



Retrospective analysis to verify the stability in dose distribution in patients with head and neck cancer undergoing radiotherapy for quality control

Dissertation zum Erwerb des Doktorgrades der Humanmedizin an der Medizinischen Fakultät der Carl von Ossietzky Universität Oldenburg

Autor: Tinei Kadenge
tineikadenge@hotmail.com

Version vom: 31.10.2023

1. Betreuer: Prof. Dr. rer. nat. Björn Poppe
2. Betreuer: PD Dr. med. Ping Jiang

Table of Contents

1. INTRODUCTION.....	- 3 -
2. THEORETICAL BACKGROUND.....	- 5 -
2.1 RISK FACTORS AND TREATMENT OPTIONS FOR HEAD AND NECK CANCER	- 6 -
2.2 SIDE EFFECTS DURING RADIOTHERAPY OF HEAD AND NECK CANCERS.....	- 8 -
2.2.1 RADIATION DERMATITIS.....	- 8 -
2.2.2 MUCOSITIS	- 10 -
2.2.3 XEROSTOMIA	- 12 -
2.2.4 DYSGEUSIA	- 12 -
2.2.5 RADIOTHERAPY INDUCED FATIGUE	- 13 -
2.2.6 OROFACIAL PAIN, ALOPECIA AND DYSPHONIA.....	- 14 -
2.3 FACTORS AFFECTING DOSE STABILITY DURING HEAD AND NECK RADIOTHERAPY	- 14 -
2.4 OBJECTIVES	- 17 -
3. MATERIALS AND METHODS.....	- 18 -
3.1 COLLECTION OF PATIENT DATA	- 18 -
3.2 CALIBRATION OF THE CONE BEAM COMPUTED TOMOGRAPHY	- 21 -
3.3 IMPORTING AND CONTOURING OF THE CBCTs	- 25 -
3.4 CALCULATION OF DOSE IN CBCTs.....	- 31 -
3.4.1 IMPORT OF THE ORIGINAL TREATMENT PLAN TO THE CBCTs	- 31 -
3.4.2 CALCULATION OF THE DOSE IN GTV/CTV AND ORGANS AT RISK	- 31 -
4. RESULTS	- 35 -
4.1 PATIENTS' VARIABLES AND ACUTE SIDE EFFECTS DOCUMENTED	- 35 -
4.2 ANALYSIS OF DOSE DEVIATION IN PATIENTS	- 37 -
4.2.1 DOSE DEVIATION IN THE SPINAL CORD.....	- 41 -
4.2.2 DOSE DEVIATION IN THE PAROTID GLANDS.....	- 47 -
4.2.3 DOSE DEVIATION IN THE MANDIBLE	- 58 -
4.2.4 DOSE DEVIATION IN THE SUBMANDIBULAR GLANDS.....	- 64 -
4.2.5 DOSE DEVIATION IN THE GROSS TUMOR VOLUME (GTV)	- 67 -
4.2.6 DOSE DEVIATION IN THE CLINICAL TARGET VOLUME (CTV)	- 69 -
4.3 SUMMARY OF THE RESULTS.....	- 71 -
5. DISCUSSION	- 73 -
5.1 CONCLUSION	- 79 -
6. SUMMARY	- 81 -
7. REFERENCES.....	- 83 -

APPENDIX - 86 -
LIST OF TABLES..... - 95 -
LIST OF FIGURES - 97 -
ACKNOWLEDGEMENTS..... - 98 -

1. Introduction

Head and neck cancers are categorized as one of the most common cancers worldwide and their incidence has increased in the last years. They are also responsible for numerous deaths in developed and developing countries (1). The treatment options for head and neck cancer include surgery, radiotherapy and chemotherapy. Details of these treatment options will be discussed in the next chapter.

Radiotherapy plays a key role in the treatment of head and neck cancers. However, large deviations in the dose distribution during radiotherapy treatment can lead to increased toxicity and acute side effects in organs at risk as well as treatment failure due to inadequate dose delivered to the tumor. In addition to this, changes in patient geometry during the course of radiotherapy may also affect the dose delivered to the organs at risk and the tumor region. Studies from Belshaw et. al (2) and Nobel et. al (3) showed an increase in the spinal cord dose due to weight loss. However, no clear correlation was found between geometrical changes and increase in the spinal cord dose during radiotherapy. In addition, a prospective study from Jellema et. al (4) included one hundred and fifty-seven patients who received bilateral radiotherapy due to head and neck cancer. This study showed that the mean parotid dose and the mean dose to the submandibular glands were the most important factors for predicting xerostomia in patients after six and twelve months.

Technical advancements in the field of radiotherapy using conformal radiotherapy (3D-CRT), intensity modulated radiotherapy (IMRT) and volumetric modulated arc therapy (VMAT) have optimized the dose delivered to the tumor and reduced the dose delivered to the organs at risk. 3D-CRT generates three-dimensional images of the internal anatomy using computerized tomography planning techniques. The IMRT technique enables higher doses to be applied to the tumor while sparing the organs at risk through the modulation of the radiation beam (5). VMAT is a modified form of IMRT that delivers radiation dose continuously during rotation of the linear accelerator. A prospective study from Kucha et. al (5) compared the acute toxicity between 3D-CRT and IMRT in seventy-eight patients with locally advanced head and

neck cancer. The study showed that patients who received IMRT had lower incidences of severe mucositis, dysphagia, weight loss and requirement for nasogastric tube insertion in comparison to those who received 3D-CRT.

Adaptive radiotherapy during treatment of patients with head and neck cancer can be applied to patients with pronounced anatomical changes during the course of treatment. Although several studies have documented dose variations in radiotherapy of head and neck cancer due to weight loss, tumor shrinkage and change in position, only a few studies have focused on identifying patients who might need re-planning before or during radiotherapy. There is therefore still limited information to identify patients who might need adaptive radiotherapy (6,7). This finding was supported by Brouwer et. al (8), who attempted to identify patients who may benefit from adaptive radiotherapy. They analyzed fifty-one studies involving anatomic and dosimetric changes in head and neck organs at risk during radiotherapy. Although some studies reported mean parotid gland doses greater than 10 Gy between planning and repeat CTs, other studies also observed mean parotid gland doses less than 1 Gy as a result of significant anatomical changes. The study therefore concluded that more studies were necessary to investigate possible relationships between anatomical and dosimetric changes as well as treatment outcome.

Our study focused on analyzing the dose stability and dose distribution during radiotherapy of fourteen patients with head and neck cancer. The analysis was done for the first twenty-five fractions of radiotherapy and involved the following organs at risk; parotid glands, submandibular glands, spinal cord and mandible. In contrast to other studies, where the dose stability and dose distribution was only analyzed in the organs at risk, this study also analyzed the dose distribution and dose stability in the tumor for inoperable patients and the tumor bed for operated patients. In addition, the severity of acute side effects as well as their impact on dose stability in our patients were analyzed with the goal of early identification of candidates for re-planning radiotherapy treatment in the future.

2. Theoretical Background

The mucosal lining covering the nasal, oral and pharyngeal tract consists of squamous epithelial cells, making squamous cell cancer (SCC) the most frequent histological diagnosis in the head and neck region. Anatomical locations of head and neck cancers are the oral cavity, nasopharynx, oropharynx, larynx and hypopharynx as shown below.

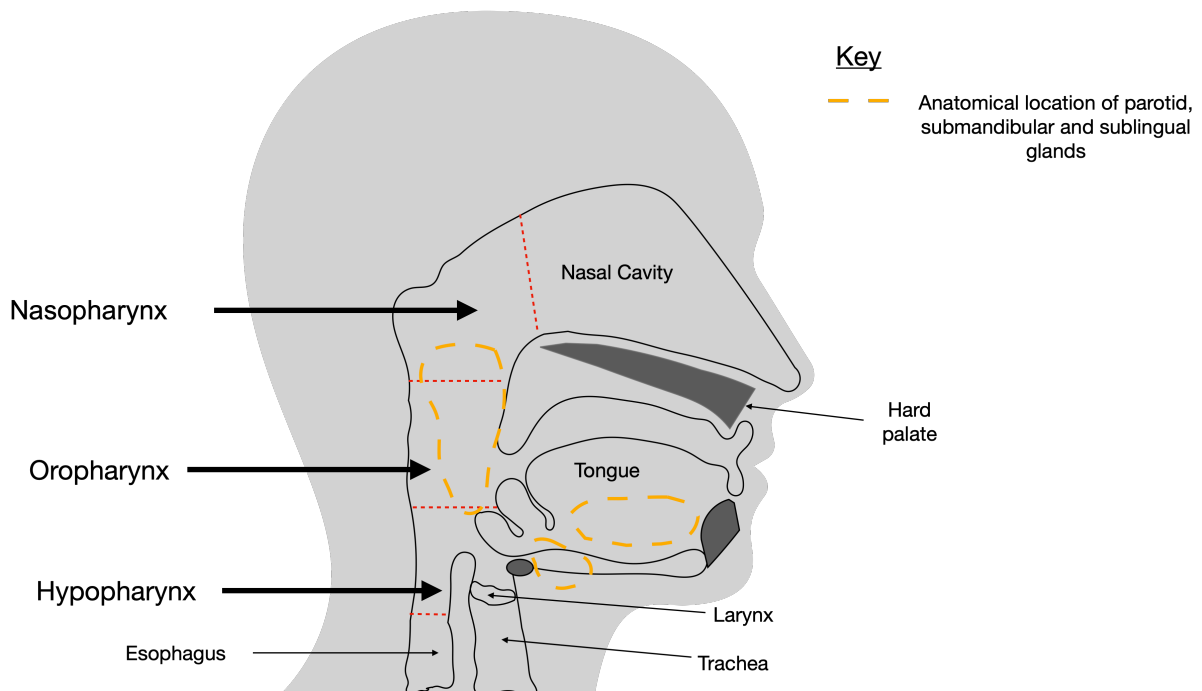


Diagram modified version from Harvard Health Publishing 2013

Figure 1: Anatomical regions and organs affected by head and neck cancer

Figure 1 above shows the anatomical regions where head and neck cancers can originate. The regions are demarcated with the red dotted lines and are called the nasopharynx, oropharynx, and hypopharynx. The patients who were analyzed in our study had either a tumor in one of these regions or a tumor overlapping the demarcations shown above. The diagram also shows important organs in the head and neck region which are in close proximity to the nasopharynx, oropharynx and hypopharynx. These organs are the salivary glands (parotid, sublingual, submandibular), esophagus, tongue and trachea. The other organs at risk during radiotherapy of the head and neck which are not indicated in the diagram are the

brain stem, optic chiasm, optic nerves, pituitary gland, spinal cord, cerebellum, thyroid gland, pharyngeal constrictor muscles and the mandible. Radiotherapy induced acute side effects in these organs and anatomical changes in the tumor region due to swelling, weight loss or tumor shrinkage can affect the stability of dose distribution during treatment as well as dose delivered to the tumor region.

2.1 Risk factors and treatment options for head and neck cancer

Worldwide head and neck cancers are ranked as the seventh most common cancer and their treatment approach differs depending on the TNM staging and anatomical locations mentioned above (9,10). Other factors which play a role in the treatment decision of patients are age, co-morbidities and patients' preferences. The three main risk factors associated with the development of oropharyngeal, laryngeal and hypopharyngeal cancers are smoking, alcohol and human papilloma virus (HPV) infection. Although smoking habits in Germany are decreasing, the incidence of oropharyngeal cancer is not decreasing. A possible explanation of this trend may be the increasing incidence of HPV infections (11). HPV associated oropharyngeal cancers have a better prognosis in comparison to HPV negative oropharyngeal cancers. Unlike oropharyngeal, laryngeal and hypopharyngeal cancers, the etiology of nasopharyngeal cancer (NPC) is an interaction of many factors. Epstein Barr virus (EBV) infection, exposure to environmental and chemical carcinogens as well as genomic variations play a role in the development of cancer in the nasopharynx (12).

Surgery is the first therapy option for patients with early-stage cancer of the head and neck. Radiotherapy is also an alternative to surgery for patients with early-stage cancer and have multiple comorbidities. Patients with locally advanced head and neck cancers and multiple lymph node involvement are treated with radio-chemotherapy (RCT) or radiotherapy alone (RT) as the first option. However, surgical resection followed by adjuvant radio-chemotherapy or adjuvant radiotherapy is also a treatment option for these patients. Patients with metastasized cancers are treated multimodally depending on symptoms and the physical condition of the patient. An overview of the management of head and neck cancers is shown in the table below.

Table 1: Overview of management of head and neck cancers according to TNM staging

T-Stage	N-Stage	M-Stage	Treatment
T0-T2	N0-N1	M0	Surgery or RT
T0-T2	N0-N2	M0	Surgery or RT Surgery + adj. RT/RCT
T3	N0-N3	M0	Surgery and/or RCT / RT Surgery + adj. RT/RCT
T3-T4	N3	M0	RCT / RT
T4	N0-N3	M0	RCT / RT
Any T	Any N	M1	Multimodal

Key: RCT – Radio-chemotherapy RT - Radiotherapy

Table 1 above gives an overview of the management of cancers in the head and neck according to the TNM staging of the tumor. As already mentioned earlier, co-morbidities and patient preferences can also influence the treatment decision of head and neck cancers.

Radiotherapy plays an important role in the treatment of SCC of the head and neck. The following treatment strategies are used for patients receiving radiotherapy due to head and neck cancer:

- **Curative Radiotherapy:** Radiotherapy is applied directly to the tumor and involved lymph nodes. However, radiation of the cervical and supraclavicular lymph node regions is only indicated when positive lymph nodes are present after clinical staging of the tumor. Combining radiotherapy with chemotherapy sensitizes the tumors cells and therefore increases the effectiveness of radiation therapy. In addition, chemotherapy reduces the risk of distant metastasis by killing microscopic tumor cells outside of the radiotherapy

treatment field. The aim of curative radiotherapy is to maximize tumor control and maintain quality of life by preserving the organ function.

- **Adjuvant Radiotherapy:** Radiotherapy is applied to the excised tumor bed and lymph node regions within eleven weeks after tumor excision and neck dissection. The following factors are indications for postoperative radiotherapy in head and neck cancers: positive margins, extranodal extension (ENE), perineural invasion (PNI), advanced T stage (pT3 and pT4), high grade, advanced N stage (N2 and N3) and involved nodes in levels IV and V (13).
- **Palliative Radiotherapy:** Radiotherapy is applied to the tumor and/or lymph nodes with the goal of improving the quality of life in patients. The majority of the patients have an extensive and incurable tumor with lymph node involvement and distant metastasis. The most common treatment goals for palliative radiotherapy are to reduce tumor associated pain (analgetic), improvement of swallowing and breathing due to tumor/lymph node compression in the esophagus or trachea and reduction of tumor associated bleeding (hemostasis). Chemotherapy and targeted therapy also play an important role in palliative treatment of head and neck cancers with distant metastasis.

2.2 *Side effects during radiotherapy of head and neck cancers*

The side effects of radiotherapy can be classified into two groups: acute and chronic side effects. The acute side effects are generally defined as reactions occurring during radiotherapy until three months after initiation of treatment. On the other hand, chronic side effects are reactions that either occur three months after the completion of radiotherapy or continue beyond three months after the completion of treatment. These are the most common acute side effects experienced by patients during radiotherapy in the head and neck region:

2.2.1 Radiation Dermatitis

The occurrence of radiotherapy-induced dermatitis during treatment is common in head and neck patients. The pathogenesis of radiation dermatitis is closely associated with basal keratinocytes, whose main function is to repair the skin. Basal

keratinocytes are the innermost layer of the epidermis and are very radiosensitive. The daily radiotherapy treatment of patients interrupts with the self-regeneration process of the epidermis by reducing the ability of basal keratinocytes to replace the damaged epithelial cells (14). As the radiotherapy treatment progresses, the basal keratinocytes activate the immune system, resulting in continuous production of cytokines. The cytokines act on blood vessels in the skin and this results in inflammation(14).

Generally, patients receiving radiotherapy administered at up to 2 Gy daily do not experience any skin reactions in the first two weeks of treatment. A radiation-induced erythema may appear after fourteen days of treatment. It is similar to a mild sunburn and is not painful. However, some patients may report having increased sensibility of the skin. Hyperpigmentation of the skin is usually observed from the twentieth day of radiotherapy treatment. In some cases, skin desquamation may occur in the last two weeks of radiotherapy. In curative radiotherapy for head and neck cancers, desquamation usually occurs from the twenty-fifth day of treatment. Skin desquamation can be either dry or moist and normally heals comprehensively two to three weeks after completion of radiotherapy.

Several risk factors are related to the development of radiation dermatitis. These risk factors can be divided into three subgroups: patient-associated factors, factors related to fractionation of radiotherapy and combination of radiotherapy with systemic therapy(14).

Patient related factors:

The most radiosensitive anatomical regions in the body are the anterior neck, chest, abdomen and face. In addition, the lifestyle of the patient also appears to increase the risk of radiation dermatitis. The most common examples are smoking, obesity, poor nutrition and exposition to the sun over long periods. Lastly, genetic abnormalities which impair the repair mechanism of DNA also increase the risk of radiation dermatitis e.g., Fanconi anemia(14).

Fractionation of radiotherapy:

The total radiotherapy dose administered, dose per fraction and the surface area of the radiation field may affect the degree of dermatitis experienced by patients during radiotherapy. Radiotherapy of head and neck cancers is usually administered once daily i.e., normofractionation. However, in rare occasions radiotherapy can also be delivered twice daily, with a period of six hours between the treatments i.e., hyperfractionation.

Combination of radiotherapy and systemic therapy:

The combination of radiotherapy with chemotherapy or targeted therapy is associated with improved loco-regional control of the tumor as well as overall survival rate. Anthracyclines, taxanes and epidermal growth factor (EGFR) inhibitors however increase the rate of radiation dermatitis (14).

Patients presenting with erythema or mild pigmentation of the skin do not require any specific treatment. The radiation oncologist however needs to reassure the patients that the skin changes will resolve a few weeks after completion of radiotherapy. Dry desquamation is treated with hydrophilic moisturizers. The use of urea-containing creams, e.g., Linola Urea Cream is recommended. Patients with itching or irritation of the skin are treated with low-potency topical corticosteroids for the relief of symptoms. The management of patients with moist desquamation involves the application of silicone foam bandages, e.g., Mepilex Lite. These provide relief for the patient and are not painful when changing dressings. However, the dressings may act as a bolus and increase the skin dose (15). In the case of secondary infections, standard therapy for bacterial infections with topical antibiotics, e.g., Fucidin cream, may be prescribed.

2.2.2 Mucositis

This is a common side effect in patients receiving radiotherapy in the head and neck region. The pathophysiology of mucositis can be divided into four phases: inflammatory phase, epithelial phase, ulcerative phase and the healing phase (16). The first phase is the inflammatory phase, which occurs around the second week of

radiotherapy. It is characterized by radiation induced cytokine production. Cytokine production results in increased permeability in the blood vessels and inflammation. The epithelial phase occurs around the third week of radiotherapy treatment and is characterized by radiation induced damage to the basal cells. This reduces the capacity of the epithelial cells to regenerate and recover. The ulcerative phase occurs from the fourth week of radiotherapy. During this phase, loss of epithelial cells causes damage to the basement membrane and development of an ulcer. The ulcer can also get a secondary bacterial infection resulting in more inflammation and pain. The last phase is the healing phase, characterized by healing and formation of fibrotic tissue (16). The classification of radiation induced mucositis is outlined in the following table.

Table 2: Classification of radiation induced mucositis

Grading of Mucositis	Clinical Presentation
Grade I	Soreness and erythema
Grade II	Erythema, ulcers; patient can swallow food
Grade III	Ulcers with extensive erythema; patient cannot swallow food
Grade IV	Mucositis to the extent that alimentation is not possible

Based on World Health Organization's oral toxicity scale

Table 2 above shows the grading of radiation induced mucositis. The following risk factors increase the risk of radiation induced mucositis: age (very young age or very old age), female gender, poor dental hygiene, decreased production of saliva, malnutrition, poor renal function and smoking(16).

The risk of developing mucositis can be reduced with scrupulous oral hygiene as well as dietary modifications. The use of an oral mouthwash (e.g., Tantum Verde solution) is used either prophylactically or after clinical observation of mucositis. Patients who develop oral thrush are treated with a mycotic like Ampho-Moronal or Nystatin suspension. Severe cases of oral thrush are treated with oral or intravenous fluconazole. Oral analgesics with non-steroidal anti-inflammatory drugs (NSAID) or

opiates are frequently prescribed due to the severe pain experienced by many patients in the last weeks of radiotherapy. Lastly, oral antibiotics can also be administered when secondary infections occur.

2.2.3 Xerostomia

Xerostomia is defined as a dry mouth due to radiation of the salivary glands during radiotherapy in the head and neck region. Reduction of saliva production may occur within the first week of radiotherapy treatment. Full recovery of the salivary glands may however take approximately two years after completion of radiotherapy (17). Xerostomia is therefore regarded as both an acute and chronic side effect of radiotherapy. Although the pathophysiology of radiotherapy induced xerostomia is not clear, studies have shown that xerostomia may be avoided if either the mean dose to one of the parotid glands is kept below 20 Gy or the mean dose to both parotid glands is less than 25 Gy (17). These dose parameters in the parotid glands can be attained using VMAT and IMRT radiotherapy techniques. However, the medial displacement of the parotid glands due to weight loss and volume reduction may increase the mean parotid gland dose during radiotherapy. In addition to the parotid glands, the radiation dose in the submandibular glands must also be controlled during treatment planning and therapy. The submandibular glands are responsible for producing saliva in the unstimulated state and therefore play an important role in the development of xerostomia (18).

Xerostomia is usually masked by more severe acute side effects like mucositis, oral thrush and radiation dermatitis during radiotherapy. It is however highlighted as a chronic side effect three months after completion of radiotherapy, when odynophagia and dysphagia have subsided. Although several treatment strategies for radiation induced xerostomia have been documented e.g., surgical transfer of the submandibular glands and treatment with oral pilocarpine solution, none of these strategies are applied frequently in clinical practice.

2.2.4 Dysgeusia

This is defined as an abnormal or impaired sense of taste. The five basic tastes are bitter, sweet, sour, salty and umami. The bitter and sour tastes are impaired the most

and the sweet taste is least impaired during radiotherapy. Dysgeusia is caused by atrophy of the taste buds due to radiotherapy in the oral cavity. Studies have shown an increased incidence of dysgeusia in patients who receive high radiation doses in the anterior two-thirds of the tongue (19,20). Mucositis may also exacerbate the altered sense of taste during radiotherapy.

Dysgeusia affects the quality of life considerably during radiotherapy treatment and should be carefully monitored by clinicians. Similar to xerostomia, this symptom can be easily overlooked due to the more severe acute side effects experienced by patients receiving radiotherapy in the head and neck region. In addition, regular use of a feeding tube due to severe dysphagia during radiotherapy decreases stimulation of the taste buds and causes an exacerbation of dysgeusia. However, many studies have reported recovery from dysgeusia four weeks after completion of radiotherapy (20).

2.2.5 Radiotherapy Induced Fatigue

Fatigue is one of the most common side effects associated with radiotherapy treatment. It is defined as a generalized weakness which is not alleviated by resting or restricting daily activities (21). Radiotherapy induced fatigue is usually reported two to three weeks after the initiation of treatment and can therefore be documented as one of the acute side effects associated with radiotherapy. However, several patients have reported persistent symptoms of fatigue three months after the completion of radiotherapy. Other factors may also cause fatigue in patients receiving radiotherapy and these also need to be considered. The most common ones are tumor-associated fatigue, anemia due to chemotherapy, medications, psychological and social issues (21).

A retrospective analysis of the data from sixty-seven patients recruited in the PASPORT trial compared the quality of IMRT to conventional radiotherapy (CRT). Although reduced incidences of xerostomia were reported in IMRT, the incidence of fatigue was significantly lower in patients who received CRT. An analysis of the dose-volume histograms of the patients revealed significantly higher doses in the posterior fossa, cerebellum and brainstem in the IMRT plans (21). This analysis revealed that

despite the recommended use of IMRT and VMAT in radiotherapy of head and neck cancers, future studies aimed at modifying the radiation dose delivered to the posterior fossa, cerebellum and brainstem are required.

2.2.6 Orofacial Pain, Alopecia and Dysphonia

These acute side effects have been less well documented in the literature but can occur during radiotherapy of the head and neck region. Orofacial pain is most likely due to irritation of the trigeminal and facial nerves during radiotherapy treatment. This symptom may persist for more than three months after the completion of radiotherapy. The pain can be controlled by nonsteroidal anti-inflammatory drugs. Alopecia is usually reported and noticed by male patients experiencing a lack of facial hair growth. It is also noticeable in the occipital part of the head. Alopecia is however reversible and many patients report a regrowth of their hair after the completion of radio-chemotherapy. Dysphonia is not a very common acute side effect in patients receiving definitive radiotherapy. Patients with a primary diagnosis of laryngeal cancer usually present with dysphonia prior to the initiation of radiotherapy. An exacerbation of the dysphonia during radiotherapy is however possible.

2.3 *Factors affecting dose stability during head and neck radiotherapy*

Maintaining a stable radiotherapy dose in the tumor region and organs at risk during the treatment period is challenging due to the following factors:

Weight loss:

Weight loss during radiotherapy treatment may result in altered dose distribution in the tumor, tumor region and organs at risk. The main reason for weight loss during radiotherapy are acute side effects, details of which were given in the last section. Weight loss is a challenge during radiotherapy because it may lead to inadequate fixation of patients during radiotherapy. This may affect the dose distribution in the tumor and organs at risk during treatment.

The introduction of modern techniques of radiotherapy, mainly volumetric modulated arc therapy (VMAT) and intensity modulated radiotherapy (IMRT), has resulted in

reduction in the severity of weight loss in comparison to the conventional radiotherapy used before. A retrospective study involving 160 patients with head and neck cancer in the oral cavity, oropharynx, hypopharynx and larynx showed a decreased extent of weight loss in patients who received conformal radiotherapy in comparison to conventional radiotherapy (22). In addition, a prospective study from Cheng et al. (23) involved nineteen patients with loco-regionally advanced NPC and showed significant weight loss in the majority of patients during radiotherapy.

Anatomical changes in the treatment region during radiotherapy:

Anatomical changes in the head and neck region during the course of radiotherapy treatment can result in dose variations in the tumor and organs at risk. These changes are usually observed in the tumor and the parotid glands. Several studies have reported volume reduction and medial shifting of the parotid glands towards high dose regions during radiotherapy. This leads to an increased dose in the parotid glands. Volume reduction and a corresponding dose increase has also been observed in the submandibular glands (8,24). However, Brouwer et al. (8) reported that volume reduction in the tumor did not affect dose stability drastically due to the use of safety margins around the tumor during treatment planning.

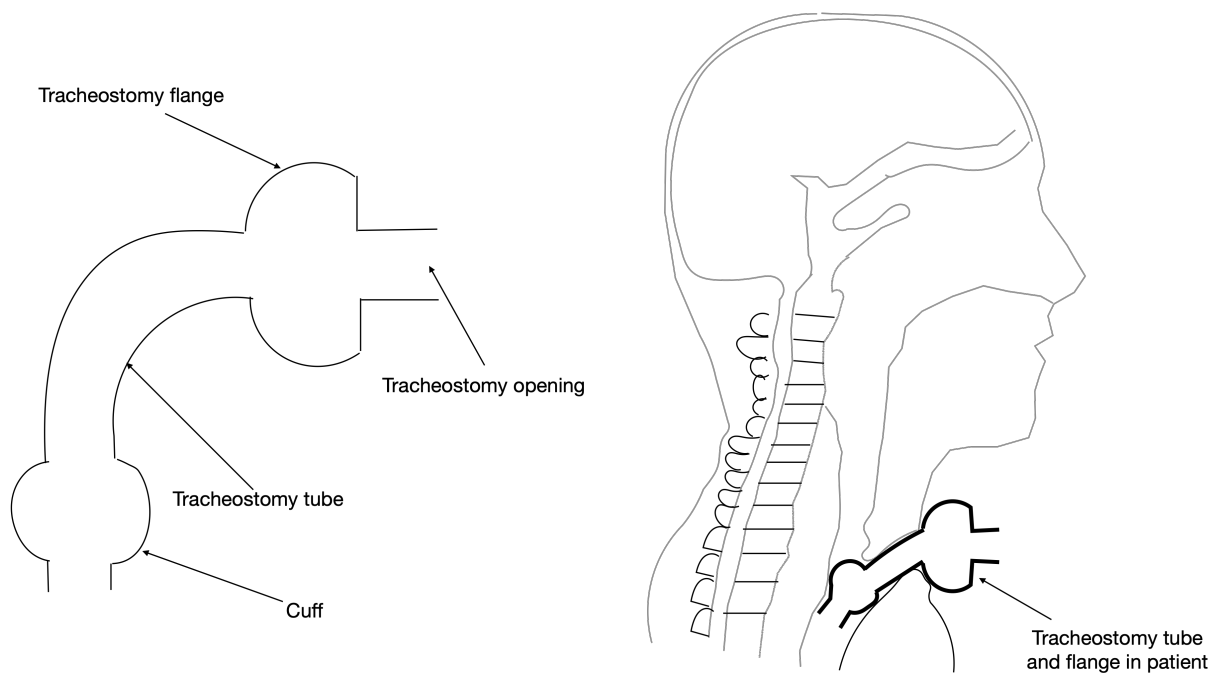
Movement of the tongue during radiotherapy:

The radiotherapy dose delivered to tumors located at the base and edge of the tongue may be affected by the movement of the tongue and the swallowing reflex. A study from Huang et al. (25) reported that use of silicone made three-dimensional bite blocks during radiotherapy reduced the dose in adjacent normal tissues and immobilized the tongue. Due to the few studies which have been carried out using bite blocks in head and neck radiotherapy, their application is not yet standard in daily practice.

Dosimetry impact of tracheostomy tube in peristomal region:

A retrospective study involving fifteen patients from Lee et al. (26) reported that the tracheostomy tube and flange had a significant impact on the radiation dose in the peristomal region during treatment. This may result in the occurrence of peristomal recurrences. The study showed that the tracheostomy flange had a bolus effect which resulted in an increased dose at the skin surface. A number of limitations in

this study were reported, the first one being that all patients included received only intensity modulated radiotherapy (IMRT). The standard treatment for patients with head and neck tumors uses volumetric modulated arc therapy (VMAT). The second limitation was that dose measurements may have been influenced by variability in placement of dosimeters on the skin surface. However, the study proved that medical devices can have a significant impact on dose delivered to adjacent structures (26).



Diagrams modified from textbook 'Tracheostomy, Information for patients and relatives', Oxford University Hospitals 2020 (p.5)

Figure 2: Bolus effect of tracheostomy flange in the peristomal region

Figure 2 above shows the different components of a tracheostomy tube on the left side. The diagram next to it shows the placement of the tube in a patient. The tracheostoma flange is in direct contact with the skin of the patient, acting as a bolus. The bolus effect may affect the dose delivered in the peristomal region by increasing the dose at the skin surface. This may result in an inadequate dose being delivered to the tumor region beneath the skin.

2.4 Objectives

Radiotherapy continues to play a key role in the treatment of head and neck cancer. As highlighted in this chapter, there are many factors which can affect the dose distribution in the tumor region and the organs at risk during the course of radiotherapy. In addition, acute side effects during radiotherapy of the head and neck region may drastically affect the quality of life in patients or even be life threatening.

The aim of this study was to verify the stability of the radiotherapy dose delivered in head and neck cancer patients during the first twenty-five fractions of treatment as well as analyze the factors which affect the dose stability. The patients included received a dose of 50 Gy during the first twenty-five fractions. These twenty-five fractions were only the first part of the radiotherapy treatment. The study was done retrospectively and analyzed treatment data for fourteen patients treated in Pius hospital. A total of 120 CT scans were analyzed during treatment data collection. For each CT scan the following structures were contoured; external outline, parotid glands, submandibular glands, spinal cord, mandible and tumor/ tumor bed. The treatment data was also collected from discharge letters written after completion of treatment as well as follow up letters written six weeks after completion of treatment.

Our study analyzed the impact of several acute side effects experienced by patients on the dose stability during these first twenty-five fractions of radiotherapy. This was done by comparing the dose calculated in the original planning CT from the treatment plan before initiation of radiotherapy, to the dose calculated in cone beam CTs (CBCT) using the same treatment plan during the course of radiotherapy. The CBCTs were performed routinely during radiotherapy of the patients to control the patient position during treatment, a concept called image guided radiotherapy (IGRT). For each patient in our study, the original planning CT and five CBCTs (one CBCT per week) were selected for analysis. The CBCTs selected for each patient to analyze dose stability needed to be calibrated first before calculating the dose delivered to the organs at risk and tumor regions. After calculation of the dose in all the CBCTs was completed, the impact of acute side effects on dose stability was assessed.

3. Materials and Methods

3.1 Collection of patient data

We initiated our study by going through a treatment register of patients treated in the radiotherapy department due to head and neck cancer at Pius Hospital in Oldenburg during a three-year period from 2015 to 2017. A total number of 155 patients with head and neck cancer received radiotherapy in Pius Hospital during this three-year period. The treatment records and register were obtained from the tumor documentation department in Pius Hospital. A total of fourteen patients were randomly picked from this register; details of the patients are given in [Table 5](#) at the end of this chapter. The treatment data was obtained from discharge letters written after completion of treatment and follow up letters written six weeks after completion of treatment.

The inclusion criteria were the following:

- All the patients included in our study were treated using an Elekta Synergy linear accelerator (Elekta, Stockholm, Sweden).
- All patients included received the standard normofractionated radiotherapy with/without combined chemotherapy (RCT), using the volumetric modulated arc therapy (VMAT) technique.
- All patients included in our study received a minimal total dose of 50 Gy with a daily dose of 2 Gy during the first 25 fractions of the treatment. This is the standard radiotherapy dose applied to the extended tumor region in patients with head and neck cancer before an additional boost dose to the tumor/tumor bed is applied.
- All patients included in our study received either definitive or adjuvant radiotherapy.

Fourteen patients who fulfilled the above-mentioned criteria were included in our study. The analysis of the dose distribution in the organs at risk as well as the extended tumor/tumor bed covered only the first twenty-five fractions of the

treatment. Subsequent to these twenty-five fractions, the patients received an additional boost dose to the tumor/tumor bed as well as to the positive lymph nodes. Due to the different location and size of the tumors treated, no analysis of the dose distribution during the boost-treatment was performed in the tumor, tumor bed and lymph nodes.

Patients receiving radiotherapy in the head and neck region due to head and neck cancer receive a five-point thermoplastic mask to fix the head, neck and shoulder regions of the patient being treated to the treatment table. The thermoplastic mask is prepared individually for each patient before initiation of radiotherapy treatment. Preparation of the mask involves immersing the mask in hot water or in a microwave to make it soft and malleable. The thermoplastic mask is molded to cover the patients' head and neck region while still soft. The mask hardens after a few minutes and maintains the form of the patient's anatomy.

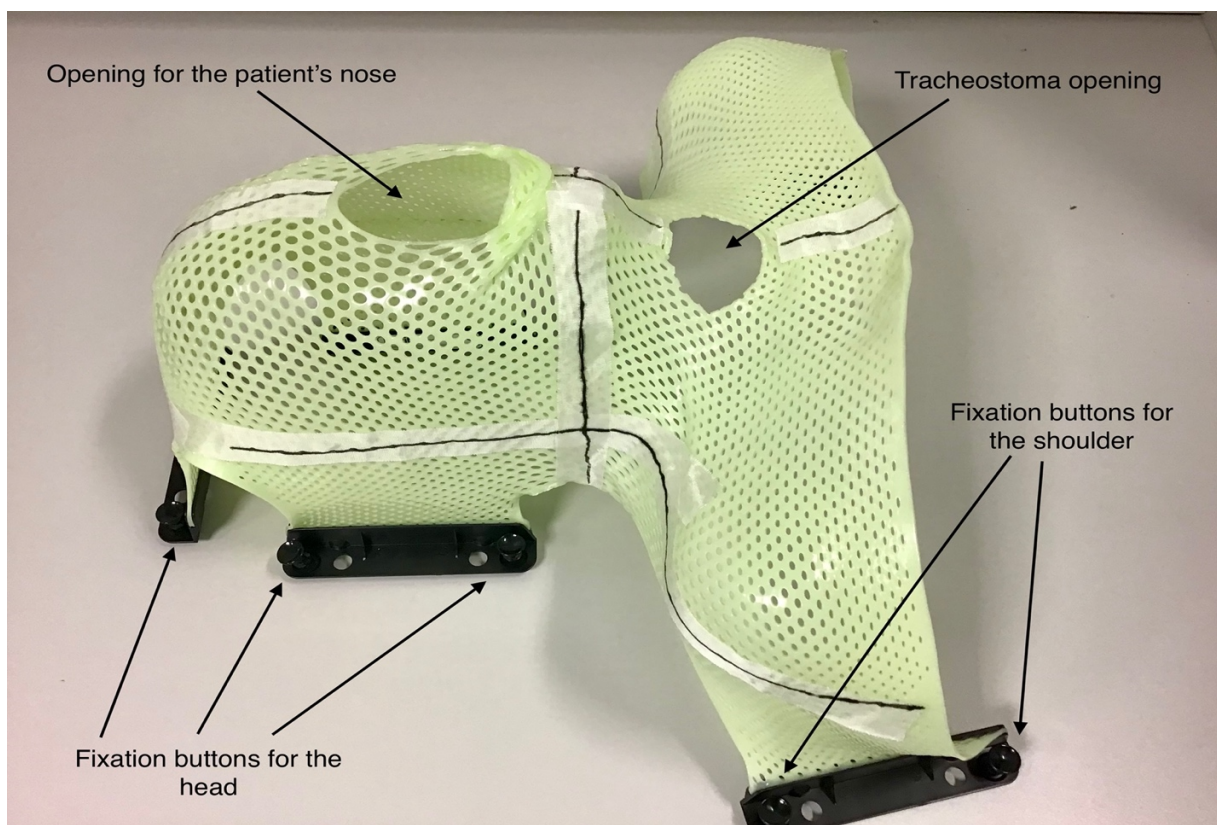


Figure 3: Five-point thermoplastic mask for fixation of radiotherapy patients

Figure 3 above shows a thermoplastic mask used for fixation in a patient with head and neck cancer. The mask has five points of fixation, three are shown in the

diagram above. Two fixation points are for both shoulders, the other two fixation points are located laterally on both sides of the head. The last fixation point is at the apex of the head. An opening for the nose allows the patient to breath during radiotherapy. An extra opening is also made for patients with a tracheostoma as shown above.

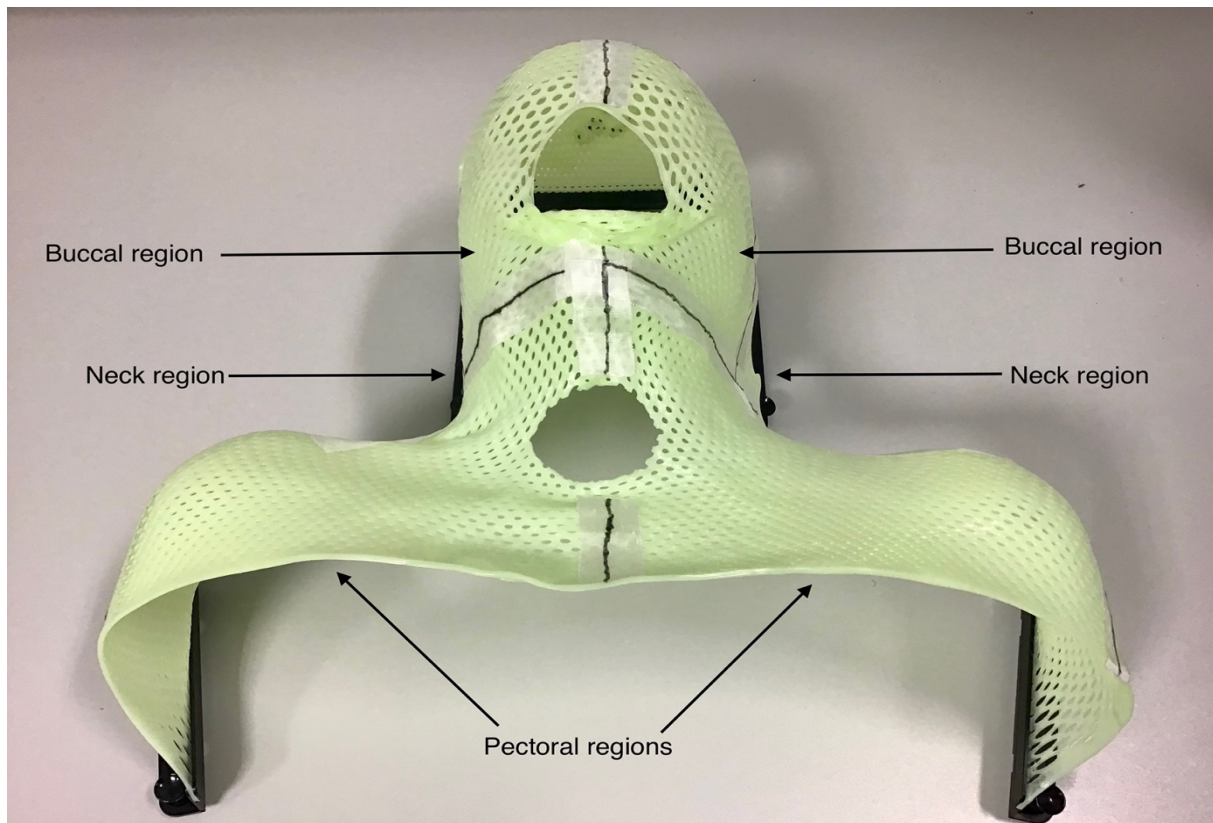


Figure 4: Anatomical regions affected by weight loss during radiotherapy of head and neck cancers

Figure 4 above shows the anatomical regions mostly affected by weight loss during radiotherapy. Loss of weight in the buccal regions may result in dose variation during radiotherapy in the region where the parotid glands are located. Weight loss in the neck region may affect the radiation dose applied to the cervical lymph nodes during radiotherapy. Loss of pectoral muscle mass in the chest may result in movement of the upper body and shoulders during radiotherapy. This may result in dose variability in the supraclavicular lymph node regions and in the spinal cord. Numerous studies have reported an increase in the spinal cord dose during radiotherapy due to weight loss. Majumdar et. al (27) found an increase in the spinal cord dose in comparison to the planned spinal cord dose in a prospective study involving forty-two patients

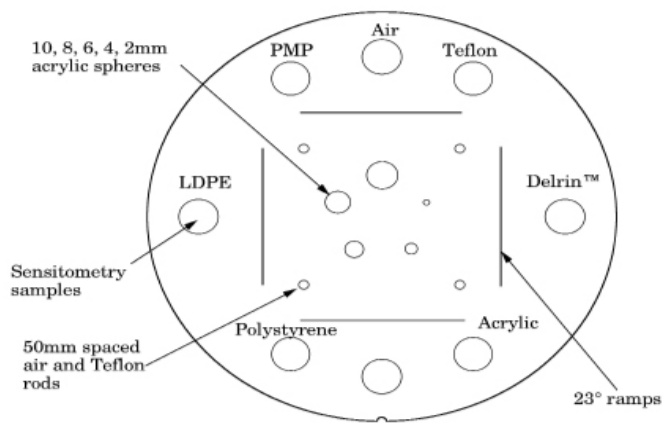
treated with head and neck cancer. However, the patients were treated with conventional radiotherapy (3D-CRT) and not the standard IMRT or VMAT radiotherapy.

In our department, patients receiving radiotherapy due to head and neck cancer using the VMAT technique received a CBCT on alternate days of treatment for the purpose of controlling the patient's position regularly during treatment. For each patient included in our study, one CBCT scan was selected weekly during the twenty-five fractions for analysis, giving a total of five CBCTs for analysis per patient.

In order to ensure the protection of patients' data, the first step in our study was to anonymize the patients' data collected. For every patient data, the original planning CT performed before initiation of treatment was exported from our Oncentra MasterPlan 4.5 (Nucletron, Columbia) planning system. A new patient case was created for each of the fourteen patients' data and renamed with the abbreviation HNO, followed by a number. For example, data for the second patient included chronologically in our study was renamed HNO 2, data for the third patient HNO 3, etc. The exported planning CT for each patient's data was then re-imported into the renamed case in the planning system. In addition, each of the five selected CBCTs for each patient were exported from the Mosaiq databank and calibrated before being imported in the renamed corresponding new cases. A detailed description of the CBCT calibration follows in sub-section 3.2 below.

3.2 Calibration of the cone beam computed tomography

Before the CBCTs could be imported into our treatment planning system for dose calculation, the grayscale values needed to be calibrated to Hounsfield units (HU) for dose calculation. The calibration phantom used in our study was the Catphan 503 phantom (The Phantom Laboratory, USA). The phantom contains inserts made of a total of seven different materials arranged in a ring around the center. The different materials in the Catphan 503 phantom are air, acrylic, delrin, PMP, LDPE, teflon and polystyrene. They have different densities and represent the different densities of materials in the human body e.g., bone, muscles, air, water, soft tissue and blood.



Source: *The Phantom Laboratory. Catphan 503 manual.*

Figure 5: Diagram of a Catphan 503 phantom

Figure 5 above shows the basic constitution of a Catphan 503 phantom with the seven inserts consisting of different materials labelled. A study from Annkah et. al (28) investigated the accuracy of the dose calculated in calibrated CBCTs using a Catphan 504 phantom, which has a similar composition to the Catphan 503 phantom. The phantom was positioned using reference lasers with a treatment isocenter. A planning CT and a CBCT were then performed on the same day on the Catphan 504 phantom. The HU values obtained for the seven different materials from the planning CT and CBCT were plotted in a graph in order to establish the correlation between the values. They found a linear relationship between the HU values from planning CT and the grey values of the CBCT. HU values for CBCTs were therefore derived using the linear calibration curve. The stability of the HU values calculated using this calibration curve was tested for a period of three months and found to be reproducible (28).

A similar process was used to calibrate the CBCTs in our study. A CBCT of the Catphan 503 phantom was taken, along with a reference CT scan of the phantom. The CT scan was performed on a Siemens Somatom Sensation 64 CT scanner under standard conditions for planning CT scans (120 kV and 3 mm slice thickness). The HU values from the planning CT and CBCT were used to plot a linear calibration curve. The calibration curve is described by the following linear relationship:

$$HU = m * x + b,$$

where x denotes the image's non-calibrated grayscale values. The m is the gradient of the plotted line and b is the value where the plotted line intersects with the y -axis.

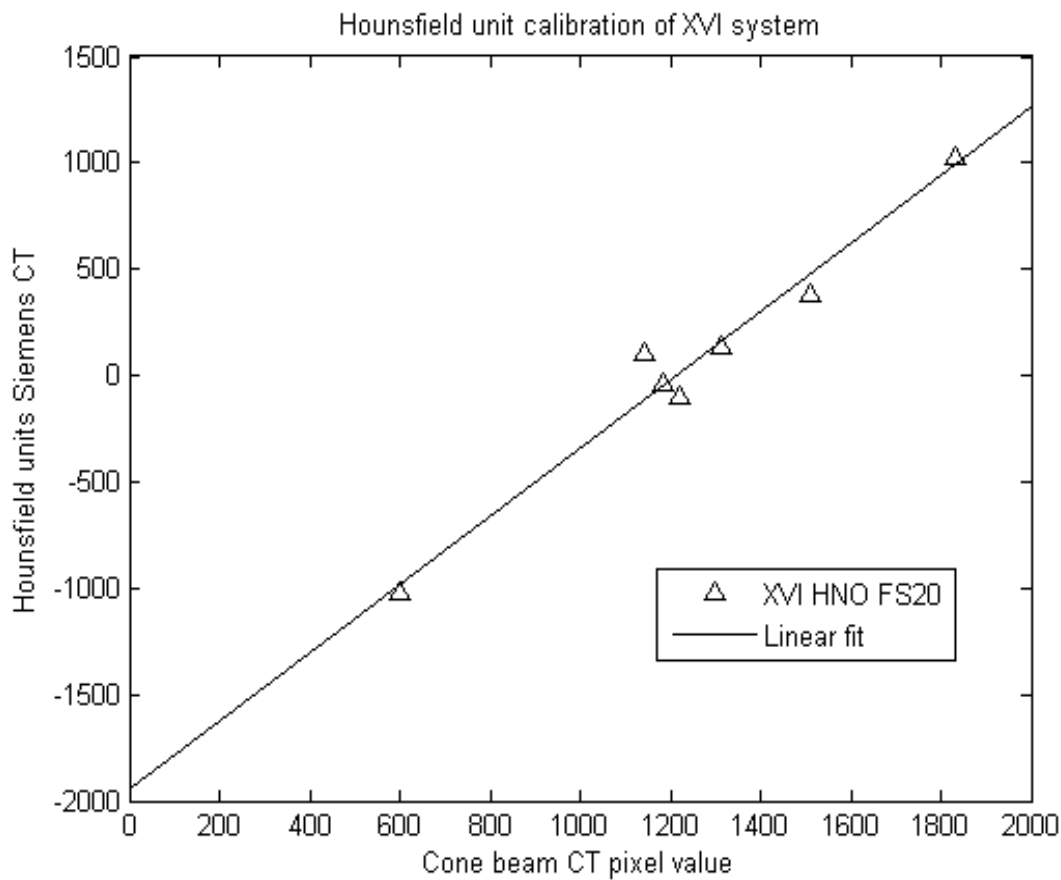


Figure 6: Graph used to calibrate CBCTs

Figure 6 above shows the plotted graph used in our study to determine the values m and b according to the equation mentioned above. Each of the seven triangles plotted in the graph represents the HU value obtained from the planning CT and the corresponding grey values in the CBCT for the seven different materials in a Catphan 503 phantom. The values m and b were derived from the linear fit. The calibration of the CBCTs into Hounsfield units has been implemented in a MATLAB (Mathworks, USA).

Table 3: Comparison of planning CT HU, uncalibrated CBCT grey values and the calibrated CBCT HU values of the seven inserts

	Planning CT HU	Uncalibrated CBCT grey values	Calibrated CBCT HU
Insert 1 - Air (Manufacturer Value: -1046 to -986)			
Average Value	-971,600	-431,000	-1000,000
Standard Deviation	1,625	32,955	0,000
Insert 2 - Teflon (Manufacturer Value: 941 to 1060)			
Average Value	921,600	817,400	1045,200
Standard Deviation	2,577	30,917	26,088
Insert 3 - Derlin (Manufacturer Value: 344 to 387)			
Average Value	327,600	503,400	452,400
Standard Deviation	3,262	29,723	17,327
Insert 4 - Acrylic (Manufacture Value: 92 to 137)			
Average Value	126,600	260,400	111,600
Standard Deviation	7,579	13,170	35,415
Insert 5 - Air (Manufacturer Value: -1046 to -986)			
Average Value	-1000,000	-417,800	-1000,000
Standard Deviation	0,000	5,913	0,000
Insert 6 - Polyesterene (Manufacturer Value: -65 to -29)			
Average Value	-55,000	206,000	-65,000
Standard Deviation	3,633	10,334	10,564
Insert 7 - LDPE (Manufacturer Value: -121 to -87)			
Average Value	-108,600	187,800	-52,200
Standard Deviation	6,829	25,143	49,773
Insert 8 - PMP (Manufacturer Value: -220 to -172)			
Average Value	-203,800	123,000	-178,600
Standard Deviation	4,261	9,381	34,949

Table 3 above compares the HU from the planning CT, the uncalibrated CBCT grey values, and the calibrated CBCT HU of the seven inserts contained in the Catphan 503 phantom. The manufacturer's provided HU value for each insert is highlighted in the gray columns. The table shows that insert three had an average HU value in the calibrated CBCT that was 65 HU above the range specified by the manufacturer. In addition, the average value of the seventh insert was 35 HU above the manufacturer's specified range. The average HU values for the other inserts were however within the specified manufacturer's range. Therefore, the calibration curve

was considered as adequate and could be used to calibrate the CBCTs for the patients selected in our study.

3.3 *Importing and contouring of the CBCTs*

The calibrated CBCTs were imported into the Oncentra Masterplan treatment planning system. A treatment case was made for each of the anonymized patients' data. The five calibrated CBCTs selected for each patient during the first twenty-five fractions were then imported into the corresponding case (one CBCT was selected per week during a period of five weeks). Each CBCT imported was labeled with the week the examination was performed. In order to accurately assess the variation of dose as well as changes in anatomy during the first twenty-five fractions of treatment, the anonymized planning CTs were also imported into the corresponding cases for all fourteen patients.

Prior to calculating the dose in the planning CTs as well as the CBCTs, contouring of the anatomical structures to be assessed had to be completed. The organs at risk selected in our analysis were the following: parotid glands, spinal cord, submandibular glands and the mandible. Each organ at risk was delineated manually using the textbook, "Target Volume Delineation for Conformal and Intensity-Modulated Radiation Therapy"(29) as a reference. In addition, the organs at risk contoured manually in the planning CT from senior consultants in the radiotherapy department at Pius Hospital were also used as a guideline during the delineation of organs at risk in the CBCTs.

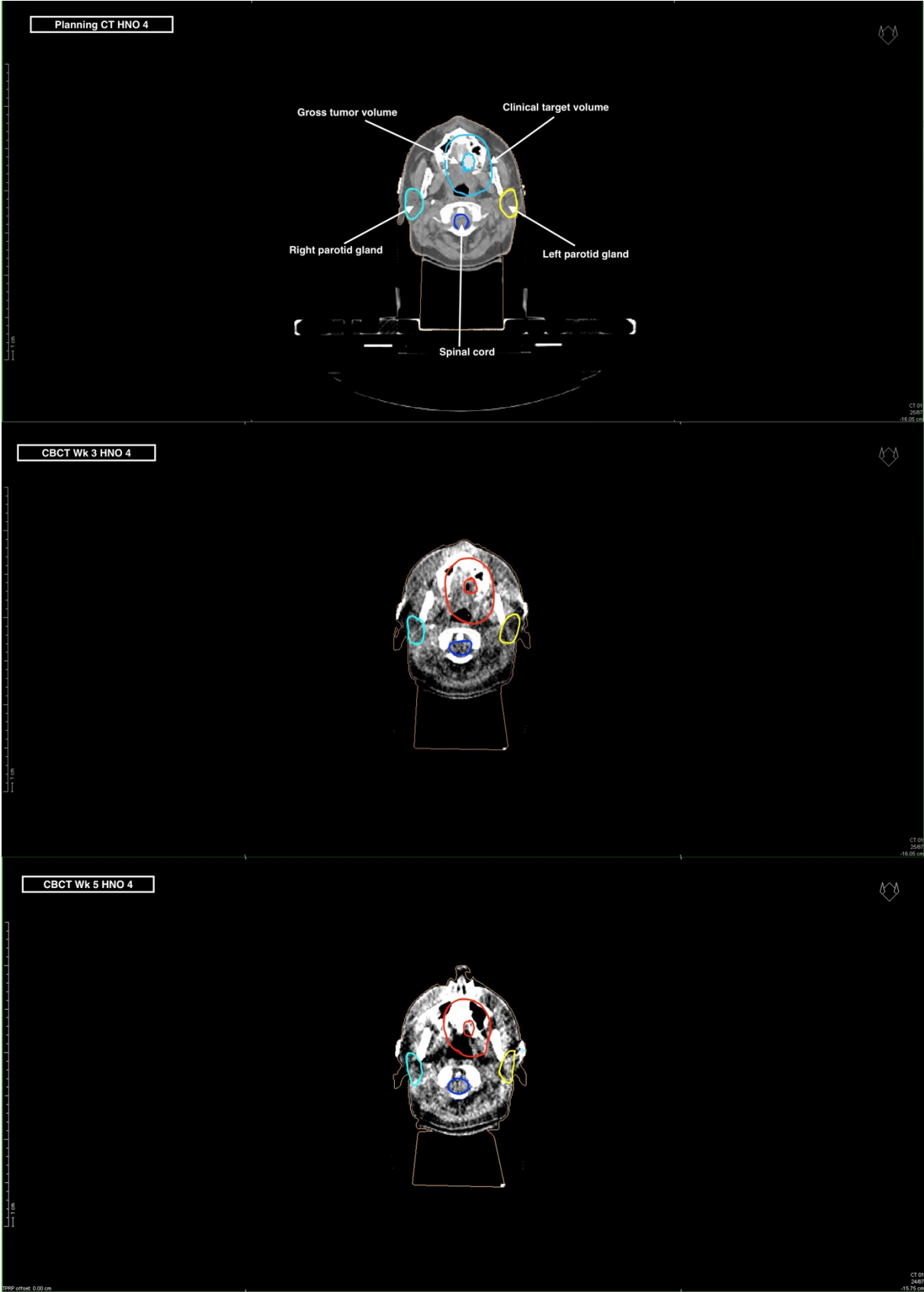


Figure 7: Example of contouring in planning CT and CBCTs for patient HNO 4

Figure 7 above shows the contouring done in the planning CT as well as the CBCTs performed weekly after the planning CT for the anonymized patient HNO 4. Only two of the five CBCTs in patient HNO 4 are shown above as an example. At the top left-hand corner of each CT is the week the CT was performed, labelled as Wk. In addition, the organs at risk contoured were labelled in the planning CT and also contoured in all the CBCTs. In this case, these were the parotid glands, spinal cord and the mandible. The gross tumor volume (GTV) and clinical target volume (CTV) were also contoured in the planning CT and in the CBCTs. More details and definitions of the GTV and CTV are given below.

In order to assess the stability of the dose in the tumor region, we contoured the gross tumor volume (GTV) and/or the clinical target volume (CTV). The GTV, CTV, as well as organs at risk (OAR), can be defined as follows:

Gross tumor volume (GTV)

- The GTV is defined as the visible tumor which can be seen physically, palpated during a clinical examination or seen radiologically. The GTV not only pertains to the primary tumor, it also includes the involved lymph nodes and adjacent organs affected by the tumor. After complete excision of a tumor, the GTV is no longer evident (30).

Clinical target volume (CTV)

- The CTV contains the GTV and a safety margin for potentially microscopic tumor cells around the GTV which cannot be fully imaged. The CTV needs to be considered and adequately treated during radiotherapy if a cure is to be achieved. During contouring in radiotherapy treatment planning, a safety margin is usually constructed around the GTV to make the CTV. The expansion margin around the GTV is however based on the clinical experience of the radiation oncologist (30).

Organs at risk (OAR)

- The organs at risk (OARs) are the healthy organs located near the clinical target volume. The radiation dose delivered to the organs at risk while delivering the treatment dose to the CTV should not exceed the tolerance dose in the organs at risk. Exceeding the tolerance dose in organs at risk increases the risk of acute and late side effects in the affected organs. For example, the median dose that the parotid glands can receive in radiotherapy is limited to 26 Gy.

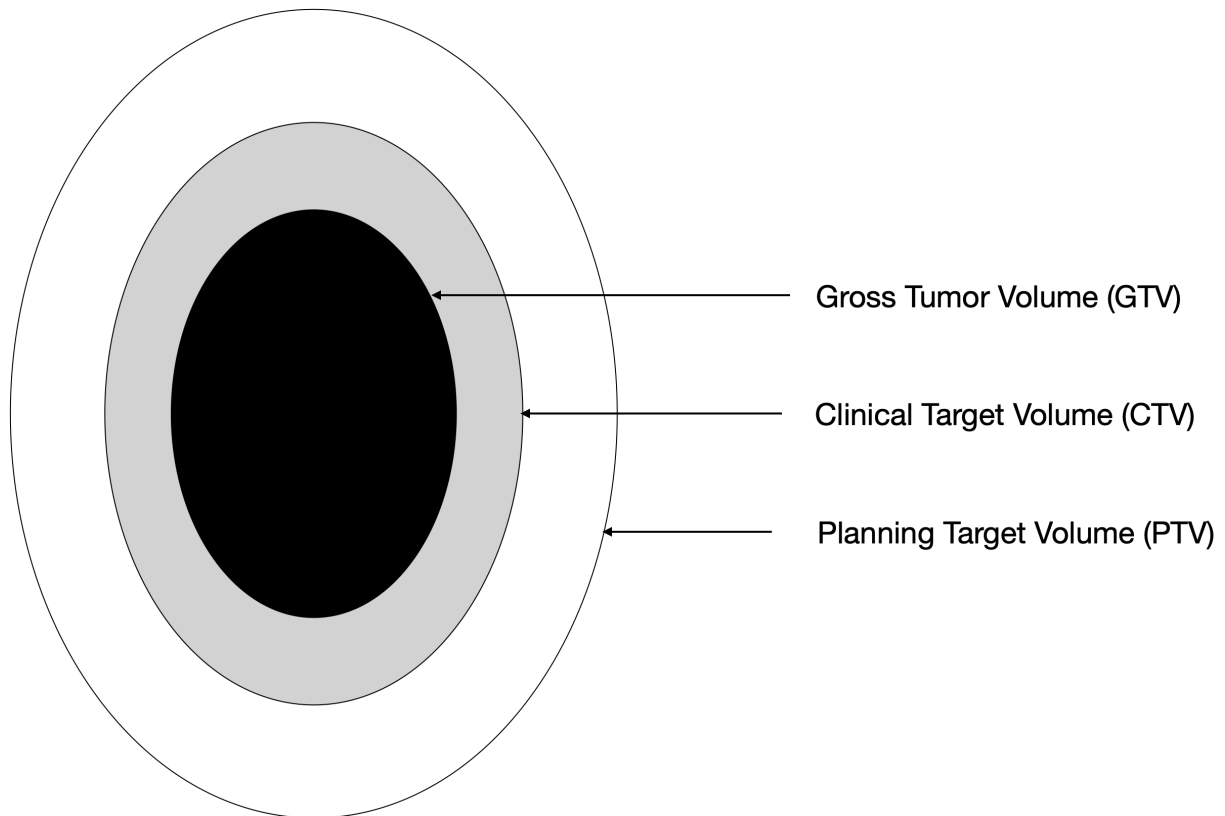


Diagram modified from ICRU Report 50

Figure 8: Illustrating gross tumor volume (GTV) and clinical target volume (CTV)

Figure 8 above illustrates the definitions of the GTV and CTV as described previously. In addition to the GTV and CTV, the planning target volume (PTV) is also depicted. The PTV considers the uncertainties in positioning of the patient, organ movement and anatomical deformations during radiotherapy.

For all the patients in our study, GTV was contoured manually in each of the five CBCTs selected per patient. The GTV was defined as the visible tumor contoured in the planning CT before initiation of radio-(chemo)therapy. The GTV contoured in the original planning CT for each patient was used as a reference during the manual contouring of each GTV in the CBCTs. Volume changes in the macroscopic tumor during treatment were however adjusted in the CBCTs. The contouring of the GTV in the original planning CT was performed by a senior consultant in the radiotherapy department at Pius Hospital. For patients who received adjuvant radio-(chemo)therapy, the CTV was contoured manually in each of the five CBCTs per patient. The CTV was defined as the tumor bed contoured in the planning CT prior to initiation of radio-(chemo)therapy. However, due to the fact that the supraclavicular

lymph node regions were cut off in our CBCT images, extensive CTVs covering the supraclavicular lymph nodes in the planning CTs could not be contoured in the CBCTs. A description of the GTV and/or CTV contoured for each patient according to anatomical localization and size is summarized in Table 4 below.

Table 4: Contouring description for GTV and CTV in patients

Patient	Diagnosis	Contouring GTV/CTV
HNO 2	Oro-and Hypopharynx Cancer	GTV: Macroscopic tumor in oro/hypopharynx and bilateral cervical lymph nodes
HNO 3	Nasopharynx Cancer	GTV: Macroscopic tumor in Nasopharynx. CTV: GTV + 1.6 cm
HNO 4	Cancer of the tongue edge	GTV: Macroscopic tumor, edge of tongue CTV: GTV + 2.0 cm
HNO 5	Cancer of the tongue base	GTV: Macroscopic tumor base of tongue
HNO 6	Cancer of the tongue base	GTV: Macroscopic tumor base of tongue
HNO 7	Cancer of the tongue base	GTV: Macroscopic tumor tongue base and bilateral cervical lymph nodes
HNO 8	Oropharynx Cancer	GTV: Macroscopic tumor oropharynx and cervical lymph nodes right
HNO 10	Oropharynx Cancer	GTV: Tumor oropharynx, PET CT positive CTV: GTV + 0.7 cm
HNO 11	Cancer of the hard palate	CTV: Tumor bed hard palate
HNO 12	Oro-, Nasopharynx and Larynx Cancer	CTV: Tumor bed oro-, nasopharynx and larynx
HNO 13	Larynx Cancer	CTV: Tumor bed larynx
HNO 15	Oropharynx Cancer	CTV: Tumor bed oropharynx and cervical lymph node region right
HNO 16	Oro-, Hypopharynx and Larynx Cancer	GTV: Macroscopic tumor oro/hypo/larynx and cervical lymph nodes left
HNO 17	Oropharynx Cancer	GTV: Macroscopic tumor tonsil left CTV: GTV + 0.7 cm

3.4 Calculation of dose in CBCTs

3.4.1 Import of the original treatment plan to the CBCTs

After completing the contouring, the original treatment plan from the planning CT was imported to each of the calibrated CBCTs. Before importing the original treatment plan, it had to be first exported from the patient's original data in the Oncentra Masterplan treatment planning system. This was done in the following steps:

- The treatment reference point marked with a cross on the left temporal side of the thermoplastic mask was first deselected, so that the adjusted coordinate parameters from the reference point to the treatment isocenter could be identified.
- After deselection of the reference point, the treatment plan was exported.
- The original treatment plan was then imported into the corresponding five calibrated CBCTs for each patient in the study.
- After importing the treatment plan, the treatment isocenter location in each CBCT was controlled and compared to the isocenter in the original planning CT.
- In all the CBCTs assessed in our study, the isocenter of the imported treatment plan was found to be in the exact same position as that of the treatment plan from the original planning CT.

3.4.2 Calculation of the dose in GTV/CTV and Organs at Risk

The next step was to calculate the expected dose distribution in the contoured organs at risk and GTV/CTV. The treatment plan and the radiation monitoring units (MU) were left exactly as they were planned and radiated in the original CT data set. In the planning system, the collapsed cone algorithm was selected among the calculation options. The calculation was then started with a dose grid of 2 mm, which takes approximately seven minutes per case for a CT slice thickness of 3 mm.

The following dose parameters were calculated from the dose distributions in the planning CT and in each of the selected CBCTs:

D50: Median dose in the organs at risk and GTV/CTV

D95: Minimum dose delivered to 95% of the GTV/CTV or organs at risk

V95: Volume of the GTV/CTV or organ at risk receiving 95% of the prescribed dose

D2: Dose received by 2% of volume, for example, the spinal cord

Table 5: Details of the patients included in our study

	Age (years)	Sex	Diagnosis, Staging Treatment	Secondary Diseases	HPV*- Status
HNO 2	65	Male	- Oro-/Hypopharynx Ca - cT4 cN2 M0 - RCT*	- Heart failure -Cerebrovascular accident (2009)	-Unknown
HNO 3	58	Male	- Nasopharynx Ca - cT3 cN0 Mo - RCT	-Cerebrovascular accident (2000) - Nicotine abuse (40 PY) - Hypertension - Hyperlipidemia	- Negative
HNO 4	26	Female	- Tongue edge Ca - pT2 pN2 M0 - RCT	- Asthma - Hyperthyroidism - Nicotine abuse (5 PY)	- Negative
HNO 5	58	Male	- Tongue Base Ca - cT4 cN2 M0 - RT*	- Multiple sclerosis - Lung emphysema	- Negative
HNO 6	58	Male	- Oro + Tongue Base Ca - cT4 cN2 M0 - RCT	- Nicotine and Alcohol abuse - Liver cysts	- Unknown
HNO 7	70	Male	- Base of Tongue Ca - cT2 cN2c M0 - RCT		- Unknown
HNO 8	78	Female	- Oropharynx Ca - cT3 cN2b Mx - RT	- Hyperthyroidism - Goiter	- Positive
HNO 10	54	Male	- Oropharynx Ca - pT3 pN0 M0 - RT	- Nicotine and Alcohol abuse - Hypertension - COPD II°, - Kidney cysts	- Negative
HNO 11	53	Female	- Hard palate Ca - pT3 cN0 M0 - RT	- Hypertension - Hyperuricemia	- Unknown
HNO 12	70	Male	- Larynx,Oro,Naso. Ca - pT4 pN1 M0 R1 - RCT	- Nicotine abuse - Hypothyroidism - Hypertension	- Positive
HNO 13	70	Male	- Larynx Ca - rpT3 pN2 M0 - RT	- Appendectomy - Cholecystectomy	- Unknown
HNO 15	73	Male	- Oropharynx Ca - pT1 pTis pN1 M0 - RT	- Restless legs - Hypertension - Morbus Scheuermann	- Positive
HNO 16	67	Male	- Oro, Hypo, Larynx Ca - cT4a cN2c M0 - RCT	- Hypertension	- Unknown
HNO 17	63	Female	- Oropharynx Ca - cT1 cN2b M0 - RCT	- Hypertension	- Positive

*HPV- Human Papilloma Virus, RCT- Radio-chemotherapy, RT- Radiotherapy

Table 5 above gives an overview of the patients included in our study. The first column shows anonymized names of the fourteen patients. The fourth column shows the diagnosis, TNM staging and the treatment applied. The patient`s comorbidities and the HPV-status are documented in the fifth and sixth columns respectively.

4. Results

4.1 Patients' variables and acute side effects documented

From January 2015 to November 2017, fourteen patients diagnosed with head and neck cancer were treated in our radiotherapy department at Pius Hospital. The age of the patients ranged from 26 years to 78 years, with a median age of 64.5 years. The variables of the patients are summarized in Table 6 below.

Table 6: Overview of patient variables

Patient variables	Number of patients	Percentage (%)
Gender		
• Males	9	64 %
• Females	5	36 %
Age (years)		
• < 70	12	86 %
• > 70	2	14 %
Weight (kg/m ²)		
• BMI < 25	8	5 %
• BMI > 25	5	36 %
• BMI unknown	1	7 %
Radio-(chemo) therapy		
• Radiotherapy (RT) alone	6	43 %
• Radio-chemotherapy (RCT)	8	57 %
Radiotherapy Concept		
• Definitve RT	8	57 %
• Adjuvant RT	6	43 %
Smoking		
• Yes	7	50 %
• No	7	50 %
Alcohol		
• Yes	3	21 %
• No	11	79 %

Table 7: Acute side effects documented during radiotherapy treatment

Acute side effects documented	Number of patients documented with side effect
Mucositis	13
Radiation dermatitis	9
Xerostomia	6
Dysgeusia	4
Other side effects	9

Table 7 above shows the acute side effects documented in the discharge and six week follow up letters during radiotherapy of the patients in our study. The most common acute side effect documented was mucositis, followed by radiation dermatitis and other acute side effects. The most common side effects documented under “Other side effects “, were increased trachea secretions during radiotherapy, nausea, vomiting and radiotherapy induced fatigue.

Table 8: Grade of mucositis documented in patients

Grade of mucositis documented	Number of patients	Percentage
Grade I	4	28,5 %
Grade II	4	28,5 %
Grade III	5	36 %
Grade IV	0	0 %
Not documented	1	7 %

Table 8 above shows the severity of mucositis documented in the patients in our study according to the WHO classification mentioned in the first chapter. Thirty-six percent of the patients experienced grade III mucositis. The majority of patients however experienced either Grad I or II mucositis.

Table 9: Grade of dermatitis documented in patients

Grade of radiation dermatitis documented	Number of patients	Percentage
Mild erythem I°	3	21,5 %
Moderate erythem II°	1	7 %
Erythem + dry desquamation	2	14 %
Erythem + moist desquamation	3	21,5 %
Not documented	5	36 %

Table 9 above shows the grade of dermatitis documented in our patients. No information on dermatitis was documented in the treatment records of five patients.

4.2 Analysis of dose deviation in patients

This section focuses on the dose deviation during the first twenty-five fractions of treatment in the organs at risk, gross tumor volume (GTV) and clinical target volume (CTV). These values were calculated weekly in the first five weeks for each patient selected in our study. The relative deviation of each value calculated weekly in the CBCT from the value calculated in the original planning CT was calculated. An example of the dose values calculated in patient HNO 4 is shown in the three tables below.

Table 10: Dose values for D50% in HNO 4 in Grays (Gy)

Week of Examination	Spinal Cord	Parotid Rt	Parotid Lt	Mandible	Tumor (GTV)	Tumor (CTV)	Submandible GI Rt	Submandible GI Lt
Planning CT	25,72	20,53	50,04	46,97	50,85	50,24	48,36	49,27
Wk 1	25,73	19,93	50,80	46,22	49,86	49,65	47,72	49,47
Wk 2	26,34	18,61	51,44	44,85	50,48	50,31	47,53	50,31
Wk 3	25,90	22,47	50,83	45,38	49,75	49,11	47,75	49,37
Wk 4	27,30	27,60	51,44	45,00	50,31	49,54	47,77	49,90
Wk 5	24,81	25,62	51,08	46,18	50,00	50,12	47,85	50,34

Table 11: Dose values for D2% in HNO 4 in Grays (Gy)

Week of Examination	Spinal Cord
Planning CT	32,22
Wk 1	29,58
Wk 2	33,03
Wk 3	30,46
Wk 4	34,47
Wk 5	30,56

Table 12: Dose values for D95% in HNO 4 in Grays (Gy)

Week of Examination	Tumorbed (CTV)
Planning CT	48,88
Wk 1	48,10
Wk 2	48,49
Wk 3	47,73
Wk 4	48,68
Wk 5	48,22

Table 10 above shows the D50% dose values calculated in the first twenty-five fractions of radiotherapy for patient HNO 4. These values were calculated weekly from CBCTs in organs at risk, GTV and CTV from week one (Wk 1) to week five (Wk 5). The D50% values for the organs at risk, GTV and CTV were also calculated in the original planning CT before initiation of radiotherapy. Table 11 and 12 above show D2% dose values in the spinal cord and D95% dose values in the clinical target volume for patient HNO 4 respectively.

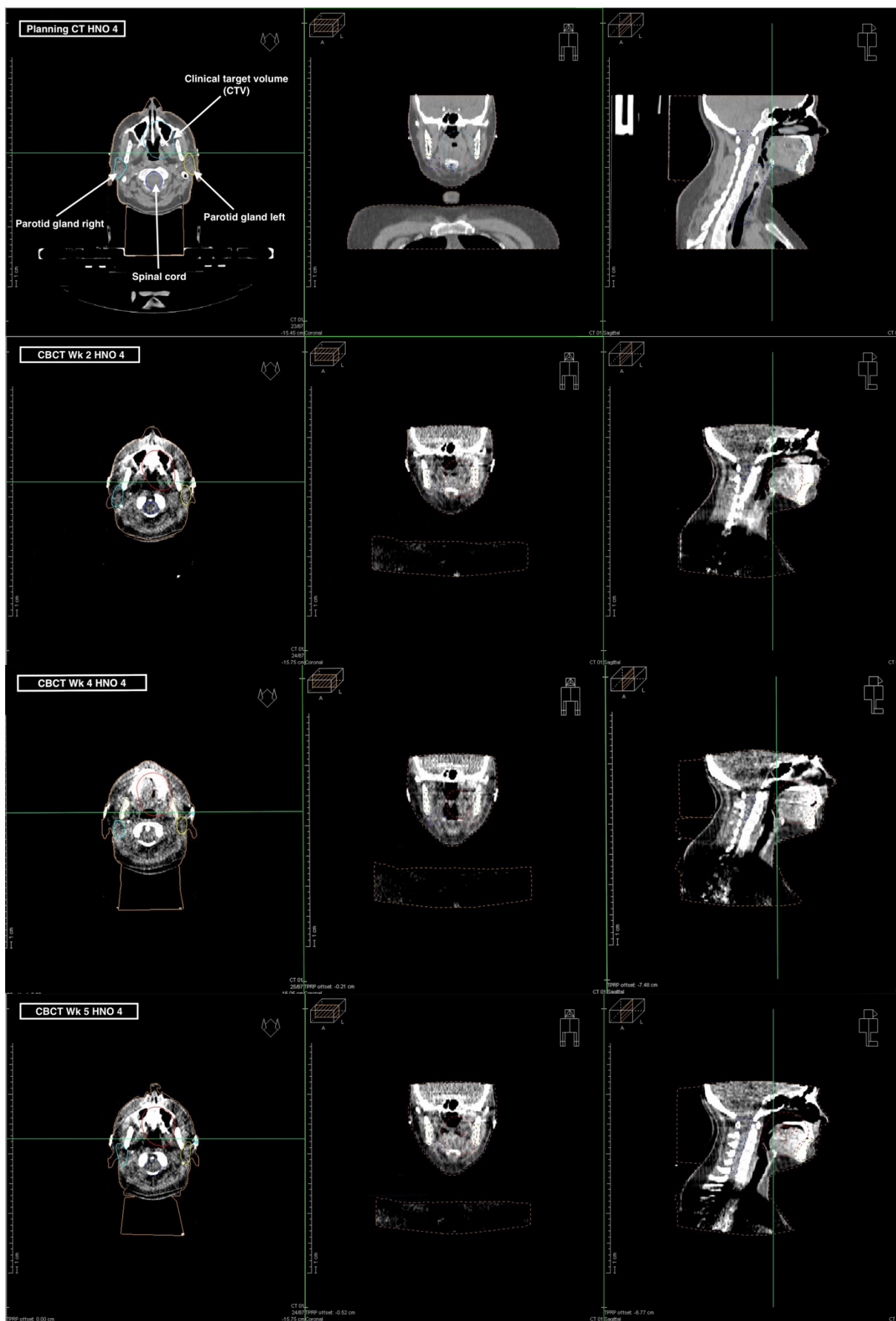


Figure 9: Planning CT and weekly CBCTs in patient HNO 4

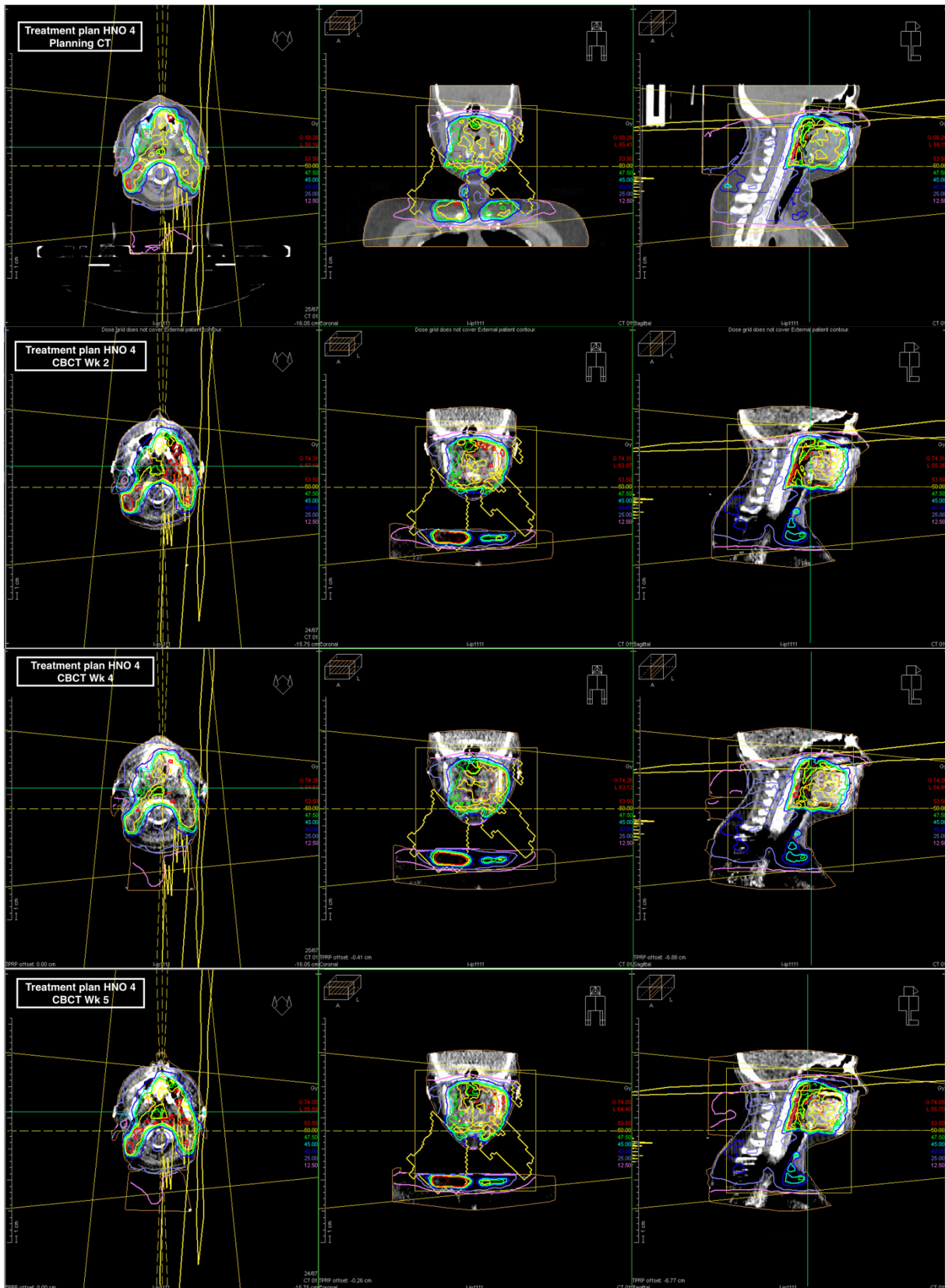


Figure 10: Radiotherapy plan in planning CT and CBCTs for patient HNO 4

Figure 9 shows axial, coronal and sagittal slices for the planning CT and three from five CBCTs in patient HNO 4. Labelled in the axial slice of the planning CT are the left and right parotid glands, the spinal cord and the clinical target volume (CTV). These structures were also contoured in all the CBCTs. Figure 10 above shows the radiotherapy plan in the planning CT and three from five CBCTs used to calculate the radiation dose in the organs at risk and CTV in patient HNO 4.

The relevance of the relative dose deviation from the planned dose in our study was defined using the following criteria:

- Dose deviation < 10%: Not relevant
- Dose deviation 10-20%: Relevant
- Dose deviation > 20%: Very relevant

4.2.1 Dose deviation in the spinal cord

D50%

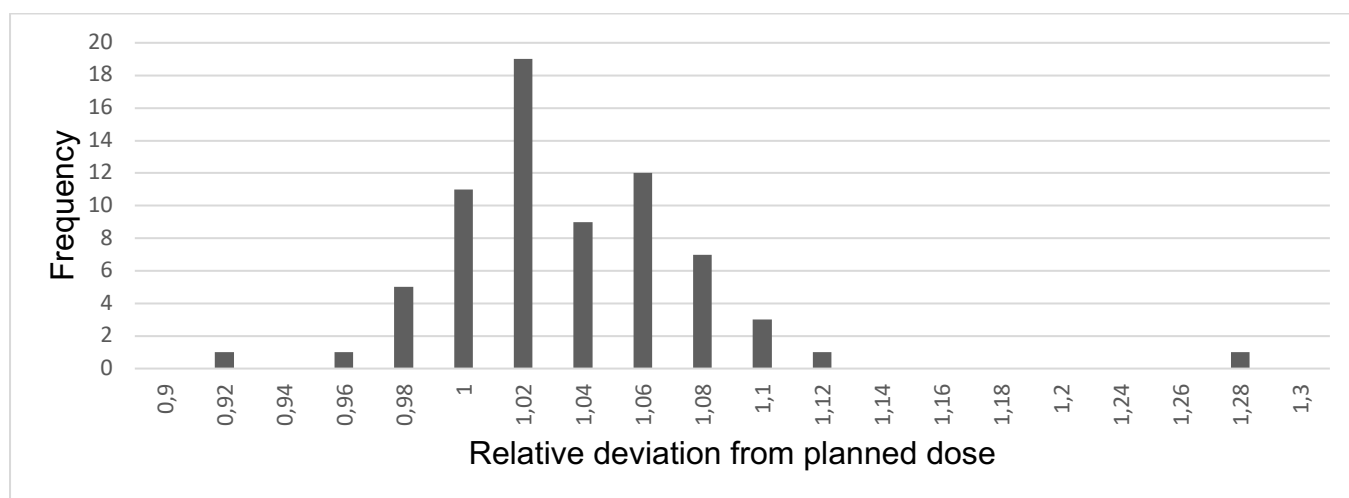


Figure 11: Frequency of daily differences from planned dose in D50% in the spinal cord

The histogram above shows the frequency of daily differences from the planned dose in D50% for the spinal cord. The relative dose deviation from the planned dose is shown on the x-axis. The frequency of the relative deviations from the planned dose is shown on the y-axis. A total of seventy CBCTs were evaluated. The most frequent relative deviation of +2% (1,02) from the planned dose was calculated in nineteen CBCTs. The second most frequent relative deviation of +6% (1,06) was calculated in twelve CBCTs. There was no relative deviation from planned dose calculated in

eleven CBCTs (1,0). Only two CBCTs had a relative deviation of more the 10% for D50% in the spinal cord. A very relevant relative deviation of 28% (1,28) was calculated in one CBCT.

Table 13: Relevant relative deviations in D50% for the spinal cord

Relative Deviations for D50% in the spinal cord		
Week	Calculated dose (Gy)	Relative deviation
HNO 11	Planning CT	25,56
	2	28,19
HNO 15	Planning CT	18,26
	1	23,21

Table 13 above shows the two relevant relative deviations in D50% for the spinal cord. The table shows the calculated D50% dose in the original planning CT for each patient and the week during treatment when the relative deviations were calculated. In patient HNO 11, the relevant relative deviation was calculated in week two of treatment and in patient HNO 15 in week one. The other sixty-eight relative deviations in D50% calculated for the spinal cord were not relevant and were therefore not tabulated.

D2%

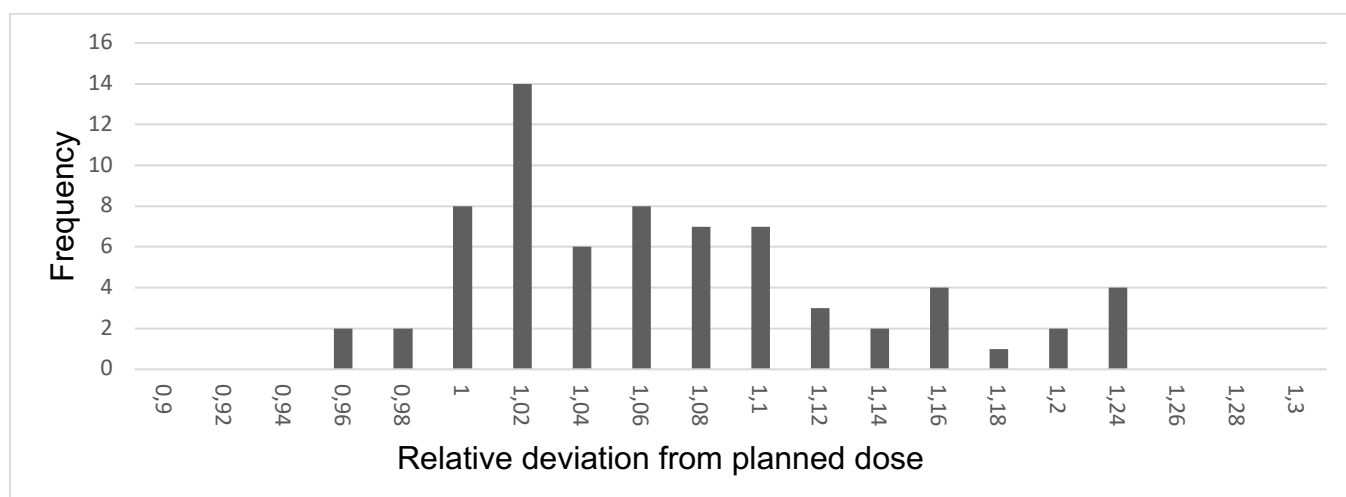


Figure 12: Frequency of daily differences from planned dose in D2% for the spinal cord

The histogram above shows the frequency of daily differences from the planned dose in D2% for the spinal cord. The relative dose deviation from the planned dose is

shown on the x-axis. The frequency of the relative deviations from the planned dose is shown on the y-axis. A total of seventy CBCTs were evaluated. The most frequent relative deviation of +2% (1,02) was calculated in fourteen CBCTs. Fifteen values had a relative deviation of more than 10% and were relevant. Four of these were very relevant with a relative deviation of more than 20%. The relevant dose values in D2% and the patients affected are summarized in the following table.

Table 14: Relevant relative deviations in D2% for the spinal cord

Relative Deviations for D2% in the spinal cord				
	Week	Calculated dose (Gy)	Relative deviation	
HNO 10	Planning CT	31,35		
	1	35,94	1,15	
	2	35,95	1,15	
	3	35,45	1,13	
	4	37,22	1,19	
HNO 11	5	36,26	1,16	
	Planning CT	31,79		
	2	35,55	1,12	
	4	35,74	1,12	
	HNO 12	Planning CT	31,79	
1		38,90	1,22	
2		39,14	1,23	
3		39,09	1,23	
4		37,72	1,19	
HNO 15	5	38,68	1,22	
	Planning CT	29,96		
	4	33,11	1,11	
	HNO 16	Planning CT	30,47	
		4	35,08	1,15
5		33,66	1,10	

Table 14 above shows the fifteen relevant relative deviations in D2% for the spinal cord. The table also shows the week during treatment when the relevant relative deviations were calculated. In patients HNO 10 and HNO 12, relevant relative dose deviations of more than 10% were calculated every week during the first five weeks of treatment. Patient HNO 12 had four very relevant relative dose deviations of more than 20% calculated. The tolerance dose of 45 Gy in D2% for the spinal cord was not exceeded in any of the calculated doses despite the relevant deviations (2). The CBCTs during the five-week treatment period of patient HNO 12 were analyzed to get more clarity about the reason for the relevant dose deviations in D2%.

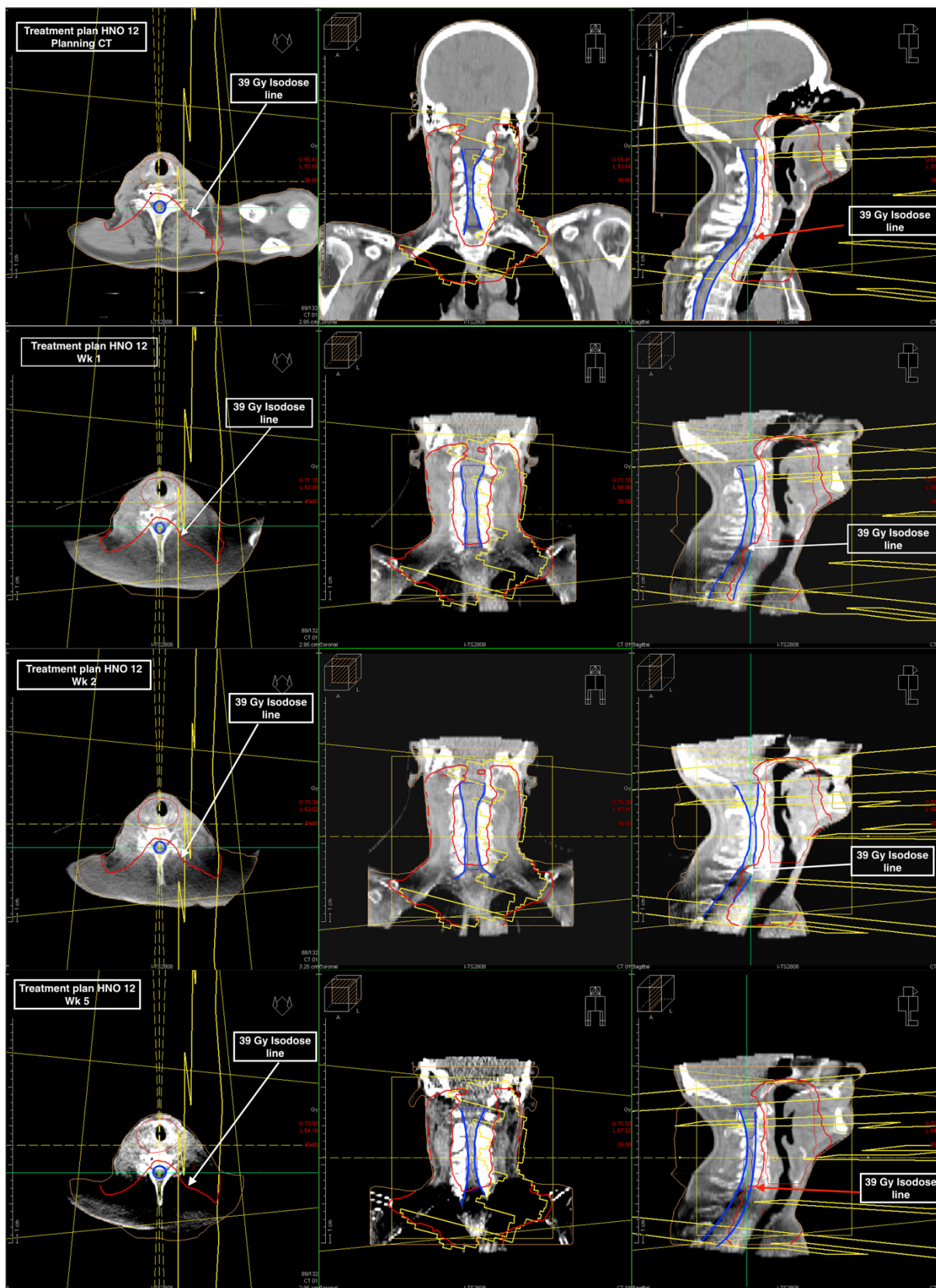


Figure 13: Radiotherapy plan in planning CT and CBCTs for patient HNO 12

Figure 13 above shows the radiotherapy plan used to calculate the radiation dose of the organs at risk and tumor bed in patient HNO 12. As already shown in [Table 14](#) above, the D2% dose in the spinal cord calculated in the five CBCTs for HNO 12 was approximately 39 Gy, whereas the D2% dose in the planning CT was 31,79 Gy. We therefore looked at the distribution pattern of the 39 Gy isodose line in the planning CT and the CBCTs. The 39 Gy isodose line is shown in red in the axial, coronal and sagittal sections of the planning CT and the CBCTs above. The spinal cord is demarcated in the dark blue outline in all axial, coronal and sagittal sections above.

The sagittal section of the planning CT in HNO 12 shows the 39 Gy isodose line in red running parallel to the spinal cord (blue line). In the CBCTs from week one to five, the 39 Gy isodose line intersects the spinal cord at level C6/C7 and continues downwards within the spinal cord. This was observed in all the sagittal sections of the CBCTs from week one to week five in patient HNO 12 above. Only three of the five CBCTs are shown in Figure 13 above. No prominent anatomical changes were observed in this region, as shown in the following diagram.

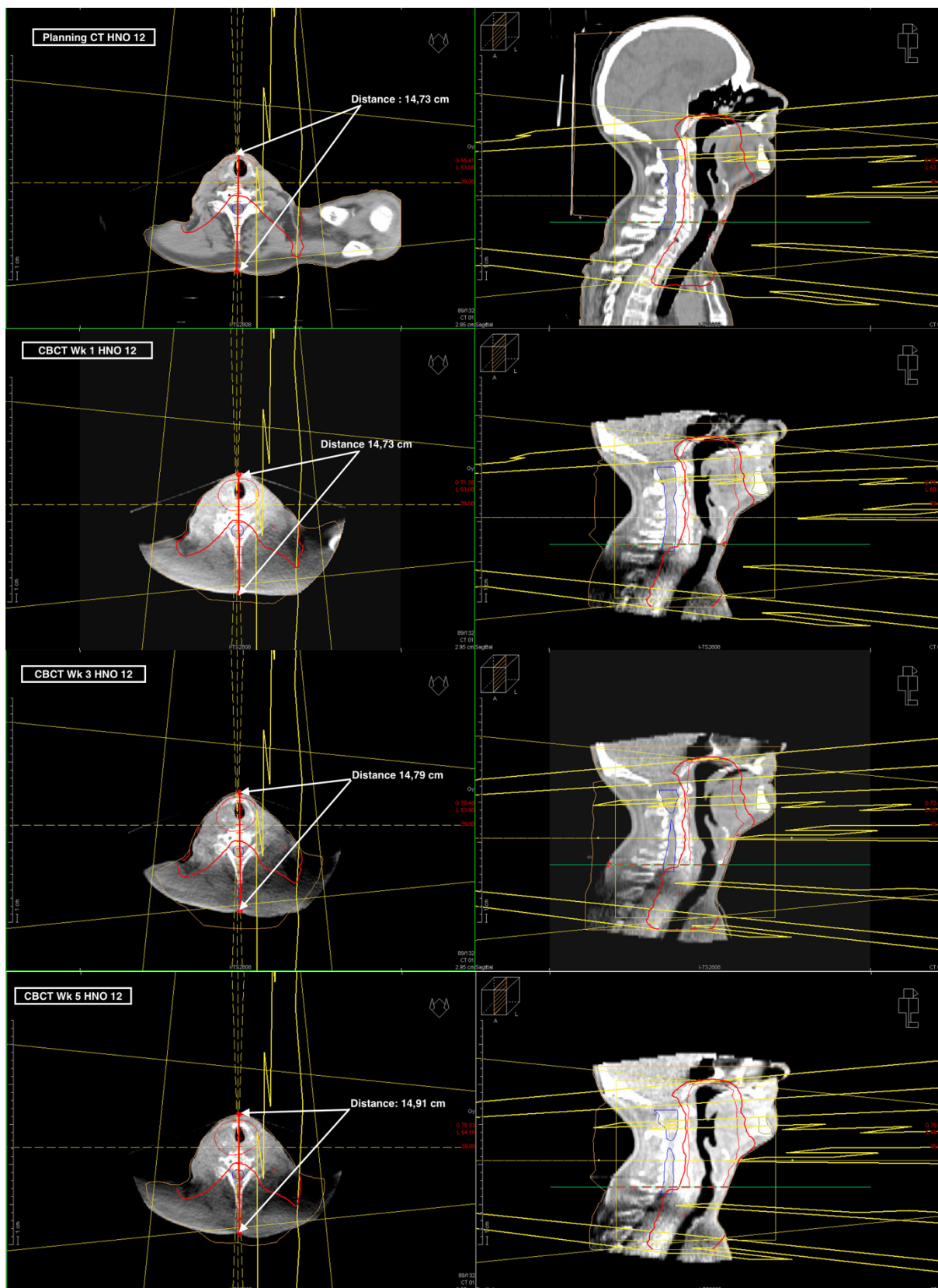


Figure 14: Evaluation of anatomical variation at level C6/C7 in patient HNO 12

Figure 14 above compares the anatomy in the planning CT and CBCTs at the level C6/C7 in patient HNO 12. As can be seen by the measured distance in the axial sections from the skin at the cricoid cartilage to the skin posterior to C6/C7, no relevant weight loss occurred in the region.

4.2.2 Dose deviation in the parotid glands

Right parotid gland

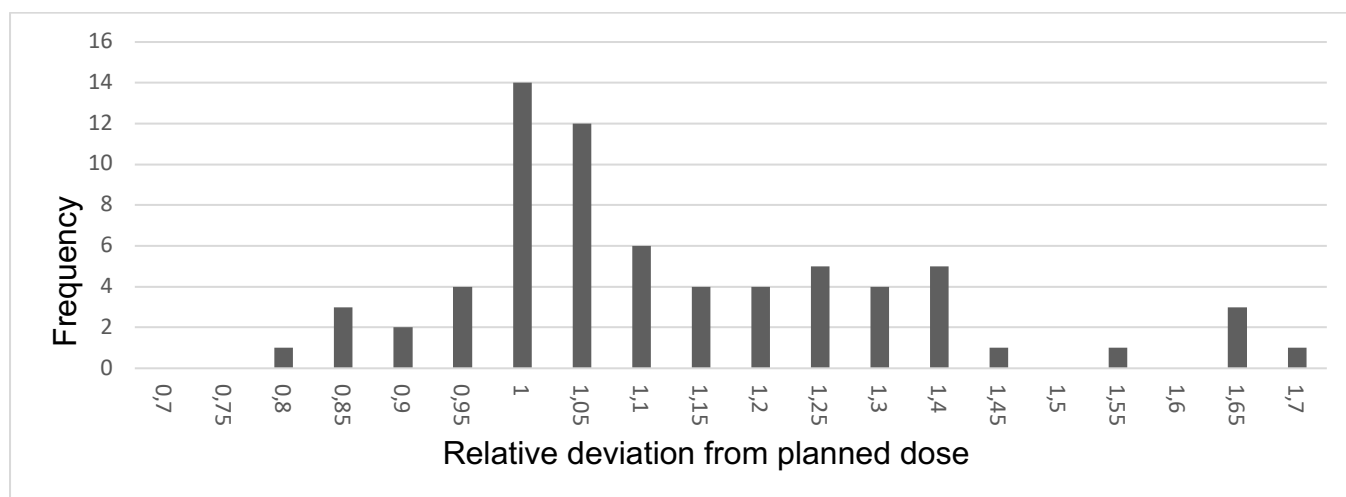


Figure 15: Frequency of daily differences from planned dose in D50% for right parotid gland

The histogram above shows the frequency of daily differences from the planned dose in D50% for the right parotid gland. The relative dose deviation from the planned dose is shown on the x-axis. The frequency of the relative deviations from the planned dose is shown on the y-axis. A total of seventy CBCTs were evaluated. No relative deviation from the planned dose was calculated in fourteen CBCTs (1,0). In twelve patients (1,05) a relative deviation from the planned dose of 5% was calculated. Relevant relative deviations from the planned dose of more than 10% were calculated in thirty-eight CBCTs. In patient HNO 7, very relevant relative dose deviations of more than 20% were calculated in the weekly CBCTs from week two to five of treatment as shown in the next table.

Table 15: Very relevant relative deviations in D50% right parotid gland in HNO 7

Relative Deviations for D50% in the right parotid gland			
Week		Calculated dose (Gy)	Relative deviation
HNO 7	Planning CT	24,67	
	2	30,00	1,21
	3	40,64	1,65
	4	40,59	1,65
	5	40,15	1,63

Table 15 above shows the relevant relative deviations calculated in the CBCTs weekly during treatment of patient HNO 7. The CBCTs for patient HNO 7 were analyzed and compared to the original planning CT.

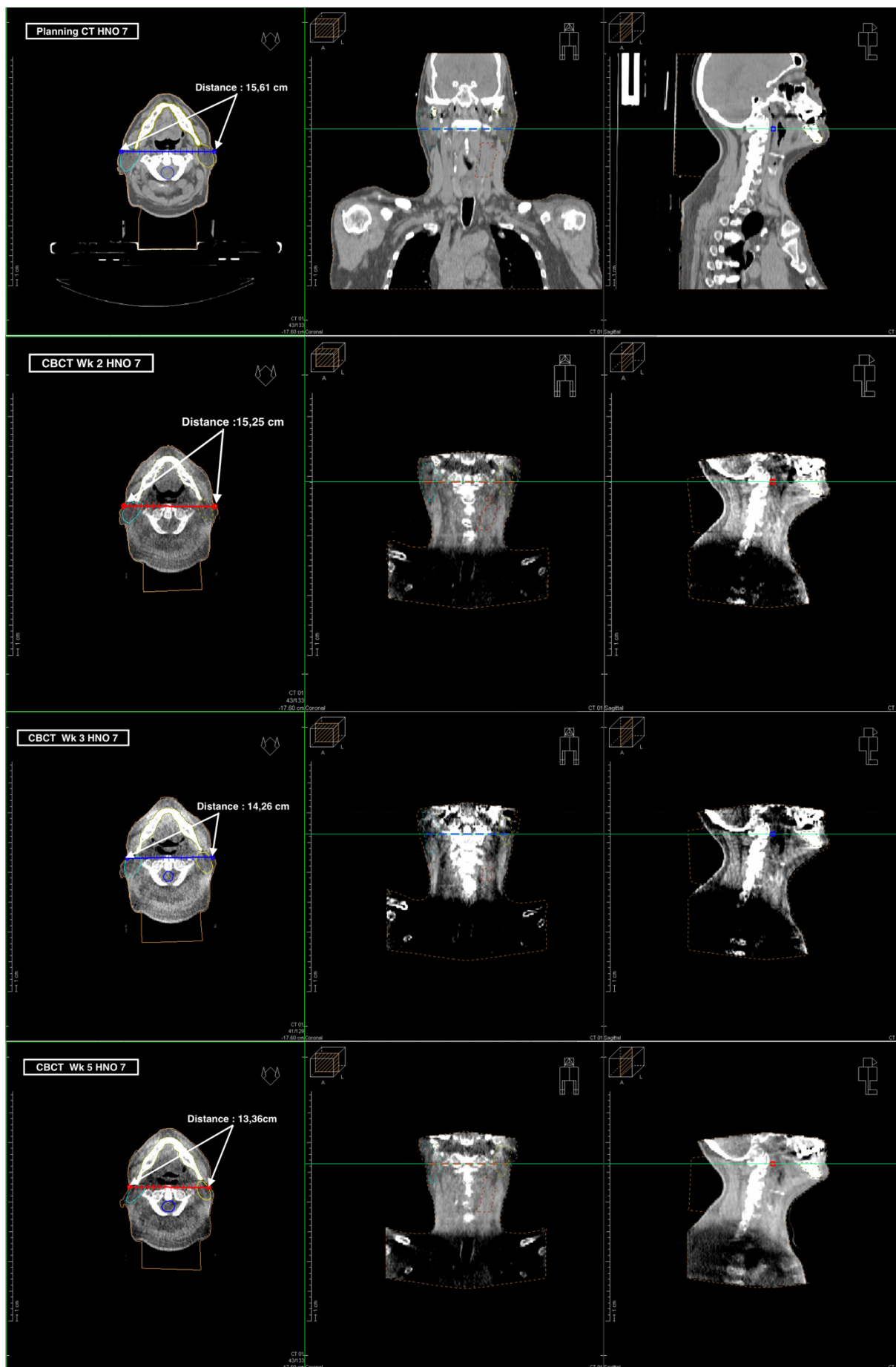


Figure 16: Weight loss during treatment in patient HNO 7

Figure 16 above shows axial, coronal and sagittal sections of the planning CT and CBCTs from week two, three and five in patient HNO 7. In order to assess weight loss in the region of the parotid glands, the skin-to-skin diameter at the level of the atlas was measured in the planning CT and the CBCTs. The diameter measured is shown in the axial sections of the planning CT and CBCTs. Weight loss in the temporal region at the level of the parotid glands was observed from week two to week five. The effect of weight loss in this region is shown in the next diagram.

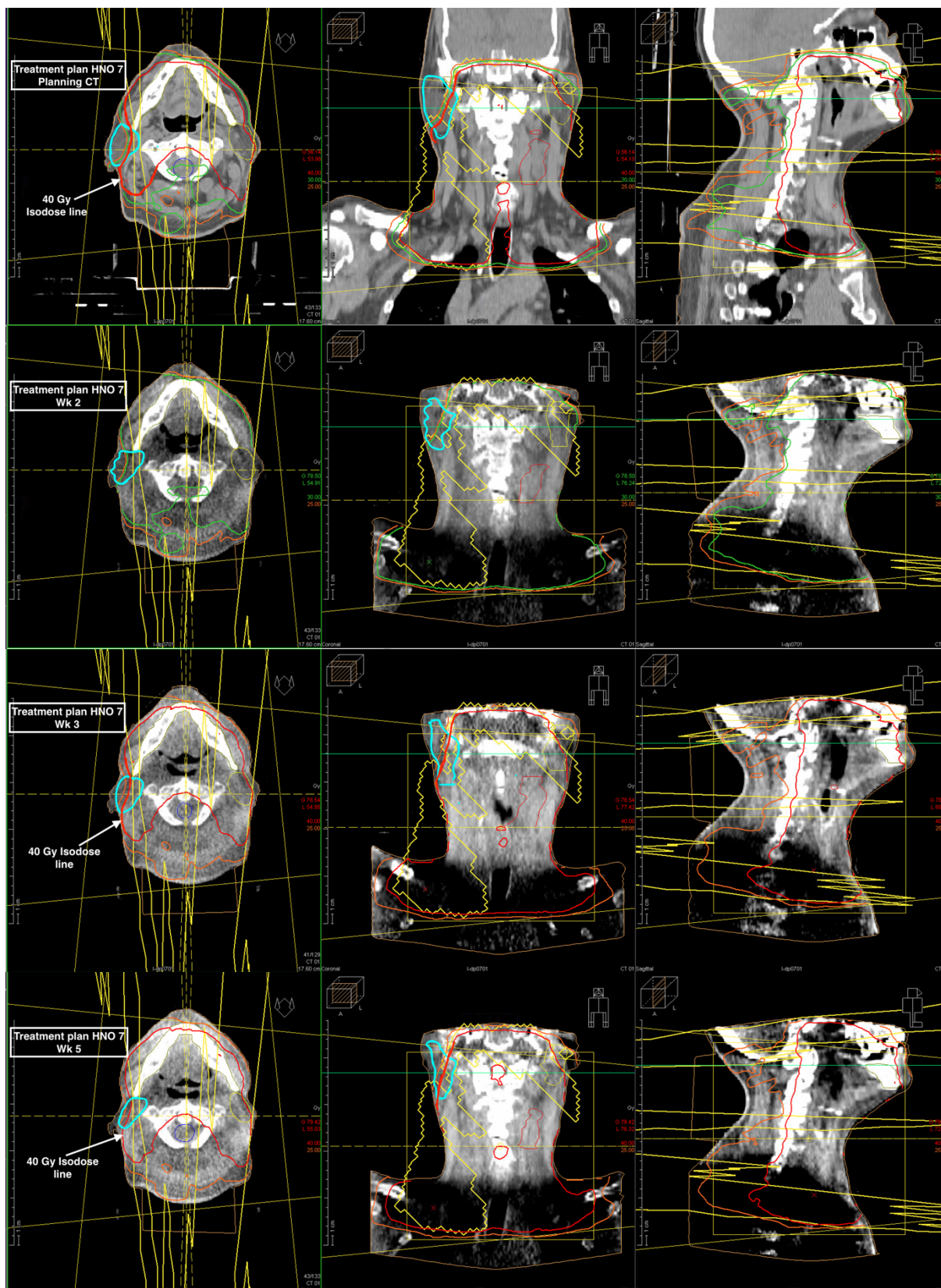


Figure 17: Medial shifting of the right parotid gland in patient HNO 7

Figure 17 above shows the axial, coronal and sagittal slices of the treatment plan in the original planning CT and CBCTs in patient HNO 7. The slices were taken at the level of the atlas vertebra. As already shown in [Table 15](#) above, the calculated D50% dose in the right parotid gland in the CBCTs from week three to week five was at least 40 Gy. The calculated D50% dose for the right parotid gland in the planning CT was 24,67 Gy. We therefore looked at the distribution pattern of the 40 Gy isodose line in the planning CT and the CBCTs in week two, three and five. The 40 Gy isodose line is shown in red in the axial, coronal and sagittal sections of the planning CT and the CBCTs. The right parotid gland is highlighted in the turquoise color in the axial and coronal sections of the planning CT and the CBCTs. Medial shifting of the right parotid gland due to weight loss can be observed in the CBCTs from week two to five. As a result, a larger volume of the right parotid gland is enclosed within the 40 Gy isodose line.

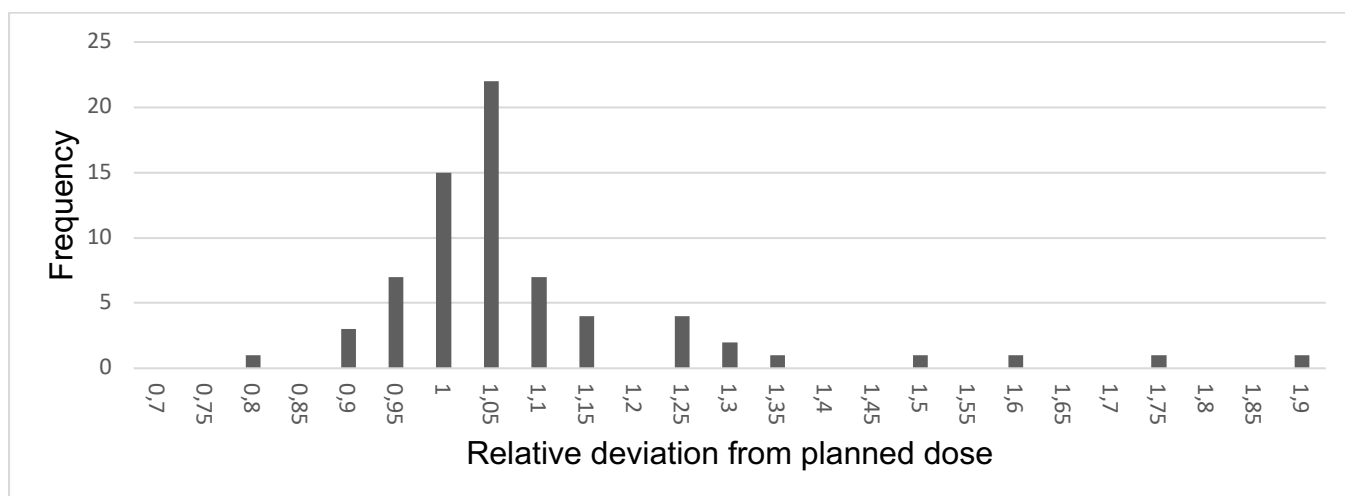
Left parotid gland

Figure 18: Frequency of daily differences from planned dose in D50% for left parotid gland

The histogram above shows the frequency of daily differences from the planned dose in D50% for the left parotid gland. The relative dose deviation from the planned dose is shown on the x-axis. The frequency of the relative deviations from the planned dose is shown on the y-axis. A total of seventy CBCTs were evaluated. No relative deviation from the planned dose was calculated in fifteen CBCTs (1,0). A relative deviation from the planned dose of 5% was calculated in the majority of the CBCTs with a total of twenty-two (1,05). Very relevant relative deviations of more than 20% were calculated in eleven CBCTs as shown in the following table.

Table 16: Very relevant relative deviations in D50% for left parotid gland

Deviations for D50% in the left parotid gland			
	Week	Calculated dose (Gy)	Relative deviation
HNO 8	Planning CT	17,10	
	1	20,68	1,21
	2	32,33	1,89
	3	29,22	1,71
	4	25,49	1,49
	5	26,64	1,56
HNO 12	Planning CT	14,11	
	3	17,10	1,21
	4	17,77	1,26
	5	18,45	1,31
HNO 13	Planning CT	17,58	
	1	21,46	1,22
	4	21,36	1,22
	5	22,46	1,28

Table 16 above shows the very relevant dose deviations in D50% for the left parotid gland calculated in patients HNO 8, HNO 12 and HNO 13. The first column shows the original planning CT and the week during treatment when the relative deviations were calculated in the CBCTs. The calculated doses are listed in the second column. Very relevant deviations were calculated weekly in patient HNO 8. The CBCTs during the five-week treatment period of patient HNO 8 were analyzed to get more clarity about the reason for the relevant dose deviations in D50% for the left parotid gland.

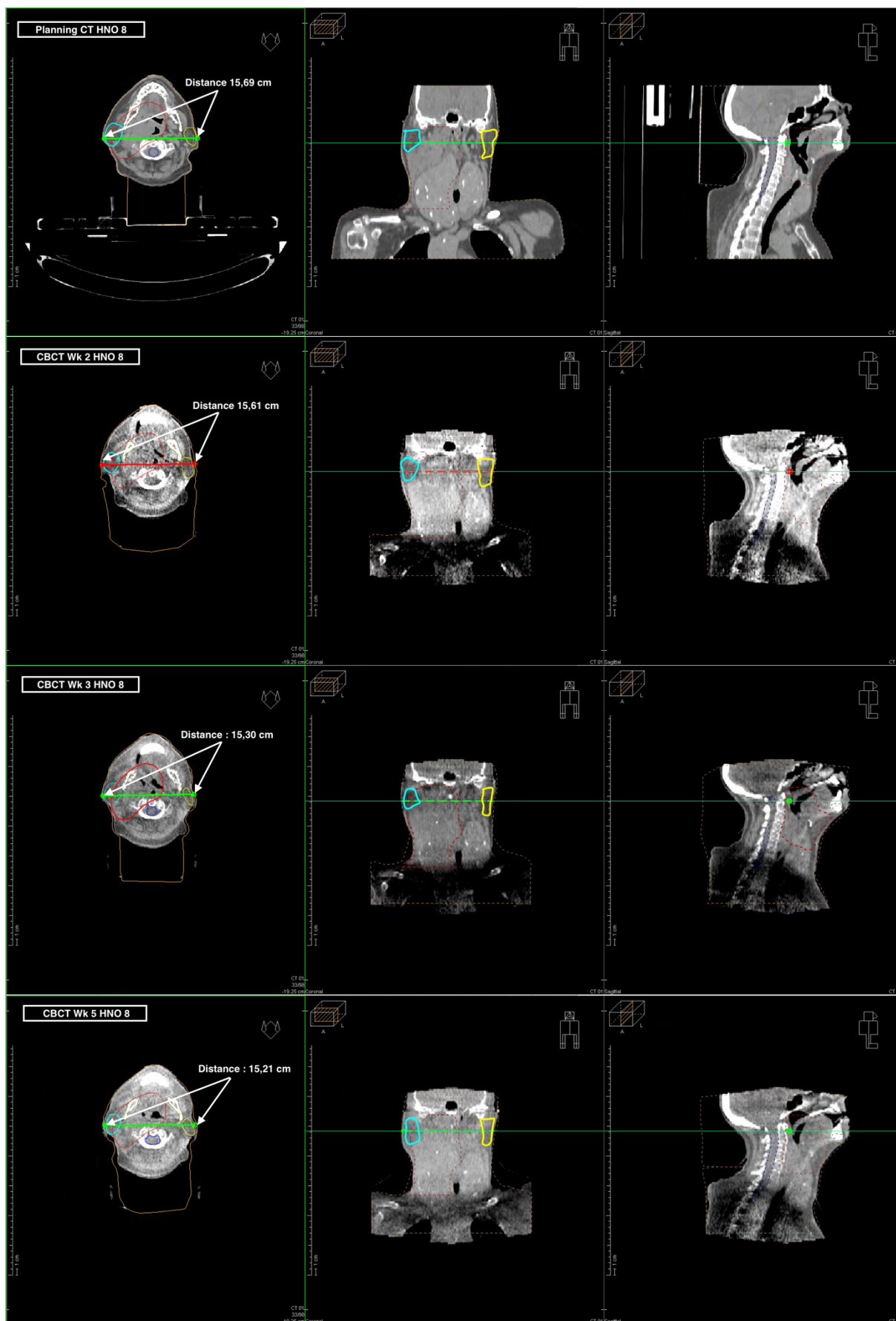


Figure 19: Weight loss during treatment in patient HNO 8

Figure 19 above shows axial, coronal and sagittal sections of the planning CT and CBCTs from week two, three and five in patient HNO 8. In order to assess weight loss in the region of the parotid glands, the skin-to-skin diameter at the level of the atlas was measured in the planning CT and the CBCTs. The diameter measured is shown in the axial sections of the planning CT and CBCTs. Weight loss in the temporal region at the level of the parotid glands was observed from week two to week five. The effect of weight loss in this region is shown in the next diagram.

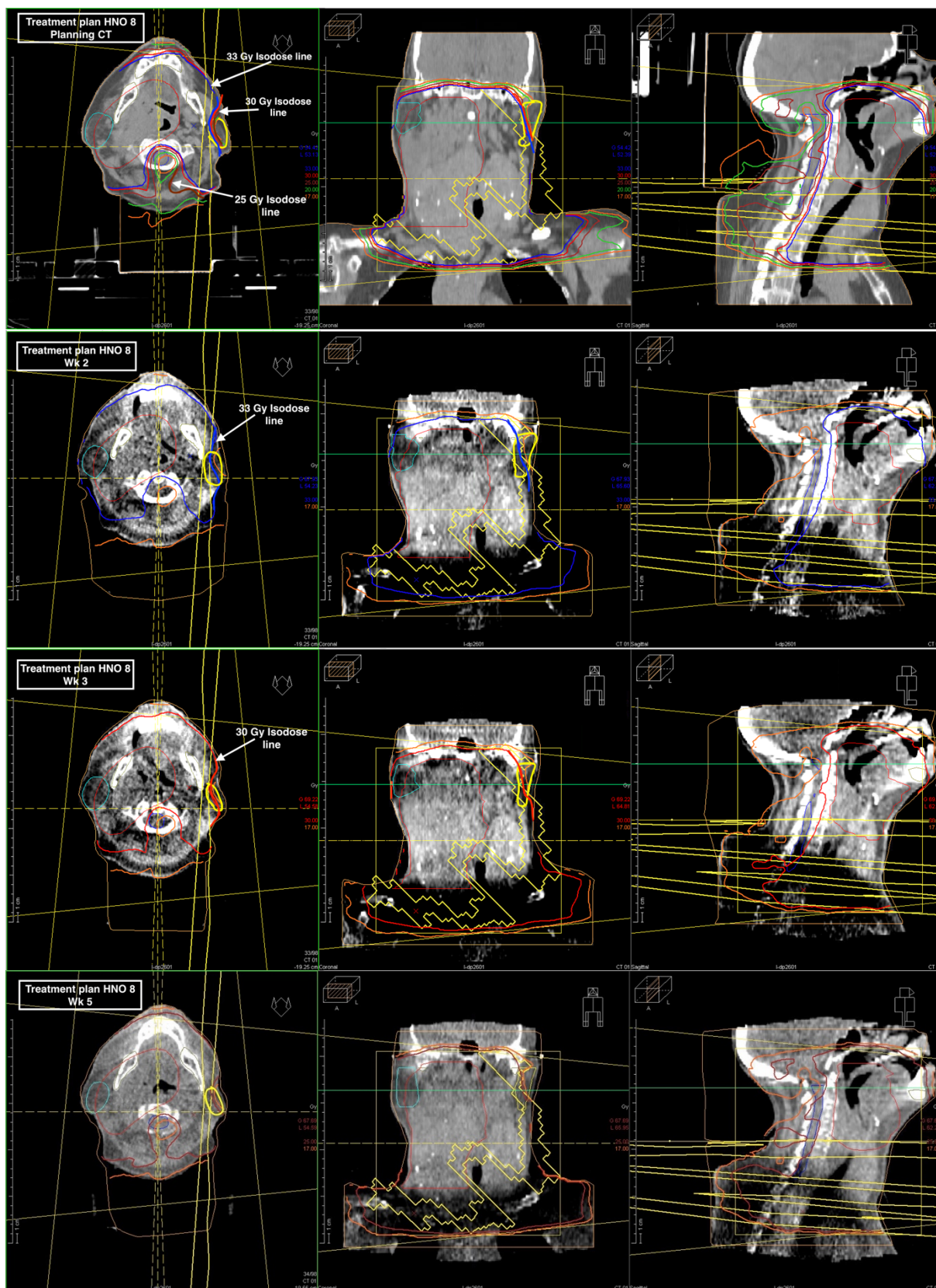


Figure 20: Medial shifting of the left parotid gland in patient HNO 8

Figure 20 above shows the axial, coronal and sagittal slices of the treatment plan in the original planning CT and CBCTs in patient HNO 8. The slices were taken at the level of the atlas vertebra. As shown in Table 16 above, the largest calculated dose deviations in the left parotid gland in the CBCTs in HNO 8 were from week two to week five. The calculated D50% dose for the left parotid gland in the planning CT was 17,10 Gy. We looked at the distribution pattern of the 25 Gy, 30 Gy and 33 Gy isodose lines in the planning CT and the CBCTs. The 25 Gy isodose line is labelled in the maroon color, the 30 Gy isodose line in the red color and the 33 Gy isodose line in the dark blue color. The left parotid gland is highlighted in the yellow color in the axial and coronal sections of the planning CT and the CBCTs. Medial shifting of the left parotid gland due to weight loss can be observed in the CBCTs from week two to five. As a result, a larger volume of the left parotid gland is enclosed in the 25 Gy, 30 Gy and 33 Gy isodose lines in comparison to the planning CT.

4.2.3 Dose deviation in the mandible

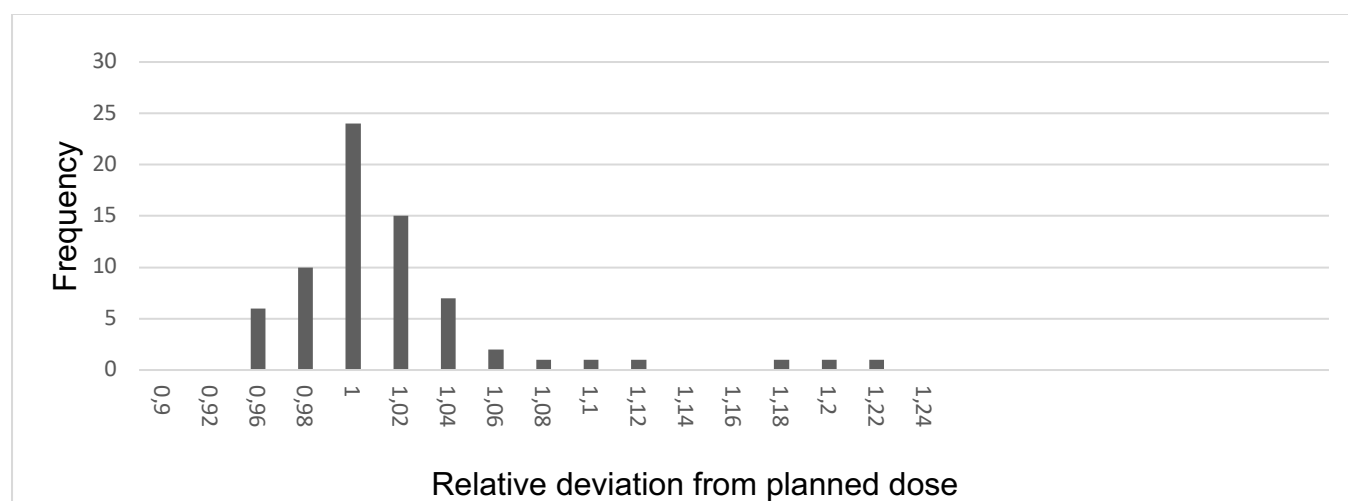


Figure 21: Frequency of daily differences from planned dose in D50% for the mandible

The histogram above shows the frequency of daily differences from the planned dose in D50% for the mandible. The relative dose deviation from the planned dose is shown on the x-axis. The frequency of the relative deviations from the planned dose is shown on the y-axis. A total of seventy CBCTs were evaluated. No relative deviation from the planned dose was calculated in twenty-four CBCTs (1,0). Very relevant relative deviations of more than 20% in D50% doses were calculated in four CBCTs. These very relevant relative deviations were calculated in patient HNO 3.

Table 17: Very relevant relative deviations in D50% for the mandible

Deviations for D50% in the mandible		
Week	Calculated dose (Gy)	Relative deviation
HNO 3	Planning CT	
	1	1,21
	2	1,19
	3	1,26
	4	1,25
	5	1,24

Table 17 above shows the relevant deviations calculated in D50% for the mandible in patient HNO 3. The first column shows the original Planning CT and the week during treatment when the deviations were calculated in the CBCTs. The calculated doses are listed in the second column. The CBCTs during the five-week treatment period of patient HNO 3 were analyzed to get more clarity about the reason for the relevant dose deviations in D50% for the mandible.

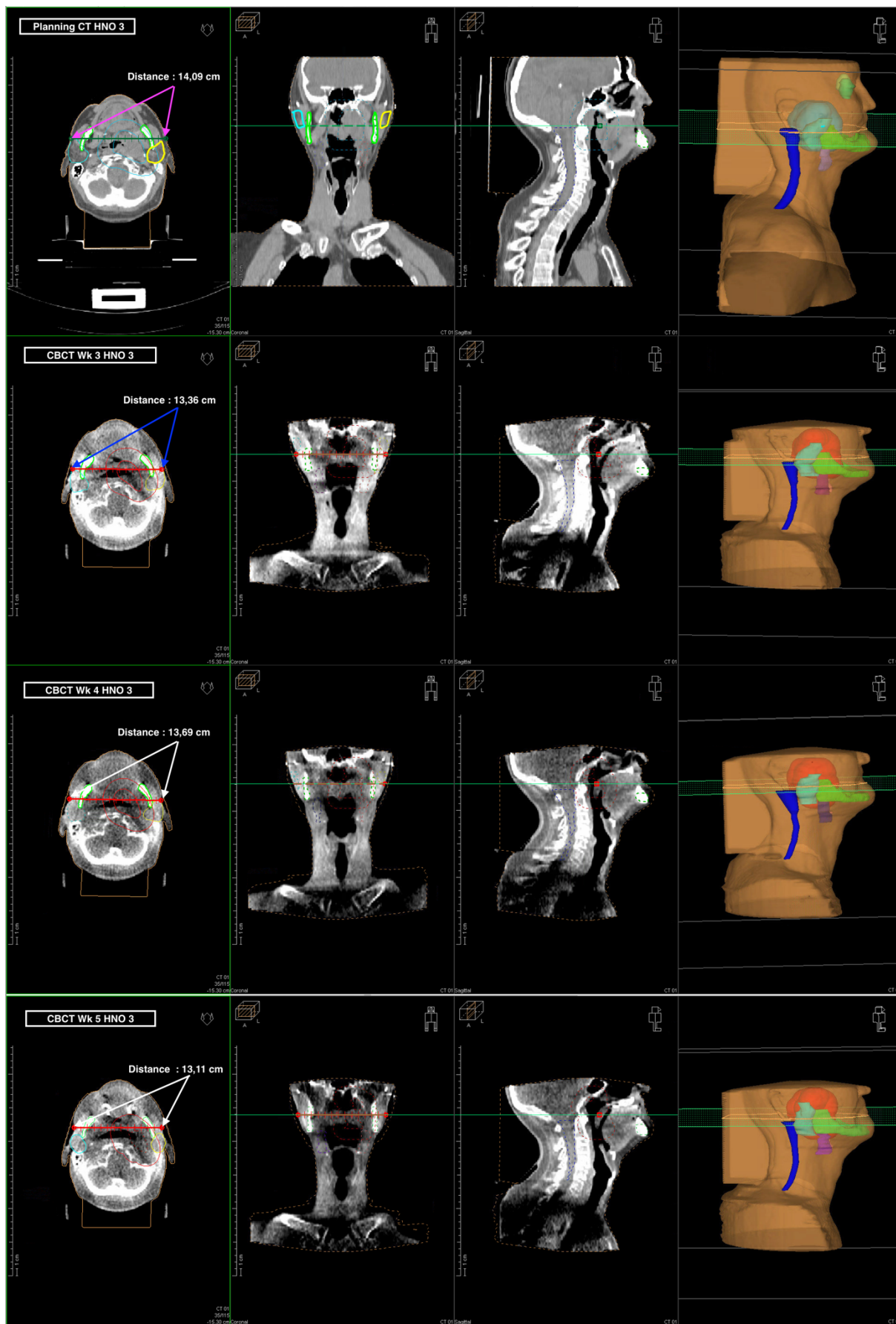


Figure 22: Weight loss during treatment in patient HNO 3

Figure 22 above shows axial, coronal, sagittal and three-dimensional sections of the planning CT and CBCTs from week three, four and five in patient HNO 3. In order to assess weight loss in the region of the mandible, the skin-to-skin diameter at the level of the base of the skull was measured in the planning CT and the CBCTs. The mandible was contoured in the light green color and can be seen in the axial, coronal and three-dimensional sections above. The diameter measured is shown in the axial sections of the planning CT and CBCTs. Weight loss in the region of the mandible was observed from week two to week five. The effect of weight loss in this region is shown in the next diagram.

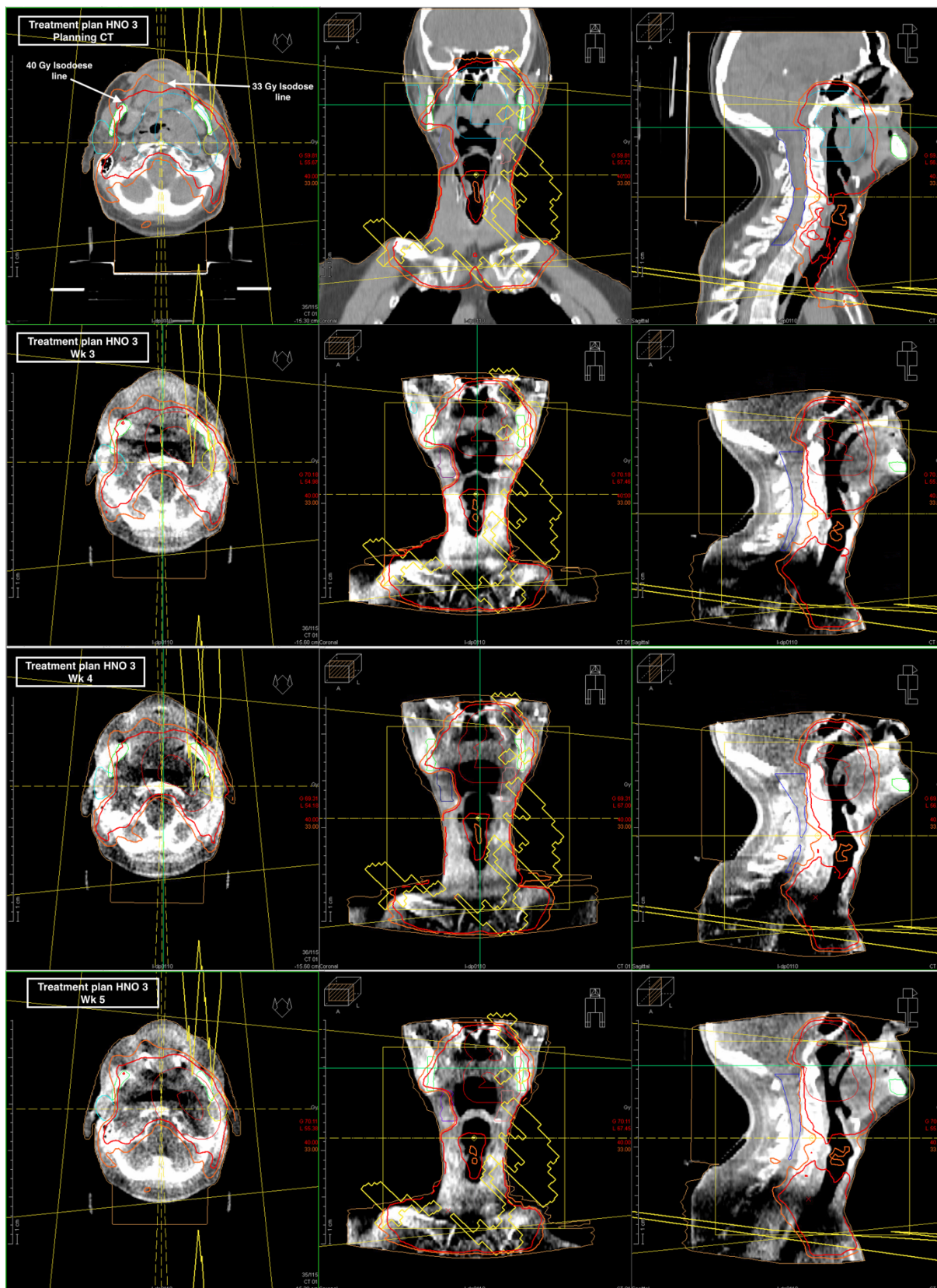


Figure 23: Treatment plan in planning CT and CBCTs in patient HNO 3

Figure 23 above shows the axial, coronal and sagittal slices of the treatment plan in the original planning CT and CBCTs in patient HNO 3. In the planning CT, the 40 Gy and 33 Gy isodose lines are labelled in red and orange respectively. Weight loss in the region of the mandible can be seen in the axial and coronal sections of the CBCTs from week three to five.

4.2.4 Dose deviation in the submandibular glands

Right submandibular gland

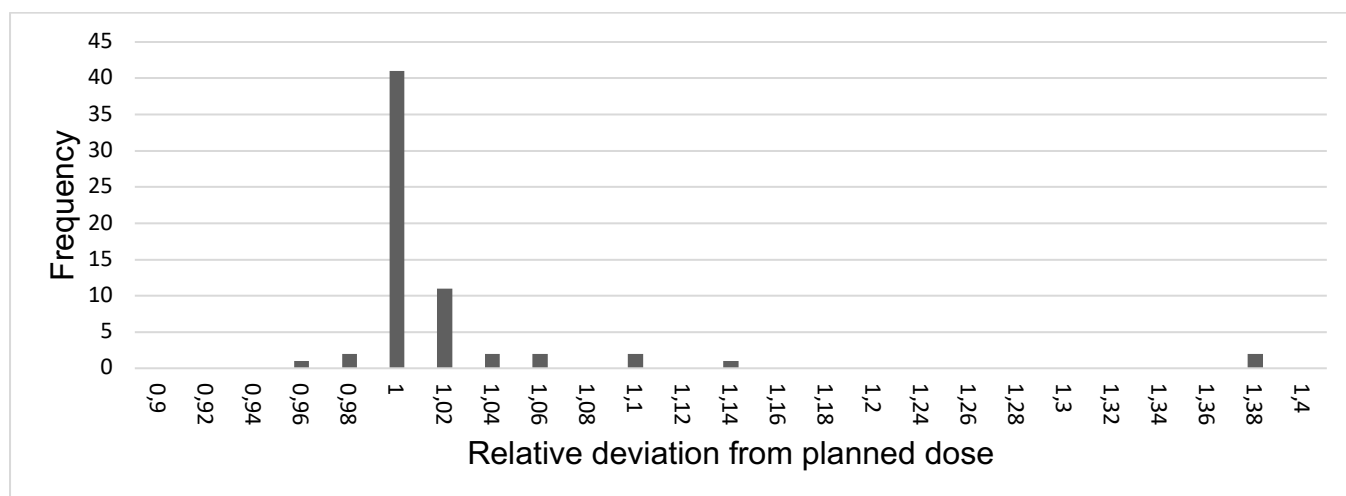


Figure 24: Frequency of daily differences from D50% planned dose in right submandibular gland

The histogram above shows the frequency of daily differences from the planned dose in D50% for the right submandibular gland. The relative dose deviation from the planned dose is shown on the x-axis. The frequency of the relative deviations from the planned dose is shown on the y-axis. A total of sixty-four CBCTs were evaluated. There was no relative dose deviation from the planned dose calculated in forty-one CBCTs (1,0). Relevant relative deviations of more than +10% were calculated in only three CBCTs. These relevant relative deviations were all calculated in patient HNO 3 as shown in the table below.

Table 18: Relevant relative deviations in D50% for the right submandibular gland

Deviations for D50% in the right submandibular gland			
	Week	Calculated dose (Gy)	Relative deviation
HNO 3	Planning CT	18,68	
	1	25,48	1,36
	2	21,16	1,13
	5	25,50	1,37

Table 18 above shows the relevant deviations in D50% for the right submandibular gland calculated in patient HNO 3. The CBCTs showing weight loss in patient HNO 3 were already shown in [Figure 22](#) in the previous subsection.

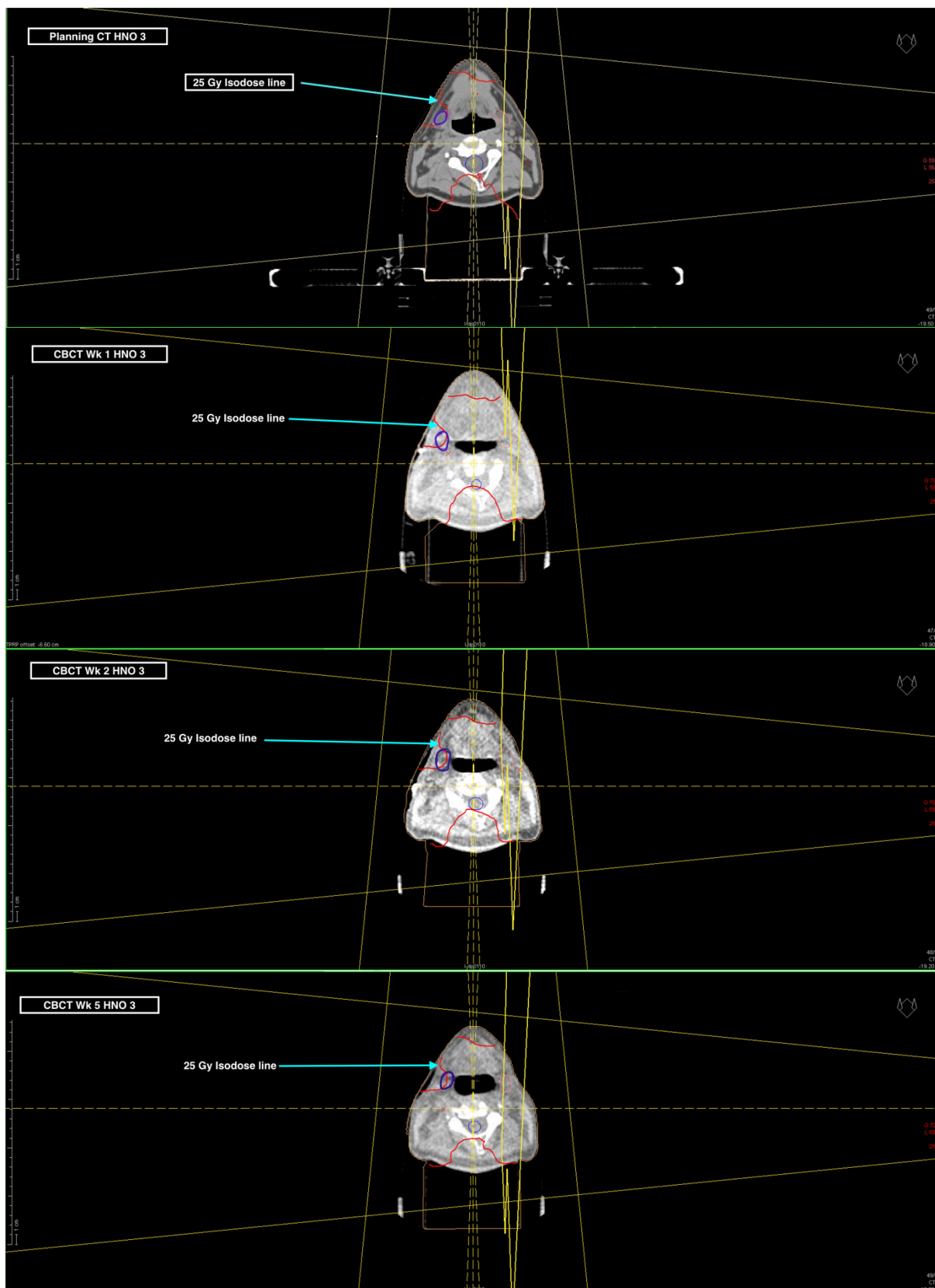


Figure 25: Treatment plan in planning CT and CBCTs in patient HNO 3

Figure 25 above shows the axial slices of the treatment plan in the original planning CT and CBCTs in patient HNO 3. The slices were taken at the level of the submandibular glands, the right submandibular gland is contoured in dark purple. As shown in Table 18 above, the largest calculated dose deviations in the right submandibular gland in the CBCTs were 25,48 Gy and 25,50 Gy in week two and five respectively. The calculated D50% dose for the right submandibular gland in the planning CT was 18,68 Gy. We looked at the distribution pattern of the 25 Gy isodose line (labelled in red) in the planning CT and the CBCTs in week one, two and five. Weight loss can be seen at the level of the submandibular glands, resulting in medial shifting towards the 25 isodose line. As a result, a larger volume of the right submandibular gland is enclosed within the 25 Gy isodose line in week one, two and five.

Left submandibular gland

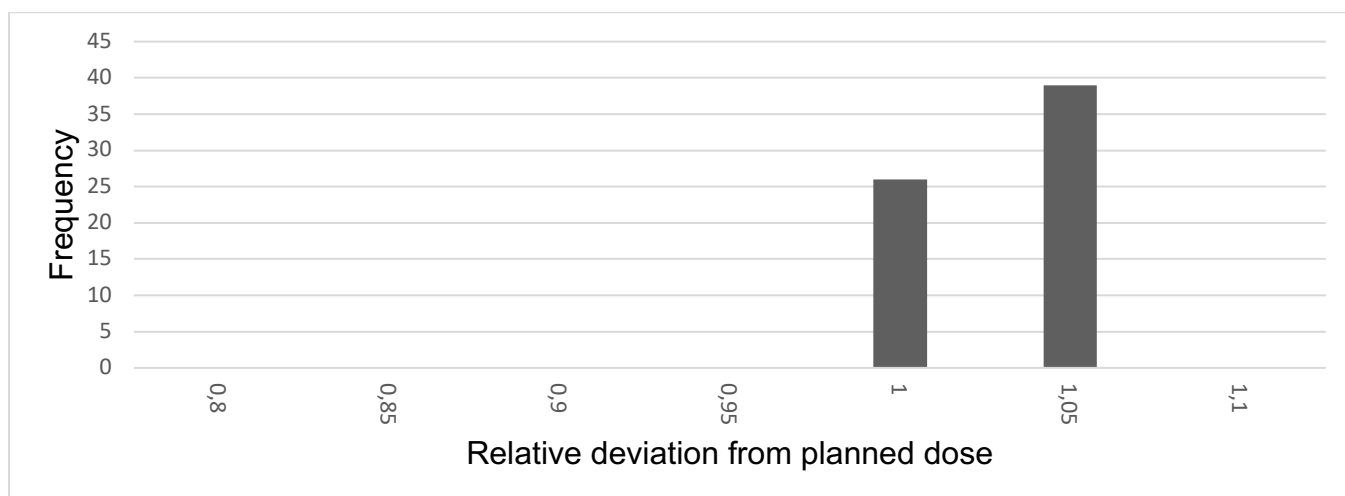


Figure 26: Frequency of daily differences from planned dose in D50% for the left submandibular gland

The histogram above shows the frequency of daily differences from planned dose in D50% for the left submandibular gland. The relative dose deviation from the planned dose is shown on the x-axis. The frequency of the relative deviations from the planned dose is shown on the y-axis. A total of sixty-five CBCTs were evaluated. In twenty-six CBCTs no relative dose deviation from the planned dose was calculated (1,0). In thirty-nine CBCTs, a relative dose deviation from the planned dose of +5% was calculated. No relevant dose deviation of more than 10% was calculated in D50% for the left submandibular gland.

4.2.5 Dose deviation in the gross tumor volume (GTV)

D50%

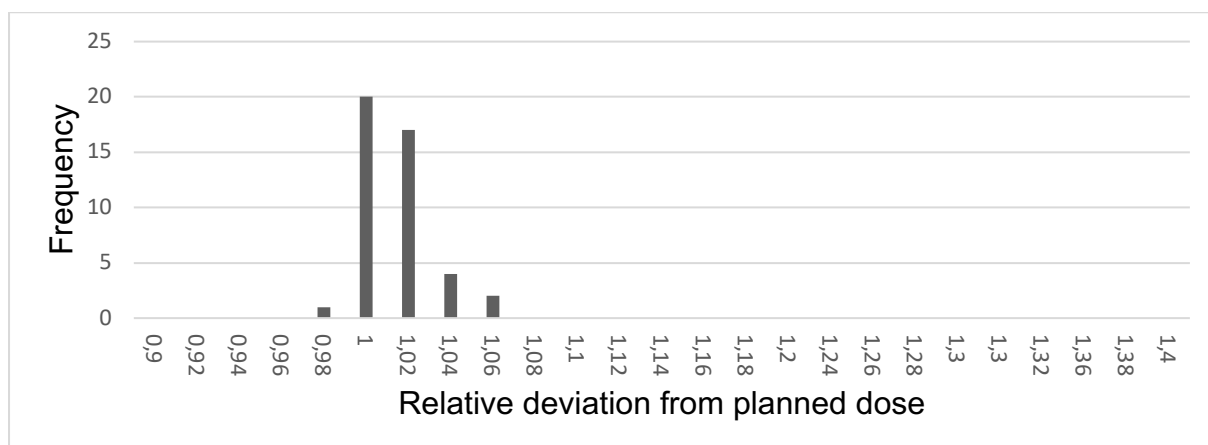


Figure 27: Frequency of daily differences from planned dose in D50% for GTV

Figure 27 above shows the frequency of daily differences from the planned dose in D50% for the GTV. The relative dose deviation from the planned dose is shown on the x-axis. The frequency of the relative deviations from the planned dose is shown on the y-axis. Forty-four CBCTs were evaluated. No dose deviation from the planned D50% dose in GTV was calculated in twenty CBCTs (1,0). A relative dose deviation of +2% from the planned dose was calculated in seventeen CBCTs. No relevant dose deviation of more than 10% was calculated in any of the CBCTs.

D95%

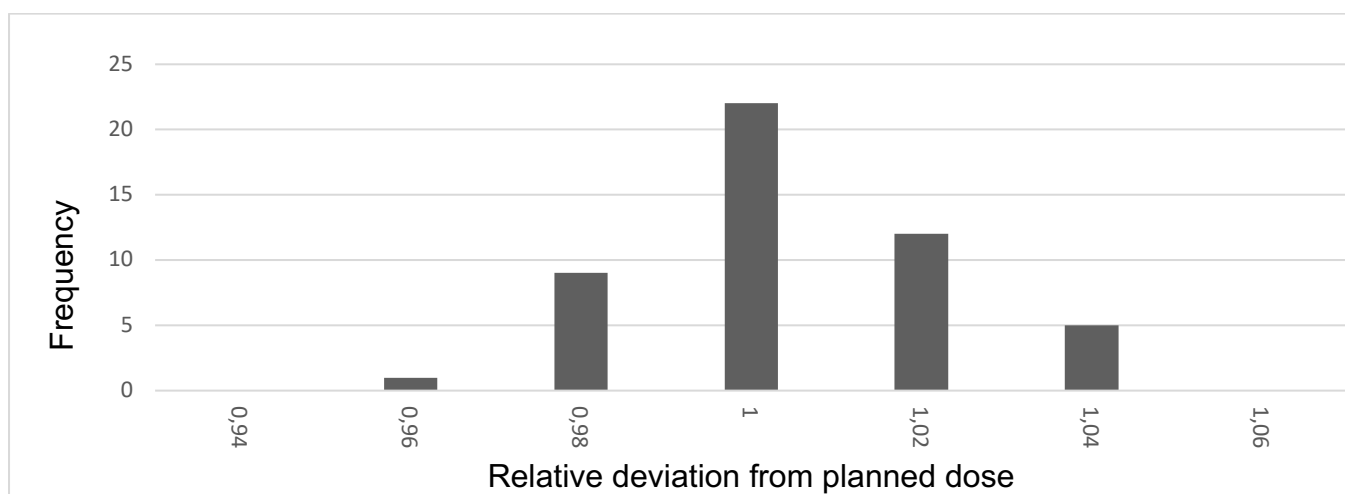


Figure 28: Frequency of daily differences from planned dose in D95% for GTV

The histogram above shows the frequency of daily differences from the planned dose in D95% for the GTV. The relative dose deviation from the planned dose is shown on

the x-axis. The frequency of the relative deviations from the planned dose is shown on the y-axis. A total of forty-nine CBCTs were evaluated. In the majority of the CBCTs (twenty-two), no relative dose deviation from the planned dose in GTV was calculated. In twenty-seven CBCTs a relative dose deviation from the planned dose of 4% or less was calculated. No relevant dose deviation of more than 10% was calculated in D95% for GTV.

4.2.6 Dose deviation in the clinical target volume (CTV)

D50%

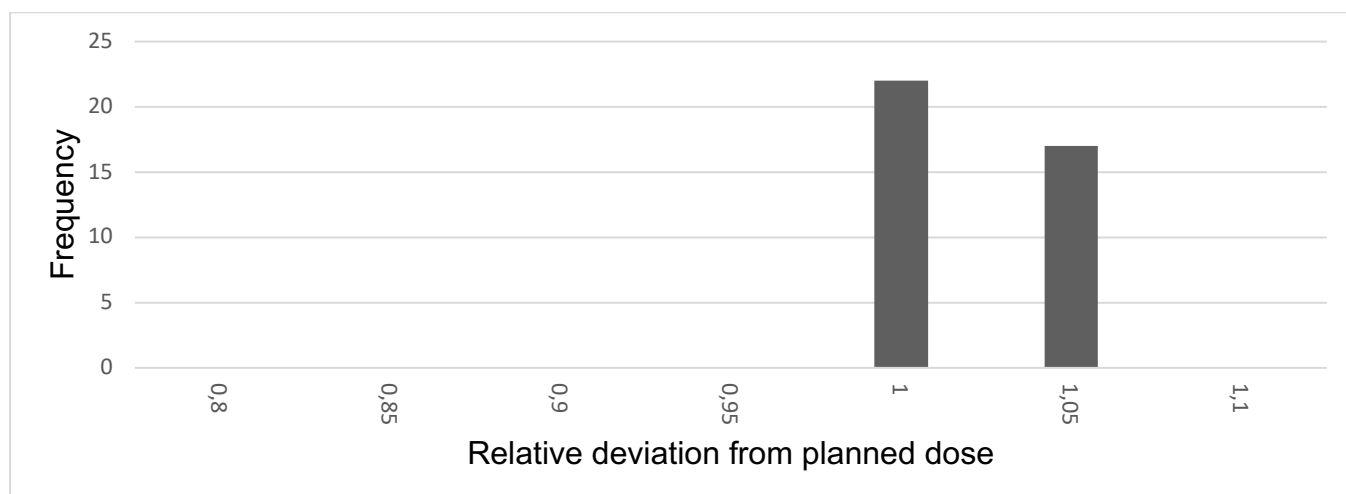


Figure 29: Frequency of daily differences from planned dose in D50% for CTV

The histogram above shows the frequency of daily differences from the planned dose in D50% for the CTV. The relative dose deviation from the planned dose is shown on the x-axis. The frequency of the relative deviations from the planned dose is shown on the y-axis. A total of thirty-nine CBCTs were evaluated. No relevant dose deviation of more than 10% was calculated in D50% for CTV.

D95%

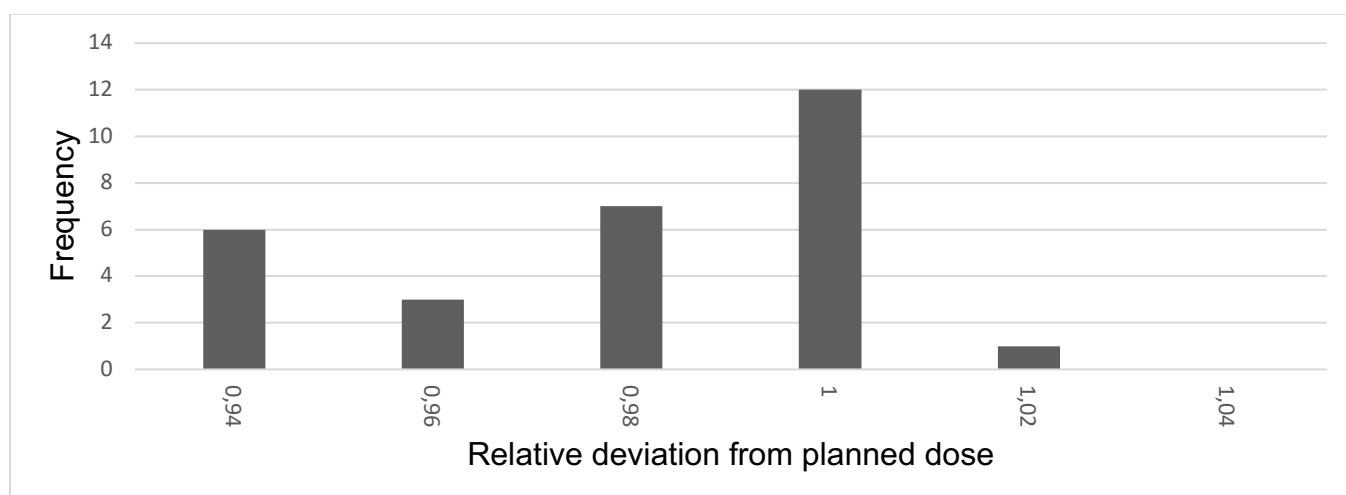


Figure 30: Frequency of daily differences from planned dose in D95% for CTV

Figure 30 above shows the frequency of daily differences from the planned dose in D95% for the CTV. The relative dose deviation from the planned dose is shown on

the x-axis. The frequency of the relative deviations from the planned dose is shown on the y-axis. A total of twenty-nine CBCTs were evaluated. In the majority of the CBCTs (twelve), no relative dose deviation from the planned dose in CTV was calculated. In six CBCTs an underdosage of -6% from the planned dose was calculated in CTV (0,94). This value was however not a relevant underdosage (<10%). In three CBCTs an underdosage of -4% was calculated and in seven patients 98% of the planned CTV dose was calculated (0,98). No relevant dose deviation of more than 10% was calculated in D95% for CTV.

4.3 *Summary of the results*

- The two most common acute side effects documented in our patients were mucositis and radiation dermatitis. None of our patients experienced grade IV mucositis or grade IV radiation dermatitis.
- The largest dose deviations in the CBCTs were calculated in the spinal cord and the parotid glands.
- The largest dose deviations calculated in the spinal cord and parotid glands were very relevant dose deviations of more than 20% in comparison to the planned dose in the planning CT.
- Patient HNO 12 had the largest relative dose deviations for D2% in the spinal cord. Very relevant dose deviations of more than 20% were calculated in all five CBCTs in patient HNO 12. No relevant anatomical changes occurred in the region where the largest D2% dose in the spinal cord was calculated in this patient.
- The largest dose deviations for D2% in the spinal cord in HNO 12 did not exceed the tolerance dose of 45 Gy (2). They were therefore clinically tolerable.
- Patient HNO 7 had the largest relative dose deviation for D50% in the right parotid gland. Temporal weight loss and medial shifting of the right parotid during treatment were seen in the CBCTs in patient HNO 7.
- No sparing of the right parotid was practiced in HNO 7 with a D50% dose of 24,67 Gy in the planning CT. Unilateral parotid gland sparing is practiced when one parotid gland receives less than 20 Gy (17). The D50% doses calculated in the CBCTs of HNO 7 were therefore clinically not relevant.
- Patient HNO 8 had the largest relative dose deviation for D50% in the left parotid gland. Temporal weight loss and medial shifting of the left parotid gland during treatment were seen in the CBCTs in patient HNO 8.
- Parotid gland sparing of the left parotid gland was practiced in HNO 8, with a D50% dose of 17,10 Gy calculated in the planning CT. The D50% doses for the left parotid gland in HNO 8 exceeded 20 Gy in all the CBCTs and were therefore clinically relevant.

- A clinically relevant dose increase in the left parotid gland was also seen in HNO 13 despite sparing of the left parotid gland (D50% dose exceeded 20 Gy in three CBCTs).
- Relevant relative dose deviations were calculated in the mandible and right submandibular gland in patient HNO 3. Weight loss was seen during treatment in the CBCTs in patient HNO 3.
- Non relevant dose deviations were calculated in the left submandibular gland, GTV and CTV. The relative dose deviations in these three structures were less than 6% in comparison to the planned dose in the planning CT.

5. Discussion

A detailed analysis of the acute side effects and relative dose deviations during the first five weeks of treatment of the patients in our study revealed valuable information. The most common acute side effect documented in our patients was oral mucositis, which was documented in ninety-three percent of our patients. These patients experienced grade I-III mucositis, with the majority of the patients having grade III mucositis (36 %). Grade IV mucositis was not documented in any of our patients. This finding correlated with that of a prospective study from Kucha et al.(5), which compared the acute toxicity between 3D-conformal radiotherapy and IMRT in patients with head and neck cancer. Seventy-eight patients were included in this study and divided equally for comparison. An assessment of the thirty-nine patients who received IMRT radiotherapy after seven weeks revealed that grade II-III mucositis was experienced by ninety-nine percent of the patients who received IMRT radiotherapy. There were also no patients in the IMRT group who experienced grade IV mucositis in this study (5). The second most common acute side effect in our study was radiation dermatitis, which was documented in sixty-four percent of our patients. The majority of these patients experienced grade I-II radiation dermatitis. Grade IV radiation dermatitis was not documented in any of our patients. This finding was also similar to the findings in the above mentioned prospective study, where eighty-five percent of the patients in the IMRT group experienced grade II radiation dermatitis and grade IV dermatitis was not documented (5).

The incidence of xerostomia after six weeks of radiotherapy in our patients was forty-three percent, similar to the incidence of xerostomia after seven weeks of radiotherapy in the prospective study mentioned above with thirty-eight percent (5). Other acute side effects documented in our study were dysgeusia, increased tracheal secretions and radiotherapy induced fatigue. In contrast, other acute side effects documented in the study from Kucha et al.(5) were dysphagia and weight loss more than ten percent. The difference in these findings is most likely due to the different methods of data collection in our retrospective study in comparison to the randomized prospective study. The data in our study was collected from patient

treatment records whereas the prospective study collected data during radiotherapy treatment and follow up appointments.

In five of the fourteen patients in our study, relevant dose deviations in D2% for the spinal cord were calculated in at least one of the weekly CBCTs. The largest dose deviations in D2% for the spinal cord were calculated weekly for five weeks in one patient. Very relevant dose deviations of more than twenty percent in comparison to D2% in the planning CT were calculated in this patient. No anatomical changes or weight loss was observed in the spinal cord region where the largest dose deviation was calculated in the CBCTs of this patient. In addition, the tolerance dose of 45 Gy for the spinal cord was not exceeded in all five patients in our study with relevant dose deviations of more than ten percent in D2% (2). This finding correlates with that of a prospective study from Noble et al.(3), where the effect of anatomical changes on the dose in the spinal cord was assessed in a cohort of one hundred and thirty-three patients with head and neck cancer. This study found no correlation between anatomical changes or weight loss and an increase in the D2% dose in the spinal cord. The D2% spinal cord dose in all the patients in this study also did not exceed the tolerance dose of 45 Gy. The authors therefore concluded that weight loss and anatomical changes did not mandate adaptive radiotherapy to protect the spinal cord from excessive radiation doses (3). Another retrospective study from Buciuman et al. (31) analyzed the treatment plans of thirteen patients who needed replanning during radiotherapy due to weight loss or anatomical changes. Although the study revealed a reduction in the final dose received to all organs at risk after replanning (including the spinal cord), the dose decrease obtained in the spinal cord was not statistically relevant (31).

Regarding the dose deviation in the parotid glands, four of the fourteen patients in our study had very relevant dose deviations in the D50% dose of more than twenty percent in one of the parotid glands. In the right parotid gland, the largest dose deviations were calculated in four of the five CBCTs performed weekly in one patient. In the left parotid gland, the largest dose deviations were calculated weekly in all five CBCTs in another patient. Weight loss in the region of the parotid glands was observed in the CBCTs during the five weeks of treatment of both these patients. An analysis of the radiotherapy plans in both patients revealed medial shifting of the

parotid glands and a reduction of the parotid gland volume during these five weeks of treatment.

Similar findings were documented in a prospective study from Wang et al.(32) involving forty-seven patients with nasopharynx cancer who got treated with IMRT radiotherapy. The study showed an increase in the parotid gland dose in the first fifteen fractions of treatment due to a decrease in size of the gross tumor volume in the nasopharynx during the same time period. Furthermore, this study documented a significant reduction in the volume of the parotid glands and their medial shifting into high-dose regions (32). A review of fifty-one studies aimed at identifying patients who might benefit from adaptive radiotherapy was done by Brouwer et al.(8). In their review, thirty-eight studies documented anatomical changes in the parotid glands. Similar to our findings, the most frequently documented anatomical changes in the parotid glands in these studies were volume loss and medial shifting. In the same literature review, twenty-four studies also documented an increase in the mean parotid gland dose (8).

Unilateral sparing of one of the parotid glands (D50% in the parotid gland less than 20 Gy in the planning CT) was practiced in three of the four patients in our study with very relevant D50% dose deviations (17). In two of these patients the D50% dose in the parotid glands exceeded 20 Gy during the five-week treatment period and was therefore clinically relevant. Although an increase in parotid gland dose was documented in the studies from Wang et al. (32) and Brouwer et al. (8), information pertaining to sparing of the parotid glands or clinical relevance of the dose increase was not given in these studies. The largest dose deviations in the parotid glands were calculated in patients with nasopharyngeal cancer in both studies. Nasopharynx cancer was therefore mentioned as a potential selection criterion for patients needing adaptive radiotherapy in these two studies (8,32). This finding did not correlate with the results in our study, where the largest dose deviations in D50% for the parotid glands were seen in patients treated with oropharyngeal cancer. The difference in these findings could be due to the different selection criterion used in our study in comparison to the other studies. Another possible explanation could be the different geographical locations where the studies were carried out. Our patients were randomly picked from a treatment register of patients who received radiotherapy due

to head and neck cancer during a three-year period. The majority of the patients in our study had oropharyngeal cancers, whose incidence is increasing in western Europe (33). In comparison, the literature review from Brouwer et al. (8) and the prospective study from Wang et al. (32) included many patients from Asia, where nasopharyngeal cancer is common.

The D50% dose variation in the mandible during the first five weeks of treatment was minimal. No relevant dose deviations in D50% for the mandible were calculated in thirteen of the fourteen patients in our study during radiotherapy. Only one patient showed very relevant dose deviations in D50% in the mandible, with more than twenty percent dose deviations calculated weekly during the first five weeks of treatment. An analysis of the weekly CBCTs performed in this patient revealed weight loss affecting the premolar region during treatment. Our findings correlated with the findings of a retrospective study from Sijtsema et al.(34), which assessed the relationship between the dose delivered in different regions of the mandible and the risk of the development of osteoradionecrosis in these regions of the mandible. The treatment records of two hundred and nineteen patients treated with oropharyngeal cancer from 2009 to 2016 were assessed with a follow up period of three years. The results of this study revealed that the incidence of osteoradionecrosis in these patients was highest in the pre-molar, molar and retro-molar regions of the mandible (34). This study however included only patients with oropharyngeal cancer whereas our patient with weekly relevant D50% doses in the mandible had nasopharyngeal cancer. In addition, the study from Sijtsema et al. (34) did not report on anatomical weight loss in the pre-molar region in their patients. According to the study, a possible explanation for the high incidence of osteoradionecrosis in the pre-molar and molar region was the high dose delivered to the tumor in the oropharynx (34). There are a few studies which have focused on the dose in the mandible during radiotherapy of patients with head and neck cancer. According to the existing literature, a mean dose of 40 to 50 Gy in the mandible is one of the predictors for the development of osteoradionecrosis in head and neck patients (35,36). In relation to this finding, the weekly calculated D50% dose in the mandible of approximately 40 Gy in our patient might be clinically relevant.

The analysis of the D50% dose in both submandibular glands in our patients also revealed stability of the dose in thirteen of the fourteen patients included. Three relevant dose deviations in D50% for the right submandibular gland were calculated in only one patient in our study. This was the same patient where relevant dose deviations in D50% for the mandible were calculated. As already mentioned in the previous paragraph, weight loss affecting the pre-molar region was observed in this patient. There were no relevant dose deviations in D50% for the left submandibular gland calculated in all fourteen patients included in our study. As stated in the second chapter of our study, the submandibular glands play an important role in the production of unstimulated saliva (saliva produced without food stimulation in the oral cavity). Radiation of the submandibular glands can therefore contribute to an increase in the incidence of xerostomia(17). In our patient, the calculated D50% doses in the right submandibular gland were 25,5 Gy, 21,4 Gy and 25,5 Gy in week one, two and five respectively. Although sparing of the parotid glands can be practiced using IMRT or VMAT radiotherapy techniques, sparing of the submandibular glands is challenging because they are included in the Ib (submandibular) lymph nodes and lie in close proximity to the II (deep cervical) lymph nodes(37). A prospective study from Murdoch-Kinsch et al. (38) aimed to assess the relationship between the dose delivered to the submandibular glands and the effect of radiation dose on their function. One hundred and forty-eight patients who received radiotherapy due to oropharyngeal, laryngeal, hypopharyngeal, oral cavity and nasopharyngeal cancer were included in the study. The salivary flow rates before, during and after radiotherapy were measured in the patients. This study reported that exceeding a threshold dose of 39 Gy resulted in a decrease in the production of stimulated and unstimulated saliva in the submandibular gland (38). Based on the report in this study, the three D50% dose deviations in the submandibular gland for our patient were not clinically relevant. However, this study did not mention whether anatomical weight loss was observed in the region of the submandibular glands.

The dose delivered in the gross tumor volume (GTV) remained stable during the first five weeks of treatment in all fourteen patients in our study. No relevant deviation of the D50% dose was calculated in our patients. Moreover, the calculated D95% dose in the GTV also remained stable in all our patients during the first five weeks of

treatment. An important finding in our study was that no relevant underdosage of more than ten percent was calculated for the GTV in any of our patients. There was also no relevant dose deviation calculated in the clinical target volume (CTV) for D50% and D95% during the first five weeks of treatment. The results from a prospective study from Beltran et al. (39) were however not in correlation with our findings. Sixteen patients were included in this study, seven of whom had oropharynx cancer and five oral cavity cancer. Three CTs were done in all the patients included: the original planning CT before initiating radiotherapy treatment, a second CT after fifteen fractions of radiotherapy and a third CT after twenty-five fractions of radiotherapy. The study reported significant loss of planning target volume (PTV) dose coverages in the parameters D95% and D98% during the treatment period. The authors of this study explained loss of PTV dose coverage as a result of anatomical changes during treatment (39).

The difference in findings between our study and that from Beltran et al. (39) is most likely due to two reasons. The first reason was that our study assessed either the dose stability in the GTV (non-operated patients) or the CTV (operated patients) whereas the study mentioned above assessed dose stability in the PTV. As already mentioned in the third chapter of our study, the GTV is defined as the visible tumor volume and the CTV is an extension of the visible tumor or tumor bed as a safety margin for potentially microscopic tumor cells around the GTV(30). Beltran et al. (39) assessed the dose distribution in the PTV, which is an extension of the CTV and takes into consideration the uncertainties in positioning of the patient as well as organ movement. Since the PTV covers a greater treatment volume, it is more likely to be affected by anatomical changes due to soft tissue swelling and weight loss in comparison to the GTV and CTV. The second reason was the difference in contouring techniques employed in the two studies. In our study, GTVs and/or CTVs were manually contoured in the five CBCTs for each patient. Anatomical changes in the tumor volume were therefore manually adjusted in the contouring of the CBCTs. This enabled a more accurate assessment of the dose stability in the GTV and/ or CTV despite anatomical changes. In contrast, the PTV from the original planning CT in the study from Beltran et al. (39) was copied on the two CTs performed at the fifteenth and twenty-fifth fractions. Modifications were only made when the PTV extended beyond the external contour or overlapped areas limited by bone. The dose

coverage in the PTV was therefore influenced significantly by anatomical changes in this study.

One of the limitations of our study was that the analysis of dose stability in the organs at risk and tumor region was only for the first twenty-five fractions of treatment. No analysis of dose stability was done for the last five to ten fractions of treatment, where the boost dose was applied in the tumor or tumor region. There is therefore need for future studies to assess dose stability during the whole treatment period. Another limitation in our study was that few patients were included in the study. The majority of the patients included in our analysis had oropharyngeal cancer and only one patient had nasopharynx cancer. Randomized studies which recruit more patients with different subtypes of head and cancer are required to identify subgroups needing adaptive radiotherapy. Lastly, a technical limitation in our study was that the weekly CBCTs carried out in our patients were limited in their lateral range of view. The shoulders of the patients were cut off in the CBCTs in comparison to the original planning CT, where both shoulders could be seen. Dose variation due to mispositioning of the shoulders in the CBCTs could therefore not be assessed.

5.1 Conclusion

Our clinical findings demonstrated a stability of the planned dose in the organs at risk during the first five weeks of treatment. Despite the occurrence of acute side effects, the most common being mucositis and radiation dermatitis, clinically relevant dose deviations in D50% in the parotid gland were calculated in only two patients. No life-threatening acute side effects were documented in the patients in our study. However, weight loss was observed in the CBCTs of some patients in our study, resulting in medial shifting and volume reduction of the parotid glands. Our study also revealed that the dose delivered to the tumor and tumor regions was not significantly affected by acute side effects or weight loss. The clinical implications of our findings include adequate nutritional support of patients receiving radiotherapy due to head and neck cancer to avoid weight loss. Implementing prophylactic medications to reduce potential acute side effects should also be investigated using randomized trials in the near future. Further studies are also needed in this field of medicine to identify patients who might benefit from adaptive radiotherapy. Our proposed method to estimate the dose stability and dose distribution by assessing the planning CT und

CBCTs of patients is therefore a helpful extension of the treatment process, especially regarding the possibility of necessary treatment replanning.

6. Summary

Our study analyzed the stability of the dose distribution in patients who received radiotherapy due to head and neck cancer retrospectively. Due to the increasing incidence of patients with head and neck cancer in western Europe, radiotherapy plays a key role as a treatment alternative to surgery in elderly and inoperable patients. One of the main challenges faced by the radiation oncologist during radiotherapy is the change in anatomy in the head and neck region due to soft tissue swelling or weight loss. Anatomical changes can impact the dose delivered in the tumor region as well as the organs at risk during the course of treatment. This may affect treatment outcome and quality of life negatively. The aim of our study was to verify the stability of the radiotherapy dose delivered in head and neck cancer patients during the first twenty-five fractions of treatment as well as analyze the factors which affect the dose stability.

Treatment records of fourteen patients were obtained from a treatment register of patients treated in the radiotherapy department due to head and neck cancer at Pius Hospital in Oldenburg during a three-year period from 2015 to 2017. For each patient, one CBCT scan was selected weekly for analysis during the twenty-five fractions, giving a total of five CBCTs for analysis per patient. The CBCTs were performed on alternate days of treatment for the purpose of controlling the patient's position regularly during radiotherapy. This treatment concept is called image guided radiotherapy (IGRT). In addition, the original planning CT performed before initiation of treatment was exported from our Oncentra MasterPlan 4.5 planning system for each patient. The original planning CT was used as the standard for comparison with the five CBCTs selected for each patient. All of the patients' data were anonymized for data protection. Before dose calculation could be performed in the selected CBCTs for comparison with the original planning CT, calibration of the CBCTs to Hounsfield units was performed. The calibration phantom used in our study was the Catphan 503 phantom (The Phantom Laboratory, USA). Prior to calculating the dose in the planning CTs as well as the CBCTs, the following organs at risk were contoured: parotid glands, spinal cord, submandibular glands and the mandible. The gross tumor volume (GTV) and clinical target volume (CTV) were also contoured in

the planning CT and in the CBCTs. The original treatment plan was then imported into the corresponding five calibrated CBCTs for each anonymized patient for dose calculation.

Mucositis and radiation dermatitis were the two most common acute side effects experienced by the patients in our study with incidences of ninety-three percent and sixty-four percent respectively. However, Grade IV mucositis and Grade IV radiation dermatitis were not documented in any of our patients. An analysis of the relative dose deviations for the organs at risk contoured in the CBCTs during the first five weeks of treatment revealed the largest dose deviations in the spinal cord and the parotid glands. Five of the fourteen patients in our study had relevant dose deviations in D2% for the spinal cord in at least one of the weekly CBCTs. No anatomical changes were associated with these relevant dose deviations. In addition, the tolerance dose of 45 Gy for the spinal cord was not exceeded in all the patients in our study. In the parotid glands, four of the fourteen patients in our study had very relevant dose deviations in the D50% dose. In two of these patients, the D50% dose in one of the parotid glands exceeded 20 Gy despite unilateral parotid gland sparing and was therefore clinically relevant. Temporal weight loss and medial shifting of the parotid glands was seen in the CBCTs of two patients with the largest dose deviations in D50%. The dose delivered in the submandibular glands, mandible, GTV and CTV was however stable in the first five weeks of treatment in all the patients.

The results of our study demonstrated a stability of the planned dose delivered in the tumor and tumor region in the first five weeks of treatment despite the occurrence of acute side effects. Our clinical findings also revealed adequate protection of the organs at risk during treatment, with clinically relevant dose deviations in D50% for the parotid glands being calculated in only two patients. Although no life-threatening acute side effects were documented in our study, close monitoring of patients to avoid excessive weight loss due to dysphagia is mandatory. In addition, further randomized studies recruiting more patients are needed in this field of medicine to identify patients who might benefit from adaptive radiotherapy. Our study therefore provided useful information to improve the quality of radiotherapy delivered and treatment outcomes for head and cancer patients in the future.

7. References

1. Johnson DE, Burtneß B, Leemans CR, Lui VWY, Bauman JE, Grandis JR. Head and neck squamous cell carcinoma. *Nat Rev Dis Primer*. 26. November 2020;6(1):1–22.
2. Belshaw L, Agnew CE, Irvine DM, Rooney KP, McGarry CK. Adaptive radiotherapy for head and neck cancer reduces the requirement for rescans during treatment due to spinal cord dose. *Radiat Oncol*. 1. November 2019;14(1):189.
3. Noble DJ, Yeap PL, Seah SYK, Harrison K, Shelley LEA, Romanchikova M, u. a. Anatomical change during radiotherapy for head and neck cancer, and its effect on delivered dose to the spinal cord. *Radiother Oncol*. 1. Januar 2019;130:32–8.
4. Jellema AP, Doornaert P, Slotman BJ, Rene Leemans C, Langendijk JA. Does radiation dose to the salivary glands and oral cavity predict patient-rated xerostomia and sticky saliva in head and neck cancer patients treated with curative radiotherapy? *Radiother Oncol*. 1. November 2005;77(2):164–71.
5. Kucha N, Soni TP, Jakhotia N, Patni N, Singh DK, Gupta AK, u. a. A prospective, comparative analysis of acute toxicity profile between three-dimensional conformal radiotherapy (3DCRT) and intensity-modulated radiotherapy (IMRT) in locally advanced head and neck cancer patients. *Cancer Treat Res Commun*. 1. Januar 2020;25:100223.
6. Figen M, Çolpan Öksüz D, Duman E, Prestwich R, Dyker K, Cardale K, u. a. Radiotherapy for Head and Neck Cancer: Evaluation of Triggered Adaptive Replanning in Routine Practice. *Front Oncol* [Internet]. 2020 [zitiert 3. März 2021];10. Verfügbar unter: <https://www.frontiersin.org/articles/10.3389/fonc.2020.579917/full>
7. Hu YC, Tsai KW, Lee CC, Peng NJ, Chien JC, Tseng HH, u. a. Which nasopharyngeal cancer patients need adaptive radiotherapy? *BMC Cancer*. 10. Dezember 2018;18:1234.
8. Brouwer CL, Steenbakkers RJHM, Langendijk JA, Sijtsema NM. Identifying patients who may benefit from adaptive radiotherapy: Does the literature on anatomic and dosimetric changes in head and neck organs at risk during radiotherapy provide information to help? *Radiother Oncol*. 1. Juni 2015;115(3):285–94.
9. Yom SS, Torres-Saavedra P, Caudell JJ, Waldron JN, Gillison ML, Xia P, u. a. Reduced-Dose Radiation Therapy for HPV-Associated Oropharyngeal Carcinoma (NRG Oncology HN002). *J Clin Oncol*. 20. März 2021;39(9):956–65.
10. Guo K, Xiao W, Chen X, Zhao Z, Lin Y, Chen G. Epidemiological Trends of Head and Neck Cancer: A Population-Based Study. *BioMed Res Int*. 14. Juli 2021;2021:e1738932.
11. Muallah D, Matschke J, Muallah S, Klimova A, Kroschwald LM, Schröder TA, u. a. Socioeconomic disparities between oral cavity cancer patients in Germany. *Front Public Health* [Internet]. 2022 [zitiert 17. Dezember 2022];10. Verfügbar unter: <https://www.frontiersin.org/articles/10.3389/fpubh.2022.831479>
12. Wang R, Kang M. Guidelines for radiotherapy of nasopharyngeal carcinoma. *Precis Radiat Oncol*. 2021;5(3):122–59.
13. Maghami E, Koyfman SA, Weiss J. Personalizing Postoperative Treatment of Head and Neck Cancers. *Am Soc Clin Oncol Educ Book*. 23. Mai 2018;(38):515–22.
14. Wolf Julie Ryan, Wazer E David. Radiation dermatitis - UpToDate [Internet]. 2022 [zitiert 7. Januar 2023]. Verfügbar unter: <https://www.uptodate.com/contents/radiation-dermatitis/print>
15. Bernier J, Bonner J, Vermorken JB, Bensadoun RJ, Dummer R, Giralt J, u. a.

Consensus guidelines for the management of radiation dermatitis and coexisting acne-like rash in patients receiving radiotherapy plus EGFR inhibitors for the treatment of squamous cell carcinoma of the head and neck. *Ann Oncol Off J Eur Soc Med Oncol*. Januar 2008;19(1):142–9.

16. Maria OM, Eliopoulos N, Muanza T. Radiation-Induced Oral Mucositis. *Front Oncol [Internet]*. 2017 [zitiert 10. Januar 2021];7. Verfügbar unter: <https://www.frontiersin.org/articles/10.3389/fonc.2017.00089/full>
17. Deasy JO, Moiseenko V, Marks L, Chao KSC, Nam J, Eisbruch A. Radiotherapy dose-volume effects on salivary gland function. *Int J Radiat Oncol Biol Phys*. 1. März 2010;76(3 Suppl):S58-63.
18. Iorgulescu G. Saliva between normal and pathological. Important factors in determining systemic and oral health. *J Med Life*. 2009;2(3):303–7.
19. Deshpande TS, Blanchard P, Wang L, Foote RL, Zhang X, Frank SJ. Radiation-Related Alterations of Taste Function in Patients With Head and Neck Cancer: a Systematic Review. *Curr Treat Options Oncol*. 2018;19(12):72.
20. Gunn L, Gilbert J, Nenclares P, Soliman H, Newbold K, Bhide S, u. a. Taste dysfunction following radiotherapy to the head and neck: A systematic review. *Radiother Oncol*. 1. April 2021;157:130–40.
21. Gulliford SL, Miah AB, Brennan S, McQuaid D, Clark CH, Partridge M, u. a. Dosimetric explanations of fatigue in head and neck radiotherapy: An analysis from the PARSPORT Phase III trial. *Radiother Oncol*. 1. August 2012;104(2):205–12.
22. Das S, Lahiri D, Mandal S, Biswas P. Weight loss during radiation therapy in patients of head & neck (H&N) cancer. *Ann Oncol*. 1. November 2018;29:ix96.
23. Cheng HCY, Wu VWC, Ngan RKC, Tang KW, Chan CCL, Wong KH, u. a. A prospective study on volumetric and dosimetric changes during intensity-modulated radiotherapy for nasopharyngeal carcinoma patients. *Radiother Oncol*. 1. September 2012;104(3):317–23.
24. Veresezan O, Troussier I, Lacout A, Kreps S, Maillard S, Toulemonde A, u. a. Adaptive radiation therapy in head and neck cancer for clinical practice: state of the art and practical challenges. *Jpn J Radiol*. 1. Oktober 2016;35:1–10.
25. Huang YM, Lee JC, Chu CM, Tai HC, Hou TC, Chen FYS, u. a. Three-Dimensional Printed Silicone Bite Blocks for Radiotherapy of Head and Neck Cancer—A Preliminary Study. *Appl Sci*. Januar 2020;10(5):1688.
26. Lee J, Ramadan S, Kim A, Alayed Y, Ravi A. Dosimetric impact of tracheostomy devices in head and neck cancer patients. *J Appl Clin Med Phys*. 6. Mai 2020;21(6):26–32.
27. Majumder D, Patra NB, Chatterjee D, Mallick SK, Kabasi AK, Majumder A. Prescribed dose versus calculated dose of spinal cord in standard head and neck irradiation assessed by 3-D plan. *South Asian J Cancer*. 2014;3(1):22–7.
28. Annkah JK, Rosenberg I, Hindocha N, Moinuddin SA, Ricketts K, Adeyemi A, u. a. Assessment of the dosimetric accuracies of CATPhan 504 and CIRS 062 using kV-CBCT for performing direct calculations. *J Med Phys Assoc Med Phys India*. 2014;39(3):133–41.
29. Nancy Y. Lee NR Jiade J Lu,. *Target Volume Delineation for Conformal and Intensity-Modulated Radiation Therapy*. 2015. Aufl. Springer;
30. Burnet NG, Thomas SJ, Burton KE, Jefferies SJ. Defining the tumour and target volumes for radiotherapy. *Cancer Imaging*. 21. Oktober 2004;4(2):153–61.
31. Buciuman N, Marcu LG. Adaptive Radiotherapy in Head and Neck Cancer Using Volumetric Modulated Arc Therapy. *J Pers Med*. 21. April 2022;12(5):668.
32. Wang W, Yang H, Mi Y, Hu W, Ding W, Xie Y, u. a. Rules of parotid gland dose variations and shift during intensity modulated radiation therapy for

- nasopharyngeal carcinoma. *Radiat Oncol*. 8. Januar 2015;10(1):3.
33. Boelke E, Gössler B, Tamaskovic B, Budach W, Matuschek C. EP-1063: Epidemiology and clinical outcome of HPV in different head and neck cancer a subgroup analysis. *Radiother Oncol*. 1. Mai 2017;123:S584–5.
34. Sijtsema ND, Verduijn GM, Nasserinejad K, Norden Y van, Mast H, Lugt A van der, u. a. Development of a local dose-response relationship for osteoradionecrosis within the mandible. *Radiother Oncol* [Internet]. 1. September 2023 [zitiert 30. September 2023];186. Verfügbar unter: [https://www.thegreenjournal.com/article/S0167-8140\(23\)00274-8/fulltext](https://www.thegreenjournal.com/article/S0167-8140(23)00274-8/fulltext)
35. Jereczek-Fossa BA, Garibaldi C, Catalano G, d'Onofrio A, Pas TD, Bocci C, u. a. Analysis of mandibular dose distribution in radiotherapy for oropharyngeal cancer: dosimetric and clinical results in 18 patients. *Radiother Oncol*. 1. Januar 2003;66(1):49–56.
36. Topkan E, Kucuk A, Somay E, Yilmaz B, Pehlivan B, Selek U. Review of Osteoradionecrosis of the Jaw: Radiotherapy Modality, Technique, and Dose as Risk Factors. *J Clin Med*. Januar 2023;12(8):3025.
37. Saarihahti K, Kouri M, Collan J, Kangasmäki A, Atula T, Joensuu H, u. a. Sparing of the submandibular glands by intensity modulated radiotherapy in the treatment of head and neck cancer. *Radiother Oncol J Eur Soc Ther Radiol Oncol*. März 2006;78(3):270–5.
38. Murdoch-Kinch CA, Kim HM, Vineberg KA, Ship JA, Eisbruch A. Dose-Effect Relationships for the Submandibular Salivary Glands and Implications for Their Sparing by Intensity Modulated Radiotherapy. *Int J Radiat Oncol Biol Phys*. 1. Oktober 2008;72(2):373–82.
39. Beltran M, Ramos M, Rovira JJ, Perez-Hoyos S, Sancho M, Puertas E, u. a. Dose variations in tumor volumes and organs at risk during IMRT for head-and-neck cancer. *J Appl Clin Med Phys*. November 2012;13(6):101–11.

Appendix

Table 19: Dose values for D50% in HNO 2

Week of Examination	Spinal Cord	Parotis Rt	Parotis Lt	Mandible	Tumor (GTV)	Submandible GI Rt	Submandible GI Lt
Planning CT	30,76	46,72	51,73	50,88	52,07	51,28	51,59
Wk 1	33,28	50,42	55,68	53,23	54,28	53,13	53,27
Wk 2	33,72	48,99	51,21	50,65	54,60	52,58	52,00
Wk 3	31,82	50,51	52,53	50,56	53,13	51,77	51,95
Wk 4	30,09	50,00	51,25	50,90	51,97	51,30	51,97
Wk 5	30,54	51,47	51,27	50,88	52,24	52,02	51,84

Table 20: Dose values for D2% in HNO 2

Week of Examination	Spinal Cord
Planning CT	30,76
Wk 1	33,28
Wk 2	33,72
Wk 3	31,82
Wk 4	30,09
Wk 5	30,54

Table 21: Dose values for D95% in HNO 2

Week of Examination	Tumor (GTV)
Planning CT	46,85
Wk 1	48,52
Wk 2	46,37
Wk 3	46,61
Wk 4	45,94
Wk 5	45,79

Table 22: Dose values for D50% in HNO 3

Week of Examination	Spinal Cord	Parotis Rt	Parotis Lt	Mandible	Tumor (GTV)	Tumor (CTV)	Submandible GI Rt	Submandible GI Lt
Planning CT	25,90	15,37	47,45	32,35	50,35	49,61	18,68	50,37
Wk 1	27,35	16,36	47,61	39,02	51,18	49,80	25,48	50,78
Wk 2	26,37	20,66	47,18	38,52	51,34	50,06	21,16	50,10
Wk 3	26,04	19,57	46,06	37,89	51,54	50,17	20,28	49,79
Wk 4	25,33	17,06	48,36	36,06	51,46	50,56	18,48	50,52
Wk 5	27,04	20,67	46,92	35,47	51,55	50,17	25,50	50,11

Table 23: Dose values for D2% in HNO 3

Week of Examination	Spinal Cord
Planning CT	33,26
Wk 1	32,77
Wk 2	35,43
Wk 3	33,17
Wk 4	33,77
Wk 5	33,18

Table 24: Dose values for D95% in HNO 3

Week of Examination	Tumor (GTV)
Planning CT	47,18
Wk 1	48,17
Wk 2	48,01
Wk 3	48,37
Wk 4	48,52
Wk 5	48,95

Table 25: Dose values for D50% in HNO 4

Week of Examination	Spinal Cord	Parotid Rt	Parotid Lt	Mandible	Tumor (GTV)	Tumor (CTV)	Submandible GI Rt	Submandible GI Lt
Planning CT	25,72	20,53	50,04	46,97	50,85	50,24	48,36	49,27
Wk 1	25,73	19,93	50,80	46,22	49,86	49,65	47,72	49,47
Wk 2	26,34	18,61	51,44	44,85	50,48	50,31	47,53	50,31
Wk 3	25,90	22,47	50,83	45,38	49,75	49,11	47,75	49,37
Wk 4	27,30	27,60	51,44	45,00	50,31	49,54	47,77	49,90
Wk 5	24,81	25,62	51,08	46,18	50,00	50,12	47,85	50,34

Table 26: Dose values for D2% in HNO 4

Week of Examination	Spinal Cord
Planning CT	32,22
Wk 1	29,58
Wk 2	33,03
Wk 3	30,46
Wk 4	34,47
Wk 5	30,56

Table 27: Dose values for D95% in HNO 4

Week of Examination	Tumorbed (CTV)
Planning CT	48,88
Wk 1	48,10
Wk 2	48,49
Wk 3	47,73
Wk 4	48,68
Wk 5	48,22

Table 28: Dose values for D50% in HNO 5

Week of Examination	Spinal Cord	Parotis Rt	Parotis Lt	Mandible	Tumor (GTV)	Submandible GI Rt	Submandible GI Lt
Planning CT	30,43	49,88	50,32	49,50	49,97	50,07	49,79
Wk 1	31,42	49,53	50,65	48,55	49,58	49,39	49,83
Wk 2	31,15	49,70	50,62	48,18	49,18	48,88	49,61
Wk 3	30,31	50,04	49,86	48,21	49,35	49,21	49,13
Wk 4	31,65	49,80	50,55	48,68	49,53	49,31	49,74
Wk 5	31,09	49,62	50,62	48,53	49,30	49,39	49,33

Table 29: Dose values for D2% in HNO5

Week of Examination	Spinal Cord
Planning CT	34,95
Wk 1	36,59
Wk 2	36,86
Wk 3	35,34
Wk 4	36,37
Wk 5	35,45

Table 30: Dose values for D95% in HNO 5

Week of Examination	Tumor (GTV)
Planning CT	48,67
Wk 1	48,03
Wk 2	47,63
Wk 3	47,75
Wk 4	47,98
Wk 5	47,73

Table 31: Dose values for D50% in HNO 6

Week of Examination	Spinal Cord	Parotis Rt	Parotis Lt	Mandible	Tumor (GTV)
Planning CT	29,39	28,45	37,16	46,01	49,97
Wk 1	29,21	31,35	39,77	47,13	49,74
Wk 2	29,89	30,17	35,89	46,75	49,46
Wk 3	31,41	34,70	42,65	46,44	49,89
Wk 4	29,86	40,69	41,15	44,63	50,20
Wk 5	29,77	26,46	37,58	45,22	50,30

Table 32: Dose values for D2% in HNO 6

Week of Examination	Spinal Cord
Planning CT	33,32
Wk 1	32,98
Wk 2	33,60
Wk 3	36,48
Wk 4	33,69
Wk 5	33,83

Table 33: Dose values for D95% in HNO 6

Week of Examination	Tumor (GTV)
Planning CT	47,98
Wk 1	47,55
Wk 2	47,29
Wk 3	47,74
Wk 4	48,12
Wk 5	48,06

Table 34: Dose values for D50% in HNO 7

Week of Examination	Spinal Cord	Parotis Rt	Parotis Lt	Mandible	Tumor (GTV)	Submandible GI Rt	Submandible GI Lt
Planning CT	28,52	24,67	44,85	46,88	49,55	49,74	48,83
Wk 1	27,69	25,46	44,43	46,54	49,08	49,25	48,74
Wk 2	27,09	30,00	44,61	46,89	49,34	49,56	49,33
Wk 3	28,88	40,64	45,05	46,67	49,50	49,76	49,41
Wk 4	29,00	40,59	45,71	46,38	49,53	49,66	49,80
Wk 5	28,88	40,15	45,94	46,68	49,73	49,52	49,70

Table 35: Dose values for D2% in HNO 7

Week of Examination	Spinal Cord
Planning CT	33,48
Wk 1	32,92
Wk 2	32,79
Wk 3	33,88
Wk 4	34,04
Wk 5	34,16

Table 36: Dose values for D95% in HNO 7

Week of Examination	Tumor (GTV)
Planning CT	45,86
Wk 1	45,13
Wk 2	44,07
Wk 3	46,44
Wk 4	46,65
Wk 5	44,45

Table 37: Dose values for D50% in HNO 8

Week of Examination	Spinal Cord	Parotis Rt	Parotis Lt	Mandible	Tumor (GTV)	Submandible GI Rt	Submandible GI Lt
Planning CT	22,59	49,68	17,10	47,76	49,56	49,68	49,18
Wk 1	22,27	49,58	20,68	47,90	49,60	49,09	49,07
Wk 2	23,97	49,23	32,33	47,85	49,64	48,81	49,54
Wk 3	22,85	49,23	29,22	47,78	49,62	48,84	49,25
Wk 4	22,95	49,95	25,49	47,79	49,81	48,88	49,46
Wk 5	24,52	49,65	26,64	47,34	49,62	48,85	49,31

Table 38: Dose values for D2% in HNO 8

Week of Examination	Spinal Cord
Planning CT	29,76
Wk 1	31,26
Wk 2	32,25
Wk 3	31,62
Wk 4	31,43
Wk 5	31,23

Table 39: Dose values for D95% in HNO 8

Week of Examination	Tumor (GTV)
Planning CT	47,87
Wk 1	46,91
Wk 2	47,24
Wk 3	47,23
Wk 4	47,31
Wk 5	47,30

Table 40: Dose values for D50% in HNO 10

Week of Examination	Spinal Cord	Parotis Rt	Parotis Lt	Mandible	Tumor (GTV)	Tumor (CTV)	Submandible GI Rt	Submandible GI Lt
Planning CT	27,02	15,59	15,45	45,87	49,57	49,55	48,88	48,82
Wk 1	28,72	13,07	16,69	45,56	49,81	49,80	48,68	48,92
Wk 2	28,62	14,78	16,48	45,43		49,76	48,74	48,86
Wk 3	28,53	18,41	15,32	45,49	49,83	49,82	48,97	49,27
Wk 4	29,02	12,73	15,56	45,76	49,99	49,94	48,97	49,23
Wk 5	28,63	16,32	17,32	45,40	49,85	49,85	48,72	49,13

Table 41: Dose values for D2% in HNO 10

Week of Examination	Spinal Cord
Planning CT	31,35
Wk 1	35,94
Wk 2	35,95
Wk 3	35,45
Wk 4	37,22
Wk 5	36,26

Table 42: Dose values for D95% in HNO 10

Week of Examination	Tumorbed (CTV)
Planning CT	47,83
Wk 1	47,95
Wk 2	
Wk 3	47,91
Wk 4	48,02
Wk 5	47,93

Table 43: Dose values for D50% in HNO 11

Week of Examination	Spinal Cord	Parotis Rt	Parotis Lt	Mandible	Tumorbed	Tumor (CTV)	Submandible GI Rt	Submandible GI Lt
Planning CT	25,56	13,29	33,80	45,16	49,56	49,61	22,24	50,41
Wk 1	26,20	15,80	26,66	44,23	49,37	49,43	23,54	50,61
Wk 2	28,19	18,39	33,67	44,68	49,59	49,55	22,02	49,81
Wk 3	26,81	16,81	33,72	44,22	49,57	49,62	20,91	50,40
Wk 4	26,80	17,26	30,82	44,06	49,46	49,51	23,29	51,31
Wk 5	26,15	17,97	36,58	43,72	49,32	49,40	24,22	51,30

Table 44: Dose values for D2% in HNO 11

Week of Examination	Spinal Cord
Planning CT	31,81
Wk 1	32,68
Wk 2	35,55
Wk 3	33,83
Wk 4	35,74
Wk 5	33,08

Table 45: Dose values for D95% in HNO 11

Week of Examination	Tumorbed (CTV)
Planning CT	47,96
Wk 1	46,37
Wk 2	46,34
Wk 3	46,66
Wk 4	46,94
Wk 5	46,83

Table 46: Dose values for D50% in HNO 12

Week of Examination	Spinal Cord	Parotis Rt	Parotis Lt	Mandible	Tumor (CTV)	Submandible GI Rt	Submandible GI Lt
Planning CT	27,52	46,30	14,11	38,70	50,09	50,11	49,78
Wk 1	27,30	45,13	13,29	40,19	49,75	49,63	49,61
Wk 2	27,78	47,40	15,00	40,01	49,87		49,30
Wk 3	27,57	45,14	17,10	38,84	49,99	49,96	49,73
Wk 4	27,53	47,27	17,77	38,52	50,00	50,33	49,77
Wk 5	27,26	46,57	18,45	38,71	49,97	49,91	49,87

Table 47: Dose values for D2% in HNO 12

Week of Examination	Spinal Cord
Planning CT	31,79
Wk 1	38,90
Wk 2	39,14
Wk 3	39,09
Wk 4	37,72
Wk 5	38,68

Table 48: Dose values for D95% in HNO 12

Week of Examination	Tumor (CTV)
Planning CT	47,37
Wk 1	47,01
Wk 2	47,16
Wk 3	46,88
Wk 4	47,09
Wk 5	47,11

Table 49: Dose values for D50% in HNO 13

Week of Examination	Spinal Cord	Parotis Rt	Parotis Lt	Mandible	Tumorbett (CTV)	Submandible GI Rt	Submandible GI Lt
Planning CT	21,70	16,31	17,58	35,21	49,81	49,99	50,56
Wk 1	21,95	20,26	21,46	35,17	49,18	49,72	50,17
Wk 2	21,72	18,84	19,99	36,57	49,25	49,78	50,74
Wk 3	21,58	18,33	19,02	36,34	49,32	49,67	50,32
Wk 4	21,81	13,96	21,36	33,85	49,56	49,54	51,45
Wk 5	22,31	16,78	22,46	35,61	49,36	49,36	51,04

Table 50: Dose values for D2% in HNO 13

Week of Examination	Spinal cord
Wk 0	28,09
Wk 1	28,18
Wk 2	28,56
Wk 3	28,55
Wk 4	28,50
Wk 5	28,29

Table 51: Dose values for D95% in HNO 13

Week of Examination	Tumorbed (CTV)
Wk 0	48,03
Wk 1	47,19
Wk 2	47,30
Wk 3	47,43
Wk 4	47,67
Wk 5	47,47

Table 52: Dose values for D50% in HNO 15

Week of Examination	Spinal Cord	Parotis Rt	Parotis Lt	Mandible	Tumorbed (CTV)	Submandible GI Rt	Submandible GI Lt
Planning CT	18,26	49,58	23,19	36,28	50,17	50,46	28,66
Wk 1	23,21	49,27	20,82	34,20		50,25	27,67
Wk 2	16,54	49,61	20,98	34,25	49,67	50,07	28,09
Wk 3	19,07	49,72	21,13	34,27	49,72	50,17	28,19
Wk 4	19,69	49,67	21,07	33,86	49,65	50,33	28,18
Wk 5	17,58	49,24	21,26	35,33	49,61	50,23	27,96

Table 53: Dose values for D2% in HNO 15

Week of Examination	Spinal cord
Planning CT	29,96
Wk 1	32,51
Wk 2	31,83
Wk 3	31,88
Wk 4	33,11
Wk 5	32,73

Table 54: Dose values for D95% in HNO 15

Week of Examination	Tumorbed (CTV)
Planning CT	48,37
Wk 1	
Wk 2	46,60
Wk 3	46,21
Wk 4	46,28
Wk 5	46,15

Table 55: Dose values for D50% in HNO 16

Week of Examination	Spinal Cord	Parotis (Rt)	Parotis (Lt)	Mandible	Tumor (GTV)	Submandibular GI (Rt)	Submandibular GI (Lt)
Planning CT	23,82	23,60	46,56	47,56	50,09	49,96	50,67
Wk 1	25,29	20,93	46,50	47,60	50,57	49,95	50,70
Wk 2	24,86	28,49	44,88	47,73	50,43	49,95	50,61
Wk 3	24,77	36,01	40,34	47,99	50,79	50,42	50,77
Wk 4	24,86	39,71	41,80	47,46	50,78	49,94	50,72
Wk 5	25,10	19,14	43,86	47,26	49,88	48,78	49,85

Table 56: Dose values for D2% in HNO 16

Week of Examination	Spinal Cord
Planning CT	30,47
Wk 1	33,27
Wk 2	35,47
Wk 3	31,81
Wk 4	35,08
Wk 5	33,66

Table 57: Dose values for D95% in HNO 16

Week of Examination	Tumor (GTV)
Planning CT	48,28
Wk 1	48,28
Wk 2	48,18
Wk 3	48,46
Wk 4	48,37
Wk 5	48,02

Table 58: Dose values for D50% in HNO 17

Week of CT-Examination	Spinal Cord	Parotid (Rt)	Parotid (Lt)	Mandible	Tumor (GTV)	Tumor (CTV)	Submandibular GI (Rt)	Submandibular GI (Lt)
Planning CT	28,53	16,96	48,47	39,28	48,84	49,24	49,80	49,02
Wk 1	28,23	12,88	49,31	40,68	49,51	49,42	49,60	48,83
Wk 2	28,16	16,32	48,99	41,28	49,46	49,37	49,56	49,27
Wk 3	28,09	21,37	48,81	42,22	49,40	49,48	49,87	49,43
Wk 4	28,55	19,81	49,01	40,08	49,95	50,06	49,85	49,73
Wk 5	28,23	15,27	49,28	39,68	49,80	49,80	49,81	50,11

Table 59: Dose values for D2% in HNO 17

Week of Examination	Spinal Cord
Planning CT	31,52
Wk 1	32,12
Wk 2	31,47
Wk 3	31,33
Wk 4	33,18
Wk 5	33,46

Table 60: Dose values for D95% in HNO 17

Week of Examination	Tumor (GTV)
Planning CT	47,54
Wk 1	45,23
Wk 2	45,78
Wk 3	46,23
Wk 4	47,85
Wk 5	46,32

List of Tables

Table 1: Overview of management of head and neck cancers according to TNM staging.....	- 7 -
Table 2: Classification of radiation induced mucositis.....	- 11 -
Table 3: Comparison of planning CT HU, uncalibrated CBCT grey values and the calibrated CBCT HU values of the seven inserts.....	- 24 -
Table 4: Contouring description for GTV and CTV in patients.....	- 30 -
Table 5: Details of the patients included in our study.....	- 33 -
Table 6: Overview of patient variables.....	- 35 -
Table 7: Acute side effects documented during radiotherapy treatment.....	- 36 -
Table 8: Grade of mucositis documented in patients.....	- 36 -
Table 9: Grade of dermatitis documented in patients.....	- 37 -
Table 10: Dose values for D50% in HNO 4 in Grays (Gy).....	- 37 -
Table 11: Dose values for D2% in HNO 4 in Grays (Gy).....	- 38 -
Table 12: Dose values for D95% in HNO 4 in Grays (Gy).....	- 38 -
Table 13: Relevant relative deviations in D50% for the spinal cord.....	- 42 -
Table 14: Relevant relative deviations in D2% for the spinal cord.....	- 43 -
Table 15: Very relevant relative deviations in D50% right parotid gland in HNO 7.....	- 48 -
Table 16: Very relevant relative deviations in D50% for left parotid gland.....	- 54 -
Table 17: Very relevant relative deviations in D50% for the mandible.....	- 59 -
Table 18: Relevant relative deviations in D50% for the right submandibular gland.....	- 64 -
Table 19: Dose values for D50% in HNO 2.....	- 86 -
Table 20: Dose values for D2% in HNO 2.....	- 86 -
Table 21: Dose values for D95% in HNO 2.....	- 86 -
Table 22: Dose values for D50% in HNO 3.....	- 86 -
Table 23: Dose values for D2% in HNO 3.....	- 87 -
Table 24: Dose values for D95% in HNO 3.....	- 87 -
Table 25: Dose values for D50% in HNO 4.....	- 87 -
Table 26: Dose values for D2% in HNO 4.....	- 87 -
Table 27: Dose values for D95% in HNO 4.....	- 87 -
Table 28: Dose values for D50% in HNO 5.....	- 88 -
Table 29: Dose values for D2% in HNO 5.....	- 88 -
Table 30: Dose values for D95% in HNO 5.....	- 88 -
Table 31: Dose values for D50% in HNO 6.....	- 88 -
Table 32: Dose values for D2% in HNO 6.....	- 89 -
Table 33: Dose values for D95% in HNO 6.....	- 89 -
Table 34: Dose values for D50% in HNO 7.....	- 89 -
Table 35: Dose values for D2% in HNO 7.....	- 89 -
Table 36: Dose values for D95% in HNO 7.....	- 89 -
Table 37: Dose values for D50% in HNO 8.....	- 90 -
Table 38: Dose values for D2% in HNO 8.....	- 90 -
Table 39: Dose values for D95% in HNO 8.....	- 90 -
Table 40: Dose values for D50% in HNO 10.....	- 90 -
Table 41: Dose values for D2% in HNO 10.....	- 90 -
Table 42: Dose values for D95% in HNO 10.....	- 91 -
Table 43: Dose values for D50% in HNO 11.....	- 91 -
Table 44: Dose values for D2% in HNO 11.....	- 91 -
Table 45: Dose values for D95% in HNO 11.....	- 91 -
Table 46: Dose values for D50% in HNO 12.....	- 92 -

Table 47: Dose values for D2% in HNO 12.....	- 92 -
Table 48: Dose values for D95% in HNO 12.....	- 92 -
Table 49: Dose values for D50% in HNO 13.....	- 92 -
Table 50: Dose values for D2% in HNO 13.....	- 92 -
Table 51: Dose values for D95% in HNO 13.....	- 93 -
Table 52: Dose values for D50% in HNO 15.....	- 93 -
Table 53: Dose values for D2% in HNO 15.....	- 93 -
Table 54: Dose values for D95% in HNO 15.....	- 93 -
Table 55: Dose values for D50% in HNO 16.....	- 93 -
Table 56: Dose values for D2% in HNO 16.....	- 94 -
Table 57: Dose values for D95% in HNO 16.....	- 94 -
Table 58: Dose values for D50% in HNO 17.....	- 94 -
Table 59: Dose values for D2% in HNO 17.....	- 94 -
Table 60: Dose values for D95% in HNO 17.....	- 94 -

List of Figures

Figure 1: Anatomical regions and organs affected by head and neck cancer.....	- 5 -
Figure 2: Bolus effect of tracheostomy flange in the peristomal region.....	- 16 -
Figure 3: Five-point thermoplastic mask for fixation of radiotherapy patients	- 19 -
Figure 4: Anatomical regions affected by weight loss during radiotherapy of head and neck cancers	- 20 -
Figure 5: Diagram of a Catphan 503 phantom	- 22 -
Figure 6: Graph used to calibrate CBCTs	- 23 -
Figure 7: Example of contouring in planning CT and CBCTs for patient HNO 4 ...	- 26 -
Figure 8: Illustrating gross tumor volume (GTV) and clinical target volume (CTV) -	- 29 -
Figure 9: Planning CT and weekly CBCTs in patient HNO 4	- 39 -
Figure 10: Radiotherapy plan in planning CT and CBCTs for patient HNO 4	- 40 -
Figure 11: Frequency of daily differences from planned dose in D50% in the spinal cord	- 41 -
Figure 12: Frequency of daily differences from planned dose in D2% for the spinal cord	- 42 -
Figure 13: Radiotherapy plan in planning CT and CBCTs for patient HNO 12	- 44 -
Figure 14: Evaluation of anatomical variation at level C6/C7 in patient HNO 12...	- 46 -
Figure 15: Frequency of daily differences from planned dose in D50% for right parotid gland	- 47 -
Figure 16: Weight loss during treatment in patient HNO 7	- 49 -
Figure 17: Medial shifting of the right parotid gland in patient HNO 7	- 51 -
Figure 18: Frequency of daily differences from planned dose in D50% for left parotid gland	- 53 -
Figure 19: Weight loss during treatment in patient HNO 8	- 55 -
Figure 20: Medial shifting of the left parotid gland in patient HNO 8.....	- 57 -
Figure 21: Frequency of daily differences from planned dose in D50% for the mandible.....	- 58 -
Figure 22: Weight loss during treatment in patient HNO 3	- 60 -
Figure 23: Treatment plan in planning CT and CBCTs in patient HNO 3.....	- 62 -
Figure 24: Frequency of daily differences from D50% planned dose in right submandibular gland.....	- 64 -
Figure 25: Treatment plan in planning CT and CBCTs in patient HNO 3.....	- 65 -
Figure 26: Frequency of daily differences from planned dose in D50% for the left submandibular gland.....	- 66 -
Figure 27: Frequency of daily differences from planned dose in D50% for GTV... -	- 67 -
Figure 28: Frequency of daily differences from planned dose in D95% for GTV... -	- 67 -
Figure 29: Frequency of daily differences from planned dose in D50% for CTV ... -	- 69 -
Figure 30: Frequency of daily differences from planned dose in D95% for CTV ... -	- 69 -

Acknowledgements

I would like to thank the following people, who helped and motivated me to complete this thesis:

A big thank you to my supervisors, Prof. Björn Poppe and Dr. Ping Jiang for providing guidance and constant feedback throughout this project. I would also like to thank Dr. Hui Khee Looe, Dr. Tenzin Stelljes, Dr. Mathius Raub and Dr. Willborn Kay for their assistance.

I am forever grateful to my family for believing in me and standing by my side during the challenging times. A special mention goes to Amai Junior Kadenge, Dr. Klaus and Marlies de Boer, Dr. Gwinyai Kadenge and Dr. Betty Kadenge. To my beautiful kids, Johanna and Taonezvi, I'm sorry for spending so many hours during the weekends writing this thesis and I thank you for allowing me to work.

To my lovely wife Antje, thanks for all your prayers, support and encouragement. I am so grateful to have you by my side.

Last but not least, I would like to dedicate this project to my father, the late Dr. Mark John Taonezvi Kadenge, who inspired me to be humble, hard-working and to never give up.